Volume 10, No. 2
November, 1961

THE SOVIET JOURNAL OF

ATOMIC ENERGY

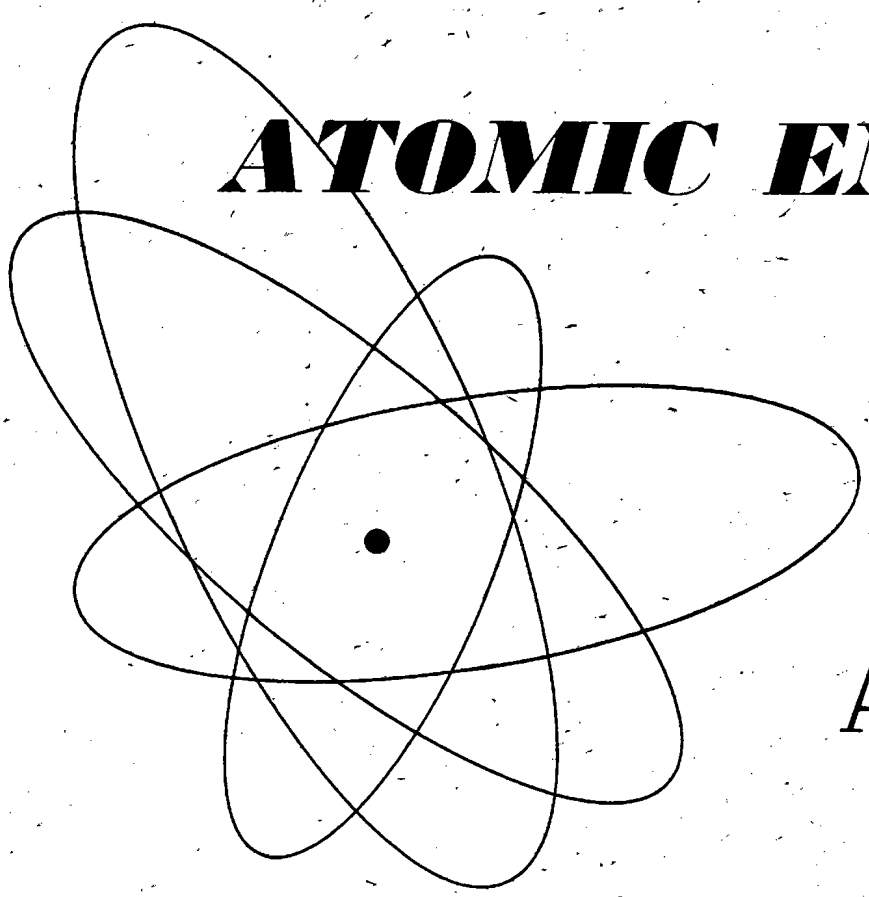

Атомная энергия

TRANSLATED FROM RUSSIAN

CONSULTANTS BUREAU

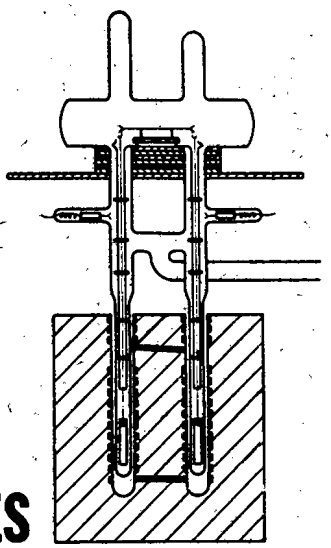

VOLUME I

VACUUM MICROBALANCE TECHNIQUES

Proceedings of the 1960 Conference Sponsored by
The Institute for Exploratory Research
U. S. Army Signal Research and Development Laboratory

Edited by
M. J. KATZ
U. S. Army Signal Research and Development Laboratory
Fort Monmouth, New Jersey

Introduction by
Thor N. Rhodin
Cornell University

The proceedings of this conference provide an authoritative introduction to the rapidly widening scope of microbalance methods which is not available elsewhere in a single publication.

The usefulness of microbalance techniques in the study of the properties of materials lies in their extreme sensitivity and versatility. This renders them particularly important in studies of properties of condensed systems. In addition to the historical use of microbalance techniques as a tool of microchemistry, they have, in recent years, found extensive application in the fields of metallurgy, physics, and chemistry. The uniqueness of the method results from the facility it provides in making a series of precise measurements of high sensitivity under carefully controlled conditions over a wide range of temperature and pressure.

This significant new volume contains papers in three major categories. The first group of reports deals with the general structural features and measuring capabilities of microbalances. In the second group, a sophisticated consideration and much needed evaluation of sources of spurious mass changes associated with microbalances is presented. The third group describes some of the most recent extensions in microbalance work to new research areas such as semiconductors, ultra-high vacuum, and high temperatures. These papers provide an interesting account of advances in the application of the microgravimetric method to three new and important fields of research on the behavior of materials.

170 pages **$6.50**

PLENUM PRESS, INC. 227 West 17th St., New York 11, N. Y.

THE SOVIET JOURNAL OF

ATOMIC ENERGY

A translation of ATOMNAYA ÉNERGIYA,
a publication of the Academy of Sciences of the USSR

(Russian original dated February, 1961)

Vol. 10, No. 2 November, 1961

CONTENTS

Annual subscription	$ 75.00
Single issue	20.00
Single article	12.50

CONTENTS (continued)

NOTE

The Table of Contents lists all materials that appears in Atomnaya Énergiya. Those items that originated in the English language are not included in the translation and are shown enclosed in brackets. Whenever possible, the English-language source containing the omitted reports will be given.

Consultants Bureau Enterprises, Inc.

USING THE METHOD OF MOMENTS TO CALCULATE THE SPACE-ENERGY DISTRIBUTION OF NEUTRON DENSITY FROM FLAT AND POINT SOURCES IN AN INFINITE MEDIUM

A. P. Ptitsyn

Translated from Atomnaya Énergiya, Vol. 10, No. 2, pp. 117-126, February, 1961
Original article submitted April 6, 1959

A method is given for calculating the space-energy distribution of neutron densities from flat and point sources in an infinite medium.

The neutron density ψ (x, E) is sought in the form $(\psi, E) = \sum_{i=1}^{N} a_i(E)\, K[b_i(E)x]$. To a large degree the form of the function K(x) is arbitrary; its selection is based on physical principles. From the 2N space moments of the function ψ(x, E), 2N parameters a_i, b_i are found. The neutron density distribution is found in hydrogen and water. The calculations for water are compared with experimental data. A comparison with the accurate solution of Wick [1] in the case of retardation of neutrons by hydrogen shows that from four moments the suggested method can, with sufficient accuracy, find the spatial distribution of neutrons at distances up to 20 free path lengths.

In [1-4] in principle the problem was solved of finding the space-energy distribution of photons and neutrons in an infinite medium. In [1,2] a study was made of the asymptotic form of the solution for very large distances from the source.

An analytical solution was found in [1] for the case of a constant free path length for strongly retarding neutrons. For cross sections depending on energy, in [3] a semianalytical method was developed to calculate the distribution at very large distances from the source.

For comparatively small distances the method of polynomial expansions can be used for the calculation [4]. It is precisely these distances (~15-20 free path lengths) which are of interest to us. The idea of the polynomial method consists of expanding the required function into a series in terms of known polynomials $U_i(x)$:

$$\psi(x,\ E) = e^{-\beta x}\Sigma A_i(E)\, U_i(\beta x), \tag{1}$$

where the coefficients $A_i(E)$ are found from a system of integral equations. This method was developed in application to photons, and at distances of 15-20 path lengths it can find the photon density by means of four polynomials, which amounts to finding four space moments.

In the case of weakly retarding media this method is also suitable for determining neutron density; however, with strong retardation, especially when the free path length decreases weakly with decrease in energy, the series in terms of polynomials converges poorly. Here the use of four terms of the series [1] at distances equal to 5-6 paths leads to negative values of neutron density. This is presumably due to the unsuitably of the polynomial expansion method for these problems, although a knowledge of the four space moments $\psi_n(E)$ is in itself sufficient to find the neutron density at the given distances for any values of E*.

As is known, neutron density mainly depends exponentially on the distance x; however, the exponent is not always a linear function. Thus, in the case of a monoenergy source $\delta(E-E_0)$ the neutron density, where there is not a single collision, at all values of x is proportional to $e^{-x/\lambda}$. Being retarded, these primary particles will give at any distances a neutron spectrum proportional to $e^{-x/\lambda}$. The accumulation of neutrons, as shown in [1,2], leads to a

* The author of [5] showed that a value of the parameter β can be chosen in the polynomial expansion (1) for which the series in terms of polynomials converges well.

still slower reduction in density at large distances. On the other hand, at small distances $x < \ln E_0/E$, according to the theory of age, the density of neutrons retarded to an energy E ($E \ll E_0$), is proportional to $e^{-x^2/4\tau}$.

An attempt could be made to find the density $\psi(x, E)$ in the form of a linear combination of functions of the given type

$$\psi(x, E) = a_1(E)\, l^{-b_1(E)\, x^2} + a_2(E)\, l^{-b_2(E)\, x}. \tag{2}$$

However, in this case to determine the coefficients a_i, b_i from the spatial moments of the function ψ, a system of nonlinear equations is obtained of a type such that the solution cannot be obtained in a clear form.

We will seek the function $\psi(x, E)$ in the form

$$\psi(x, E) = \sum_{i=1}^{N} a_i(E)\, K[b_i(E)\, x] \tag{3}$$

(with regard to the form of the functions $K(x)$ see section 3). The advantage of this form of approximation is that approximations of any order can be obtained in the same way, and the main advantage is that the system of equations for the coefficients a_i, b_i permits an accurate analytical solution. As will be shown, two terms of the sum (3) describe with sufficient accuracy the neutron density for any energy E at distances of x to 20 free path lengths.

1. Integral Equations for Moments

To obtain equations which are satisfied by the spatial moments of neutron density in the case of a flat monoenergy source we will proceed, as usual, from the kinetic equation

$$\mu \frac{\partial \psi'}{\partial x} + \sigma(u)\, \psi' - \Sigma \alpha_i \int_0^u du' \sigma_{s_i}(u') \int d\Omega' G_i(\mu_0, u - u')\, \psi'(x, u', \mu') = \delta(x)\, \delta(u)\, S(\mu), \tag{1.1}$$

where $u = \ln E_0/E$; E_0 is the energy of the source neutrons; μ is the cosine of the angle between the axis x and the direction of movement of the neutron; μ_0 is the cosine of the scatter angle of the neutron; $\psi'(x, u, \mu) = vn(x, u, \mu)$; v is the speed of the neutron; $n(x, u, \mu)\, dx\, du\, d\Omega$ is the number of neutrons in an element $dx\, du\, d\Omega$;

$$G_i(\mu_0, u) = \frac{1}{2\pi} e^{-u} \delta \left[\mu_0 - \left(\frac{M_i + 1}{2} e^{-u/2} - \frac{M_i - 1}{2} e^{u/2} \right) \right];$$

$S(\mu)$ is the angular distribution of neutrons leaving the source; $\sigma(u)$ and $\sigma_{s_i}(u)$ are the macroscopic cross sections (total and elastic scatter at nuclei with a mass M_i, respectively); $\alpha_i = (M_i + 1)^2/4M_i$.

For simplicity the scatter is assumed to be elastic and isotropic in a system of a center of masses. Extension to the case of inelastic and nonisotropic scatter is elementary. Nonisotropicity is allowed for by introducing after the integral sign the factor $\omega_i[(M_i + 1)^2/2M_i] \times e^{-(u-u')} - [(M_i^2 + 1)/2M_i]\}$, where $\omega_i(\cos\vartheta)$ is the indicatrix of scatter at nuclei of the type i, standardized $\frac{1}{4\pi} \int \omega_i(\cos\vartheta)\, d\Omega = 1$. Inelastic scatter is allowed for by introducing the integral of nonelastic collisions

$$\frac{1}{4\pi} \int_0^u \sigma_i^{\text{inel}}(u')\, W_i(u', u)\, \psi'_0(x, u')\, du',$$

where $\sigma_i^{\text{inel.}}$ is the cross section of inelastic scatter; $W_i(u', u)$ is the probability of inelastic scatter from u' to u, standardized so that $\int_{u'}^{\infty} W_i(u', u)\, du = 1$.

To eliminate peculiarities in the right side of equation (1.1) we will separate from the function $\psi'(x, u, \mu)$ the part which describes those neutrons of the source which have not undergone a single collision with nuclei, i.e. we will represent ψ' in the form

$$\psi'(x, u, \mu) = \psi(x, u, \mu) + \psi^{\text{tr}}(x, \mu)\, \delta(u). \tag{1.2}$$

The function $\psi^{tr}(x, \mu)$ apparently satisfies equation (1.1) without an integral of collisions

$$\mu \frac{\partial \psi^{tr}}{\partial x} + \sigma(0)\psi^{tr} = \delta(x) S(\mu). \tag{1.3}$$

The solution of this equation is

$$\psi^{tr}(x, \mu) = \frac{S(\mu)}{|\mu|} e^{-\sigma(0)x/\mu} \theta(\mu x), \tag{1.4}$$

where $\theta(y)$ is a known discontinuous function

$$\theta(y) = \begin{cases} 1, & y > 0, \\ 0, & y < 0. \end{cases} \tag{1.5}$$

We will multiply equation (1.3) by $P_l(\mu)$ [$P_l(\mu)$ Legendre polynomials] and integrate for all angles Ω. We obtain

$$\frac{1}{2l+1}\left[(l+1)\frac{\partial \psi_{l+1}^{tr}}{\partial x} + l\frac{\partial \psi_{l-1}^{tr}}{\partial x}\right] + \sigma(0)\psi_l^{tr} = \delta(x) S_l. \tag{1.6}$$

Here ψ_l and S_l are the coefficients of expansion of the functions $\psi(\mu)$ and $S(\mu)$ in terms of Legendre polynomials

$$\psi_l = \int d\Omega P_l(\mu)\psi(\mu),$$

$$S_l = \int d\Omega P_l(\mu) S(\mu).$$

Let

$$m_{ln} = \frac{\beta^{n+1}}{n!}\int_{-\infty}^{\infty} x^n \psi_l^{tr}(x)\, dx, \tag{1.7}$$

where β is a certain constant. Multiplying equation (1.6) by $(\beta^{n+1}/n!)\, x^n$ and integrating with respect to x from $-\infty$ to $+\infty$, we find for the coefficients m_{ln} the following systems of algebraic equations:

$$m_{l0} = \gamma S_l;$$

$$m_{ln} = \frac{\gamma}{2l+1}\left[(l+1)m_{l+1,\,n-1} + l m_{l-1,\,n-1}\right], \tag{1.8}$$

$$n = 1, 2, \ldots$$

where

$$\gamma = \frac{\beta}{\sigma(0)}. \tag{1.9}$$

The system of equations (1.8) is recurrent. Each coefficient with an index n is expressed only through a coefficient with an index n-1. The system is solved in the following order: from a determination of the coefficients ($m_{l0} = \gamma S_l$) it follows that

$$m_{l1} = \frac{\gamma}{2l+1}\left[(l+1)m_{l+1,\,0} + l m_{l-1,\,0}\right].$$

Hence it is possible to find m_{l2}, etc.

The coefficients m_{ln} can be obtained directly by substituting in the integrals (1.6) and (1.7) the function ψ^{tr} from (1.4).

We will deal with the system of equations (1.8) in detail since this will be useful at a later stage.

Assuming similar to (1.7) that

$$M_{ln}(u) = \frac{\beta^{n+1}}{n!}\int_{-\infty}^{\infty} x^n \psi_l(x, u)\, dx. \tag{1.10}$$

Substituting $\psi'(x, u, \mu) = \psi(x, u, \mu) + \psi^{tr} \times (x, \mu)\,\delta(u)$ in equation (1.1), multiplying it by $(\beta^{n+1}/n!)\,x^n P_l(\mu)$, and integrating with respect to $d\Omega$ and dx, we obtain, considering the determination of (1.10) and (1.7), the system of integral equations which we require to determine the functions $M_{ln}(u)$*:

$$\sigma(u)\,M_{ln}(u) - \sum_i \alpha_i \int_0^u \theta(q_i - u + u')\,\sigma_{si}(u')\,e^{-(u-u')}\,P_l(\mu_i)M_{ln}(u')\,du' = \frac{\beta}{2l+1} \times$$

$$\times \left[(l+1)\,M_{l+1,\,n-1} + lM_{l-1,\,n-1} \right] + m_{ln}e^{-u}\sum_i \alpha_i\sigma_{si}(0)\,P_l(\mu_i^0)\theta(q_i - u); \tag{1.11}$$

$$M_{l,\,-1}(u) = 0,$$

where

$$\mu_i \equiv \mu_i(u-u') = \frac{M_i+1}{2}\,e^{\frac{u-u'}{2}} - \frac{M_i-1}{2}\,e^{\frac{u-u'}{2}};$$

$$\mu_i^0 = \mu_i(u-u')\Big|_{u'=0}, \quad q_i = \ln\left(\frac{M_i+1}{M_i-1}\right)^2. \tag{1.12}$$

The system of integral equations (1.11) for M_{ln} and also the system (1.8), is recurrent and is solved in exactly the same order.

The initial values of the functions M_{ln} can readily be found. In fact, for $u = 0$ the integrals in the left side of (1.11) revert to zero, the Lengendre polynomials in the right side revert to unity ($\mu_i(0) = 1$) and for $M_{ln}(0)$ we obtain a system of algebraic equations

$$\sigma(0)\,M_{ln}(0) = \frac{\beta}{2l+1}\left[(l+1)\,M_{l+1,\,n-1}(0) + lM_{l-1,\,n-1}(0) \right] + m_{ln}\sum_i \alpha_i\sigma_{si}(0). \tag{1.13}$$

Since the coefficients m_{ln} satisfy the system of equations (1.8) we find the solution of the system (1.13) [6]:

$$M_{ln}(0) = (n+1)\,m_{ln}\frac{\sum_i \alpha_i\sigma_{si}(0)}{\sigma(0)}. \tag{1.14}$$

For the direct solution of equations (1.11) the coefficients m_{ln} must be found in a clear form; in their turn these depend on the coefficients S_l of angular distribution of the source $S(\mu)$.

Since the kinetic equation (1.1) and hence the system of equations (1.11) are linear, the solution of the latter for an arbitrary source

$$S(\mu) = S^+(\mu) + S^-(\mu),$$

where

$$S^+(\mu) = S^+(-\mu), \quad S^-(\mu) = -S^-(-\mu), \tag{1.15}$$

can be found as the sum of solutions corresponding tosymmetrical $S^+(\mu)$ and antisymmetrical $S^-(\mu)$ sources. Therefore

* In the case of nonisotropic scatter instead of $P_l(\mu)$ in equation (1.11) it is essential to substitute $\omega(\cos v)\,P_l(\mu)$. Allowing for inelastic scatter leads to an additional integral term $\delta_{l0}\sum_i \int_0^u \sigma_i^{inel}(u')\,W_i(u', u)\psi_{0n}(u')du'$ and to a corresponding free term $\delta_{l0}m_{ln}\sum_i \sigma_i^{inel}(0)\,W_i(0, u)$.

we will later assume that the source $S(\mu)$ is either an even or an odd function of μ. Without limiting the generalization it is apparently sufficient to find the coefficients m^{+}_{ln} and m^{-}_{ln} for the symmetrical

$$S^{+}(\mu)=\frac{1}{4\pi}\left[\delta(\mu-\mu_0)+\delta(\mu+\mu_0)\right] \tag{1.16}$$

and the antisymmetrical

$$S^{-}(\mu)=\frac{1}{4\pi}\left[\delta(\mu-\mu_0)-\delta(\mu+\mu_0)\right] \tag{1.17}$$

δ-sources, respectively.

As mentioned above, the coefficients m_{ln} can be found not only from the system (1.8) but also directly, substituting $\psi^{tr}(x, \mu)$ in (1.7). Taking as $S(\mu)$ (1.16) we find

$$m^{+}_{ln}=\frac{\beta^{n+1}}{n!}\int_{-1}^{1}2\pi d\mu\frac{P_l(\mu)}{4\pi(\mu)}\left[\delta(\mu-\mu_0)+\delta(\mu+\mu_0)\right]\int_{-\infty}^{\infty}e^{-\sigma(0)x/\mu}\theta(\mu x)\,x^n dx=$$

$$=\frac{\gamma^{n+1}}{2(n!)}\frac{P_l(\mu_0)}{|\mu_0|}\int_{-\infty}^{\infty}e^{-y/\mu_0}\theta(\mu_0 y)\,y^n dy+\frac{\gamma^{n+1}}{2(n!)}\frac{P_l(-\mu_0)}{|\mu_0|}\int_{-\infty}^{\infty}e^{y/\mu_0}\theta(-\mu_0 y)\,y^n dy \tag{1.18}$$

(the value of γ is determined by formula (1.9). Hence

$$m^{+}_{ln}=\begin{cases}0 & \text{for odd } (l+n),\\ \gamma^{n+1}P_l(\mu_0)\,\mu_0^n & \text{for even } (l+n).\end{cases} \tag{1.19}$$

Similarly, using (1.17) we find

$$m^{-}_{ln}=\begin{cases}\gamma^{n+1}P_l(\mu_0)\,\mu_0^n & \text{for odd } (l+n),\\ 0 & \text{for even } (l+n).\end{cases} \tag{1.20}$$

We will consider one particularly important case of a symmetrical source, where the angular distribution $S(\mu)$ is independent of the direction (isotropic source):

$$S(\mu)=\frac{1}{4\pi}. \tag{1.21}$$

For the coefficients m_{ln} according to (1.21) and (1.8) we have [5]

$$m_{ln}=\frac{\beta^{n+1}}{n!}\int_{-1}^{1}\frac{2\pi\,d\mu}{4\pi\,|\mu|}P_l(\mu)\int_{-\infty}^{\infty}e^{-\sigma(0)x/\mu}\;\theta(\mu x)\,x^n\,dx=\gamma^{n+1}\varkappa_{ln}, \tag{1.22}$$

where

$$\varkappa_{ln}=\frac{1}{2}\int_{-1}^{1}\mu^n P_l(\mu)\,d\mu\;=\begin{cases}0 & \text{for odd } (n-l) \text{ or } n<l,\\ \dfrac{2^l n!\left(\frac{n+l}{2}\right)!}{\left(\frac{n-l}{2}\right)!\,(n+l+1)!}, & \text{if } (n-l) \text{ is a non-negative even number.}\end{cases} \tag{1.23}$$

An important equality follows from (1.23) and system (1.11) as well as the obvious relationship $M_{ln}(u)=0$, if $(l+n)$ is an odd number.

$$M_{ln}(u)=0, \quad \text{if} \quad n<l. \tag{1.24}$$

2. Point Isotropic Source

The "moments" M^{pt}_{ln} in the case of a point isotropic source

$$M_{ln}^{pt}(u) = \frac{\beta^{n+1}}{n!}\int_0^\infty r^n \psi_l^{pt}(r, u)\, 4\pi r^2\, dr \quad (2.1) \tag{2.1}$$

for even values of $l + n$ can be found knowing the moments M_{ln} for a plane isotropic source. In fact, with regard to the known connections between the solutions for plane and point sources [2],

$$\psi_l^{pl}(x, u) = 2\pi \int_{|x|}^\infty dr r \psi_l^{pt}(r, u)\, P_l\left(\frac{x}{r}\right) \tag{2.2}$$

We have [5]

$$M_{ln}(u) = 2\pi \frac{\beta^{n+1}}{n!}\int_{-\infty}^\infty dx x^n \int_{|x|}^\infty dr r \psi_l^{pt}(r, u)\, P_l\left(\frac{x}{r}\right) = \varkappa_{ln} M_{ln}^{pt}. \tag{2.3}$$

In particular, for moments M_{0n}^{pt} the neutron density

$$M_{0,2k}^{pt} = (2k+1)\, M_{0,2n}\ k = 0, 1, 2, \ldots \tag{2.4}$$

3. Method of Approximating a Function With Respect to Its Moments

Let there be 2N space moments

$$g_n = \int_0^\infty x^n g(x)\, dx$$

of a certain function g(x), given for the range, $(0, \infty)$. We wish to approximate the function g(x) by the sum

$$g(x) \simeq \sum_{i=1}^N a_i K(b_i x), \tag{3.1}$$

where the function K(x) is such that its moment

$$K_n = \int_0^\infty x^n K(x)\, dx$$

exist. In [3] a method is given which can be used to express the coefficients a_i, b_i by moments g_n. This method is essentially as follows. We will write the sum of (3.1), somewhat changing the designations, in the form

$$g(x) = \sum_{i=1}^N (\eta_i/s_i) K(x/s_i). \tag{3.2}$$

Multiplying (3.2) by x^n and integrating from 0 to ∞, we obtain a system of nonlinear equations

$$g_n = \sum_{i=1}^N \eta_i s_i^n K_n \tag{3.3}$$

or, dividing (3.3) by K_n and introducing the designations $f_n = g_n/K_n$, we obtain

$$\begin{gathered} \eta_1 + \eta_2 + \ldots + \eta_N = f_0; \\ \eta_1 s_1 + \eta_2 s_2 + \ldots + \eta_N s_N = f_1; \\ \eta_1 s_1^{2N-1} + \eta_2 s_2^{2N-1} + \ldots + \eta_N s_N^{2N-1} = f_{2N-1}. \end{gathered} \tag{3.4}$$

Let $f(s)$ be a function such that the right sides f_n of the system (3.4) are its moments. We then obtain this system of equations if in the N-point quadratic formula of the Gauss type with weight $f(s)$

$$\int_0^\infty f(s) H(s)\, ds \simeq \sum_{i=1}^N \eta_i H(s_i) \tag{3.5}$$

we substitute instead of H(s) successively all powers of s from zero to 2N-1, for which the equality in the approximate expression (3.5) is fulfilled accurately. As is known, s_i in expression (3.5) is the zero of the polynomial $h_N(s)$, orthogonal with the weight f (s) to all polynomials of lower powers, and η_i are the so-called Christoffel numbers, determined by the formula

$$\eta_i = \left[\frac{dh_N(s)}{ds}\right]^{-1}_{s_i} \int_0^\infty f(s)\,\frac{h_N(s)}{s-s_i}\,ds. \tag{3.6}$$

Therefore, the solution of the system of equations (3.4) is given by formula (3.6) and by the roots of the equation

$$h_N(s) = 0. \tag{3.7}$$

If the function f (s) is positive, then all roots of equation (3.7) are real and different. In the general case among the roots s_i there can be some which are related in a complex way. Let s_α and $s_{\alpha+1}$ be two such roots. Then the two complex related terms in formula (3.2) will give

$$(\eta_\alpha/s_\alpha)\,K(x/s_\alpha) + (\eta_{\alpha+1}/s_{\alpha+1})\,K(x/s_{\alpha+1}) = 2Re\,[(\eta_\alpha/s_\alpha)\,K(x/s_\alpha)]. \tag{3.8}$$

Among the roots of equation (3.7) there can also be multiple roots. We will consider this case in greater detail.

Let a certain root s_α have a multiplicity m. To be precise we will assume that these are the roots

$$s_1 = s_2 = \ldots = s_m \equiv \beta^{-1}.$$

Formula (3.2) in this case then becomes

$$g(x) = \beta\Big(\sum_{\alpha=1}^{m}\eta_\alpha\Big)K(\beta x) + \sum_{i=m+1}^{N}(\eta_i/s_i)\,K(x/s_i), \tag{3.9}$$

and the Christoffel numbers η_α according to (3.6) revert to infinity. It is true that their sum $\left(\sum_{\alpha=1}^{m}\eta_\alpha\right)$ is finite and according to the first equation of system (3.4) is equal to

$$\sum_{\alpha=1}^{m}\eta_\alpha = f_0 - \sum_{i=m+1}^{N}\eta_i = C, \tag{3.10}$$

however, the function

$$\beta C K(\beta x) + \sum_{i=m+1}^{N}(\eta_i/s_i)\,K(x/s_i)$$

in the general case will not be a solution of the problem. Generally speaking, 2N moments of this function do not coincide with 2N given moments g_n of the function g(x). This is not a contradiction of system (3.4) since formally this system is "satisfied" by finite additions arising on the addition of infinite terms

$$\sum_{\alpha=1}^{m}\eta_\alpha s_\alpha^n = \beta^{-n}C + \text{arbitrary constant}.$$

The solution of the problem in this case will be the function

$$g(x) = K(\beta x)\sum_{n=1}^{2m}a_n x^n + \sum_{i=m+1}^{N}(\eta_i/s_i)\,K(x/s_i). \tag{3.11}$$

In particular, if all N roots of equation (3.7) are equal, then according to (3.11) for g(x) we have

$$g(x) = K(\beta x)\sum_{n=1}^{2N}a_n x^n, \tag{3.12}$$

and this is a polynomial expansion [1].

Returning now to the problem of finding the neutron density it can be stated that at the distances we are concerned with the neutron density behaves mainly as $K(\beta x)$ (for example as $e^{-\beta x}$), then the solution can be found in the form of a polynomial expansion (3.12). If the density at small and large distances is very different (different exponents) then the solution must be sought in a general form (3.2).

We will write in a clear form all formulas for the case when the four moments g_0, g_1, g_2, g_3 of the function $g(x)$ are known. The coefficients of the polynomial

$$h_2(s) = s^2 - as + b,$$

of the orthogonal with weight $f(s)$ to all polynomials of a lower power, i.e. to 1 and s, are equal to

$$a = \frac{f_3 f_0 - f_2 f_1}{f_2 f_0 - f_1^2}, \quad b = \frac{f_3 f_1 - f_2^2}{f_2 f_0 - f_1^2}. \tag{3.13}$$

The roots of equation $h_2(s) = 0$ are

$$s_1 = \frac{1}{2}[a - (a^2 - 4b)^{1/2}];$$
$$s_2 = \frac{1}{2}[a + (a^2 - 4b)^{1/2}]. \tag{3.14}$$

Hence

$$\eta_1 = \frac{1}{2s_1 - a}\int_0^\infty (s - s_2) f(s)\, ds = \frac{s_2 f_0 - f_1}{(a^2 - 4b)^{1/2}};$$
$$\eta_2 = f_0 - \eta_1. \tag{3.15}$$

We will use the obtained formulas to approximate the neutron density $\psi_0(x, u)$ using the moment $\psi_{0n}(u)$. If the angular distribution of the source $S(\mu)$ is symmetrical, then the neutron density $\psi_0(x, u)$ is an even function x. If $S(\mu)$ is antisymmetrical, then the function $\psi_0(x,u)$ is odd. It is therefore sufficient to approximate it only for positive values of x, i.e. for the range $0 \le x < \infty$; toward negative values of x the function $\psi_0(x, u)$ should be continued symmetrically or antisymmetrically. For an even value of $\psi_0(x)$ the function $K(x)$ should therefore be taken in the form

$$K^{\text{even}}(x) = e^{-x}, \tag{3.16}$$

and for an odd value, in the form

$$K^{\text{odd}}(x) = xe^{-x}. \tag{3.17}$$

For even functions from the system of integral equation (1.11), different-from-zero even moments are obtained, and for odd functions, odd moments are obtained. Therefore, in the range $(0,\infty)$ for the required function $\psi_0(x)$ we will only know whether the moments are even or uneven. So that the above-described method of approximation of (3.1) can be used in this case, the even and the odd functions must be sought in the form

$$\psi(x) = \sum_{i=1}^{N} (\eta_i/\sqrt{s_i})\, K^{\text{even}}(x/\sqrt{s_i}) = \sum_{i=1}^{N} (\eta_i/\sqrt{s_i})\, e^{-x/\sqrt{s_i}}, \quad \psi(x) \text{ even}; \tag{3.18}$$

$$\psi(x) \sum_{i=1}^{N} (\eta_i/s_i) K^{\text{odd}}(x/\sqrt{s_i}) = x \sum_{i=1}^{N} (\eta_i/s_i\sqrt{s_i})\, e^{-x/\sqrt{s_i}}, \quad \psi(x) \text{ odd}. \tag{3.19}$$

Then for η_i, s_i all the formulas derived above are valid if f_n is taken to mean $\psi_{2n}/K_{2n}^{\text{even}}$ and $\psi_{2n}/K_{2n+1}^{\text{odd}}$. The functions $M_{1n}(u)$ according to (1.10) were determined by the formula

$$M_{ln} = \frac{\beta^{n+1}}{n!} \int_{-\infty}^{\infty} x^n \psi_l(x, u)\, dx,$$

which in view of the symmetry (or antisymmetry) $\psi_l(x)$ can be rewritten in the form

$$M_{ln}(u) = 2\frac{\beta^{n+1}}{n!} \int_{0}^{\infty} x^n \psi_l(x, u)\, dx = \frac{2\beta^{n+1}}{n!} \psi_{ln}(u), \tag{3.20}$$

where ψ_{ln} represents the nth space moment of the function $\psi_l(x)$ in the range $(0,\infty)$. From (3.20)

$$\psi_{ln} = \frac{n!}{2\beta^{n+1}} M_{ln}. \tag{3.21}$$

According to (3.16) and (3.17) for $K_{2n}^{even} + K_{2n+1}^{odd}$ we have

$$K_{2n}^{even} = (2n)!; \tag{3.22}$$

$$K_{2n+1}^{odd} = (2n+2)! \tag{3.23}$$

Using (3.21)–(3.23), for moments f_n fron (3.4), determining the values s_i and η_i, we obtain

$$f_n = \frac{\psi_{0,2n}}{K_{2n}^{even}} = \frac{M_{0,2n}}{2\beta^{2n+1}}, \quad \psi_0(x) \text{ even}; \tag{3.24}$$

$$f_n = \frac{\psi_{0,2n+1}}{K_{2n+1}^{odd}} = \frac{M_{0,2n+1}}{4(n+1)\beta^{2n+2}}, \quad \psi_0(x) \text{ odd}. \tag{3.25}$$

We will write the corresponding formulas for the neutron density from a point isotropic source. According to (2.1) and (2.5) we have

$$M_{0,2n}^{pt} = (2n+1) M_{0,2n} = \frac{\beta^{2n+1}}{(2n)!} \int_{0}^{\infty} r^{2n} \varphi(r, u)\, dr = \frac{\beta^{2n+1}}{(2n)!} \varphi_{2n}(u)$$

or

$$\varphi_{2n} = \frac{(2n+1)!}{\beta^{2n+1}} M_{0,2n},$$

where

$$\varphi(r, u) = 4\pi r^2 \psi_0(r, u). \tag{3.26}$$

Hence, for moments f_n we obtain

$$f_n = \frac{\varphi_{2n}}{K_{2n}^{even}} = \frac{2n+1}{\beta^{2n+1}} M_{0,2n}, \tag{3.27}$$

and for the density $\psi_0(r, u)$

$$\varphi(r, u) \equiv 4\pi r^2 \psi_0(r, u) = \sum_{i=1}^{N} (\eta_i / \sqrt{s_i})\, e^{-r/\sqrt{s_i}}. \tag{3.28}$$

If the roots s_1 and s_2 are connected in a complex way then, for example, to approximate the even function $\psi_0(x)$ with respect to its four even moments we obtain, according to (3.18)

$$\psi_0(x) = 2Re\left[(\eta_i/\sqrt{s_i})\, e^{-x/\sqrt{s_1}}\right] = 2\left[A\cos\left(\frac{\sin\frac{w}{2}}{b^{1/4}} x\right) + B\sin\left(\frac{\sin\frac{w}{2}}{b^{1/4}} x\right) \exp\left(-\frac{\cos\frac{w}{2}}{b^{1/4}} x\right)\right., \tag{3.29}$$

where

$$\left.\begin{aligned} &\operatorname{tg} w = -\frac{\delta}{a}, \quad \delta = \sqrt{4b - a^2}\,; \\ &A = \frac{1}{b^{1/4}}\left(\frac{1}{2} f_0 \cos\frac{w}{2} - \gamma \sin\frac{w}{2}\right); \\ &B = \frac{1}{b^{1/4}}\left(\frac{1}{2} f_0 \sin\frac{w}{2} + \gamma \cos\frac{w}{2}\right); \\ &\gamma = \frac{1}{\delta}\left(\frac{1}{2} f_0 a - f_1\right). \end{aligned}\right\} \tag{3.30}$$

The values of a and b in (3.30) are given by formulas (3.13).

4. Neutron Density in Hydrogen and Water

Hydrogen. We will find the solution of the system of equations (1.11) for a plane isotropic source in hydrogen, assuming the free path length of the neutron to be constant (which is the case in the range of energies 10^4-1 ev), $\sigma(u) = \sigma_s(u) = \beta = 1$. We will introduce instead of $M_{ln}(u)$ the functions $N_{ln}(u) = e^u M_{ln}(u)$. According to (1.11) the functions $N_{ln}(u)$ are satisfied by the equations

$$N_{ln}(u) - \int_0^u P_l\left(e^{-\frac{u-u'}{2}}\right) N_{ln}(u')\,du' = \frac{1}{2l+1}\left[(l+1)\,N_{l+1,\,n-1} + lN_{l-1,\,n-1}\right] + \varkappa_{ln} P_l(e^{-u/2}); \tag{4.1}$$

$$N_{l,\,-1}(u) = 0.$$

To find four moments of neutron density it is necessary to solve the following ten integral equations of system (4.1):

1) $N_{00} - \int_0^u N_{00}\,du' = 1,$

2) $N_{11} - \int_0^u e^{-\frac{u-u'}{2}} N_{11}\,du' = \frac{1}{3} N_{00}(u) + \frac{1}{3} e^{-u/2};$

3) $N_{02} - \int_0^u N_{02}\,du' = N_{11}(u) + \frac{1}{3};$

4) $N_{22} - \frac{1}{2}\int_0^u [3e^{-(u-u')} - 1]\,N_{22}\,du' = \frac{2}{5} N_{11}(u) + \frac{1}{15}(3e^{-u} - 1);$

5) $N_{13} - \int_0^u e^{-\frac{u-u'}{2}} N_{13}\,du' = \frac{1}{3}(2N_{22} + N_{02}) + \frac{1}{5} e^{-u/2};$

6) $N_{04} - \int_0^u N_{04}\,du' = N_{13} + \frac{1}{5};$

7) $N_{33} - \frac{1}{2}\int_0^u e^{-\frac{u-u'}{2}} [5e^{-(u-u')} - 3]\,N_{33}\,du' = \frac{3}{7} N_{22} + \frac{1}{35} e^{-u/2}(5e^{-u} - 3);$

8) $N_{24} - \frac{1}{2}\int_0^u [3e^{-(u-u')} - 1]\,N_{24}\,du' = \frac{1}{5}(3N_{33} + 2N_{13}) + \frac{2}{35}(3e^{-u} - 1);$

9) $N_{15} - \int_0^u e^{-\frac{u-u'}{2}} N_{15}\,du' = \frac{1}{3}(2N_{24} + N_{04}) + \frac{1}{7} e^{-u/2};$

10) $N_{06} - \int_0^u N_{06}\,du' = N_{15} + \frac{1}{7}.$

By differentiation with respect to u all these equations become differential equations and are solved in an elementary way. In fact, from the first equation by differentiation with respect to u we obtain

$$N'_{00}(u) - N_{00}(u) = 0, \quad N_{00}(0) = 1.$$

Hence

$$N_{00}(u) = e^u. \tag{4.2}$$

From the second and third equations we find

$$N_{11}(u) = e^u - \frac{1}{3} e^{u/2}; \tag{4.3}$$

$$N_{02}(u) = \frac{2}{3} e^u + ue^u + \frac{1}{3} e^{u/2}. \tag{4.4}$$

We will consider the fourth equation:

$$N_{22}(u) - \frac{1}{2} \int_0^u [3e^{-(u-u')} - 1] N_{22}(u')\, du' = \frac{2}{5} N_{11}(u) + \frac{1}{15}(3e^{-u} - 1) \equiv q(u).$$

Differentiating twice with respect to u, we obtain

$$N''_{22} + \frac{1}{2} N_{22} = q'(u) + q''(u) = \frac{4}{5} e^u - \frac{1}{10} e^{u/2};$$

$$N_{22}(0) = q(0) = \frac{2}{5},$$

$$N'_{22}(0) = q(0) + q'(0) = \frac{8}{15}.$$

Hence

$$N_{22}(u) = \frac{8}{15} e^u - \frac{2}{15} e^{u/2} + \frac{\sqrt{2}}{15} \sin(u/\sqrt{2}). \tag{4.5}$$

Omitting such simple calculations, we will write the final solution for the moments $M_{0,2k}(u)$:

$$\left.\begin{aligned}
&M_{00}(u) = 1;\\
&M_{02}(u) = u + \frac{2}{3} + \frac{1}{3} e^{-u/2};\\
&M_{04}(u) = \frac{1}{2} u^2 + \frac{7}{5} u + \frac{47}{45} +\\
&+ \frac{68}{135}(1 - e^{-u/2}) - \frac{1}{45} e^{-u/2}(u+2) +\\
&+ \frac{8}{405}\left[1 - e^{-u}\left(\cos\frac{u}{\sqrt{2}} + \right.\right.\\
&\left.\left. + \sqrt{2}\sin\frac{u}{\sqrt{2}}\right)\right] +\\
&+ \frac{4}{405}\left[1 - e^{-u}\left(\cos\frac{u}{\sqrt{2}} - \right.\right.\\
&\left.\left. - \frac{1}{\sqrt{2}}\sin\frac{u}{\sqrt{2}}\right)\right];\\
&M_{06}(u)|_{u\gg 1} = -\frac{157}{45} u + \frac{31}{15} u^2 +\\
&+ \frac{1}{2}\left(\frac{u^3}{3} - 2u^2 + 8u\right).
\end{aligned}\right\} \tag{4.6}$$

In [1] for u = 10 the accurate space distribution of density $\psi_0(x)$ was found. We will calculate it for u = 10 from equations (4.6) and compare it with the Wick solution.

From formulas (4.6) we find

$$M_{00}(10) = 1, \qquad M_{04}(10) = 65{,}578,$$
$$M_{02}(10) = 10{,}667, \qquad M_{06}(10) = 278{,}44.$$

TABLE 1. Comparison of the Results for Determining Neutron Density by Different Methods

	βx								
	0	1	2	4	5	8	10	15	20
lg $\psi_0(x)$ from Eq. (4.7)	−1,140	−1,046	−1,065	−1,229	−1,346	−1,773	−2,102	−3,052	−4,254
lg $\psi_0(x)$ from Wick's solution	−1,046	−1,057	−1,089	−1,240	−1,340	−1,741	−2,100	−3,070	−4,250

The relationships (3.13) and (3.24) give

$$a = 8{,}7289, \quad b = 27{,}558, \quad 4b - a^2 = 34{,}038 > 0;$$

i.e. the roots s_1 and s_2 are connected in a complex way. According to (3.30)

$$\delta = 5{,}8342, \quad A = 0{,}03598, \quad \gamma = -0{,}54010, \quad w = -0{,}5892, \quad B = -0{,}25725.$$

Substituting the values in (3.29), we obtain the formula for the neutron density

$$\psi_0(x) = e^{-0{,}41725\beta x}[0{,}07196\cos(0{,}1267\beta x) + 0{,}51450\sin(0{,}1267\beta x)]. \tag{4.7}$$

In Table 1 the solution of (4.7) is compared with the Wick solution.

Water. The solution of the system of equations (1.11) for a plane isotropic source of neutrons with energy $E_0 = 2.5$ Mev in water was found numerically. Formulas (3.27) and (3.28) should be used to transfer to a point source.

In experiments carried out by I. S. Pogrevov (1957) the distribution of density was measured by a chamber from U^{235}, surrounded by a cadmium cover of thickness 0.5 mm. To obtain the distribution of the number of reactions R(r) in the chamber we find the moments of the function R(r). According to (2.5) we have

$$R_{2n}^{pt} = (2n+1)\,R_{2n}^{pl} = (2n+1)\int_0^{15{,}7} M_{0,2n}(u)\,\sigma_f^{235}(u)\,du. \tag{4.8}$$

Hence, according to (3.27) and (3.28)

$$f_n = \frac{2n+1}{\beta^{2n+1}} R_{2n}^{pl}$$

and

$$4\pi r^2 R(r) = (\eta_1/\sqrt{s_1})\,e^{-r/\sqrt{s_1}} + (\eta_2/\sqrt{s_2})\,e^{-r/\sqrt{s_2}}. \tag{4.9}$$

Here, R(r) is the number of reactions in the chamber, per one atom of U^{235} and one neutron of the source. We will introduce the designation

$$B(r) = e^{\beta r} 4\pi r^2 R(r), \tag{4.10}$$

where

$$\frac{1}{\beta} = \lambda(0) = 5 \text{ cm}.$$

In Table 2 the results of calculation using formulas (4.8)-(4.10) are compared with experimental data.

Unfortunately, due to the insufficient source strength the measurements could not be taken for distances r greater than 36 cm.

In conclusion the author would like to thank Yu. A. Romanov and L. P. Feoktistov for their valuable discussions, L. S. Bychenkova and M. N. Kopylova for performing the numerical calculations.

TABLE 2. A Comparison of Calculated and Experimental Results

	βr										
	1,72	2,22	2,72	3,22	4,22	5,22	6,22	7,22	10	15	20
$10^{24} B(r)$ from equation (4.10)	94,4	131	168	210	294	385	479	580	879	1485	2068
$10^{24} B(r)$, experimental data	79	120	166	198	307	423	517	611	—	—	—

LITERATURE CITED

1. G. Wick, Phys. Rev. 75, 738 (1949).
2. U. Fano. J. Res. Nat. Bur. Standards 51, 95 (1953).
3. L. Spencer. Phys. Rev. 88, 793 (1952).
4. L. Spencer, and U. Fano. J. Res. Nat. Bur. Standards 46, 446 (1951).
5. A. R. Ptitsyn, Atomnaya Energiya 9, 3, 216 (1960).*
6. H. Goldstein, and J. Wilkins. NYO-3075, Final Report. New York, 1954.

*Original Russian pagination. See C. B. translation.

THE CREATION OF A MAGNETIC FIELD WITH AN AZIMUTHAL VARIATION

R. A. Meshcherov and E. S. Mironov

Translated from Atomnaya Énergiya, Vol. 10, No. 2, pp. 127-130, February, 1961
Original article submitted June 22, 1960

A method is given for calculating the form of pole surfaces for creating a magnetic field with an azimuthal variation of given depth and with a certain law of change of the mean field intensity along the radius. Experiments are described on the modeling of a magnetic field of a 1½-meter cyclotron with azimuthal variation of the magnetic field.

Calculating the Shape of Pole Surfaces

To calculate the shape of poles from a given distribution of intensity of magnetic fields in the middle plane $H_z = F(r, \varphi)$ a method can be used which is based on the assumption that pole surfaces are magnetic equipotentials. As for axially symmetrical fields [1], the scalar magnetic potential in a cylindrical system of coordinates can be represented in the form of a series

$$P(r, \varphi, z) = \sum_{k=1}^{\infty} v_{2k-1}(r, \varphi)\, z^{2k-1}. \tag{1}$$

For the coefficients of these series the following recurrent relationship holds, obtained from the Laplace equation:

$$v_{2k+1} = -\frac{1}{2k(2k+1)}\left(\frac{\partial^2 v_{2k-1}}{\partial r^2} + \frac{1}{r}\frac{\partial v_{2k-1}}{\partial r} + \frac{1}{r^2}\frac{\partial^2 v_{2k-1}}{\partial \varphi^2}\right). \tag{2}$$

Obviously

$$v_1 = \frac{\partial P}{\partial z}\Big|_{z=0} = -H_z(r, \varphi). \tag{3}$$

Using formulas (1)-(3) it is possible to calculate the shape of pole surfaces for an arbitrary distribution $H_z(r, \varphi)$, which can be given both analytically and graphically. In particular, this method can calculate poles for creating a field $H_z = H_0(1 + Ar^2 + Br\cos n\varphi)$, first suggested by Thomas [2]. However, the poles of the magnet in this case have a very complex profile, and their preparation involves considerable technological difficulties.

The variation of the magnetic field can be achieved much more simply (by means of plane sector covers [3]).

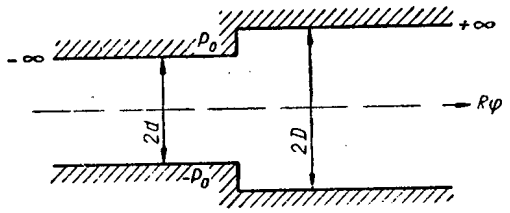

Fig. 1. Shape of plane-parallel poles used to calculate the distribution of magnetic field intensity.

There are no accurate methods for calculating the magnetic field of these poles. The problem was therefore solved on the assumption that the magnetic field intensity between the middle of the sector and the middle of the recess depends on φ the same as in the case of plane-parallel poles, the shape of which is shown in Fig. 1. This assumption obviously holds only under the condition

$$R\alpha \gg d\ ,\quad R\left(\frac{2\pi}{n} - \alpha\right) \gg d,$$

where R is the radius; α is the angle of the sector; n is the number of sectors.

Figure 2 gives regions on complex planes which are converted into one another by means of the formula

$$w = \frac{d}{\pi}\ln\frac{\sqrt{e^{\pi\frac{z}{d}} + \varkappa^2} - \varkappa\sqrt{e^{\pi\frac{z}{d}} + 1}}{\sqrt{e^{\pi\frac{z}{d}} + \varkappa^2} + \varkappa\sqrt{e^{\pi\frac{z}{d}} + 1}} - \frac{D}{\pi}\ln\frac{\sqrt{e^{\pi\frac{z}{d}} + 1} - \sqrt{e^{\pi\frac{z}{d}} + \varkappa^2}}{\sqrt{e^{\pi\frac{z}{d}} + 1} + \sqrt{e^{\pi\frac{z}{d}} + \varkappa^2}}, \tag{4}$$

where $\varkappa = d/D$.

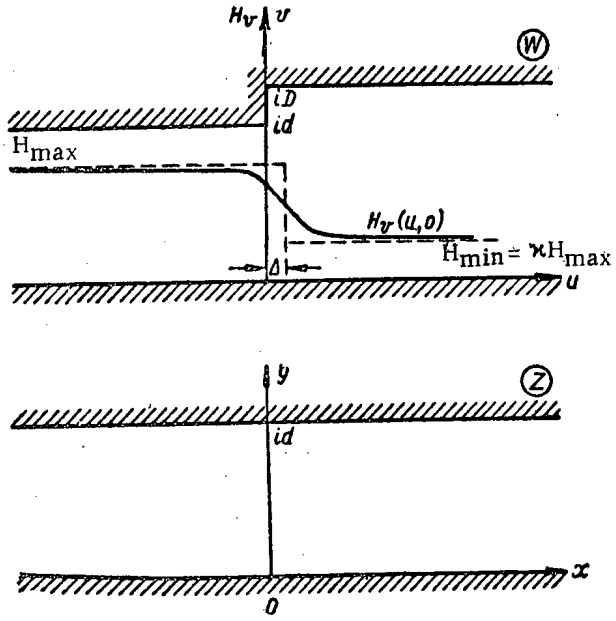

Fig. 2. Regions on complex planes w and z.

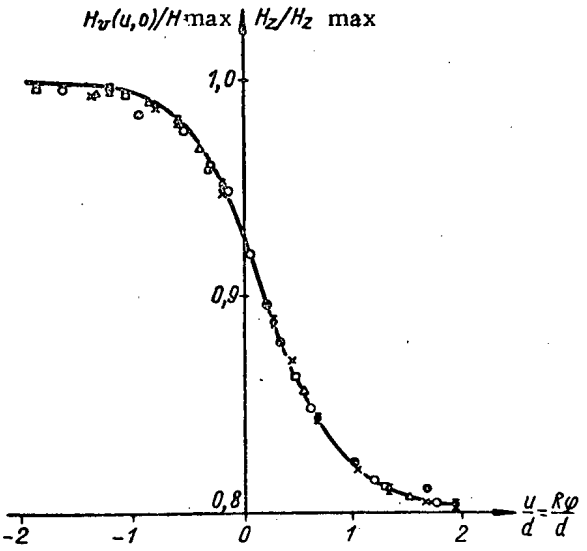

Fig. 3. A comparison of the calculated and experimental data. The continuous curve represents the calculated data; the points show the results of the measurements at different radii (in millimeters): ⊛—50; ×—70; □—90; △—110; ○—130; ◆—145.

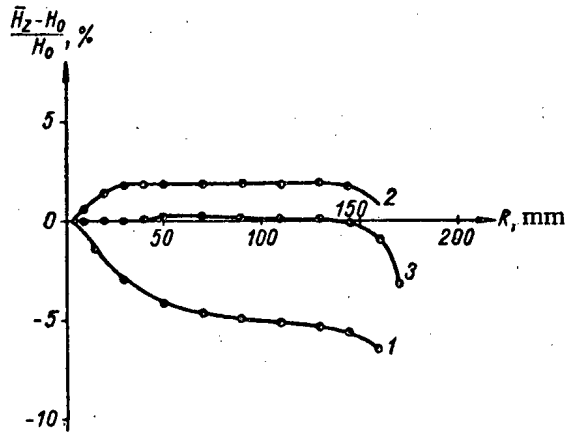

Fig. 4. Dependence of the magnetic field intensity, averaged with respect to φ, on the radius.

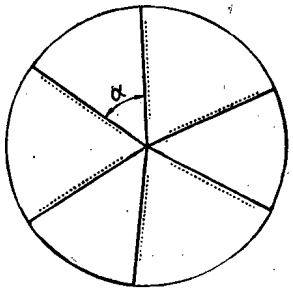

Fig. 5. Shape of sector covers and boundary of equivalent magnetic field (dotted lines).

From the theory of the complex potential it follows that the magnetic field between stepped poles (see Fig. 1) is equal to

$$H(w) = H_u + iH_v = -iH_{max}\varkappa \frac{\sqrt{e^{\pi\frac{z}{d}}+1}}{\sqrt{e^{\pi\frac{z}{d}}+\varkappa^2}}, \qquad (5)$$

where H_{max} is the field intensity on moving an infinite distance to the left.

Using formulas (4) and (5) a calculation was made of the distribution of intensity $H_v = f(u)$ in the middle plane between the stepped poles of infinite length. The results of the calculation are given in the form of a curve in Fig. 3.

In many cases, especially when studying the movement of ions in an idealized magnetic field of the sector type [4], $H_v = f(u)$ is best represented in the form of an equivalent stepped field (see Fig. 2). A characteristic value of this field is the parameter Δ—the difference in coordinates of the steps of the pole surface and the equivalent magnetic field:

$$\Delta = \frac{1}{H_{\max}(1-\varkappa)} \left\{ \int_{-\infty}^{\infty} H_z(u)\,du - \int_{-\infty}^{0} H_{\max}\,du - \int_{0}^{\infty} \varkappa H_{\max}\,du \right\} = \frac{d}{\pi(1-\varkappa)} \left[\frac{1+\varkappa^2}{\varkappa} \ln \frac{1+\varkappa}{1-\varkappa} - \ln \frac{16\varkappa^2}{(1-\varkappa^2)^2} \right]. \quad (6)$$

Preliminary Experiments

The experiments were carried out with an electromagnet with pole pieces of diameter 370 mm and 90 mm between them. Between the cylindrical poles there were two steel discs of diameter 370 mm and thickness 16 mm with sectors fastened to them at an angle of 52.5° and thickness 5 mm. The gap between the sectors was 40 mm, consequently d = 20 mm, D = 25 mm and $\varkappa = 0.8$. The measurements were carried out with a magnetic field intensity in the center $H_0 = 6000$ oe. The points of Fig. 3 show the values of the function $H_z(R,\varphi)/H_{z\,max}$ obtained from experimental data, H_{zmax} being the greatest of all values of magnetic field intensity near the middle of the sector. As should be expected, the best coincidence is observed at large distances from the center. At R = 50 mm the experimental data differ considerably from the calculated data.

In the range of radii 50 < R < 150 mm it can be assumed that

$$\varkappa = \frac{d}{D} \simeq \frac{H_{z\,r}}{H_{z\,sec}},$$

where $H_{z\,sec}$ and $H_{z\,r}$ are the values of the magnetic field intensity near the center of the sector and near the center of the recess respectively for R = const. Consequently, in this range the boundaries of the equivalent magnetic field created by the sector covers will be straight lines not passing through the origin of the coordinates. The magentic field intensity averaged with respect to φ therefore decreases smoothly with increase in R from 50 to 145 mm (curve 1 of Fig. 4). The boundaries of the equivalent magnetic field are shown in Fig. 5 by dotted lines and the boundaries of the sector coveres are shown by continuous or bold lines.

Using formula (6) it is possible to calculate the shape of the sector covers in the range of radii 50 < R < 145 mm for any relationship of $\overline{H}_z(R)$. For example, to create $\overline{H}_z(R) = \text{const}$ the sector covers were reduced parallel to their edges by 4 mm on each side since for 4 mm on each side since for $\varkappa = 0.8$ and d = 20 mm $\Delta \simeq 4$ mm. Measurements of the magnetic field with this shape of covers showed that in the range of radii 50 < R < 145 mm $\overline{H}_z(R) \simeq$ const (see curve 2 of Fig. 4). However, for small values of R, when the described method of calculation is unsuitable, the mean value of the field intensity, as before, differs considerably from $\overline{H}_z$ for large values of R. To even out the field the apexes of the sectors were cut off and discs of 40 mm diameter were placed in the center. The thickness of the discs, calculated from the condition $H_0 = \overline{H}_z$, equalled

$$\delta_0 = D - \frac{d}{\frac{n\alpha}{2\pi} + \frac{d}{D}\left(1 - \frac{n\alpha}{2\pi}\right)} = 2{,}5 \text{ mm}. \quad (7)$$

To make the field smooth a two-stage transition was made from the sectors to the central disc (the continuous bolder lines of Fig. 6).

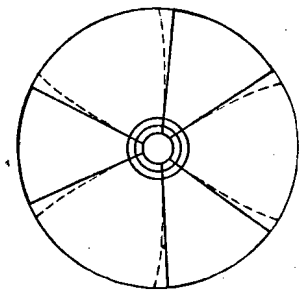

Fig. 6. Shape of covers providing a given relationship of $\overline{H}_z(R)$ radii O < R < 145 mm. For $\overline{H}_z(R) = \text{const}$ the boundaries of the sectors are shown by continuous bolder lines; for $\overline{H}_z(R)$ – a monotonously increasing function – the boundaries of the sectors are shown by broken lines.

Figure 4 (curve 3) shows the distribution of the mean value of magnetic field intensity obtained with this center. As can be seen from this diagram, $\overline{H}_z$ is constant with a good approximation.

The shape of the sectors was then changed so that (broken lines of Fig. 6) the mean value of the magnetic field intensity increased with increase in R. The increase in the mean value of the field intensity $\Delta\overline{H}_z = f(R)$ due to change in the shape of the sectors is shown in Fig. 7. The difference between the experimental and calculated data (~0.1%) is explained by the inaccuracy in preparing the sectors and errors in the measurements.

Modeling the Magnetic Field of a 1½-Meter Cyclotron

The magnetic field of a 1½-meter cyclotron was modeled on the mentioned electromagnet, the cylindrical pole pieces being replaced by tapered pieces of 300

mm diameter. Between the poles there were 300 mm diameter steel discs which served as a model of the covers in the accelerating chamber of the cyclotron. In order to create a magnetic field with a maximum depth of variation of approximately ± 15% (allowing for the design of the chamber) we chode d = 16 and D = 22 mm. Three sectors were fastened on each disc with an angle of 60° and thickness D-d to 6 mm. Based on a value Δ for x = 0.73, each sector was reduced parallel to its edges by 4.4 mm on each side. The apexes of the sectors were cut off and in the center there was a disc of 42 mm diameter and thickness 3.5 mm. The measurements were carried out at $H_0 = 14{,}500$ oe, therefore during the measurements the thickness of the central disc ($\delta_0 = 3.2$ mm) was made more accurate.

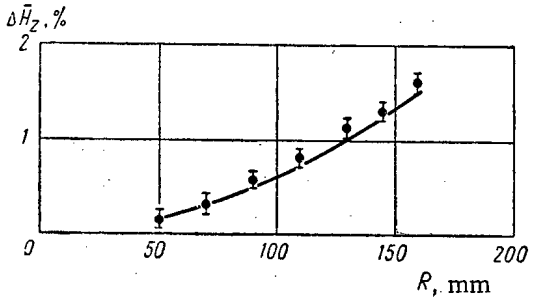

Fig. 7. Increase in mean value of field intensity $\Delta\bar{H}_z = f(R)$ due to a change in shape of sectors

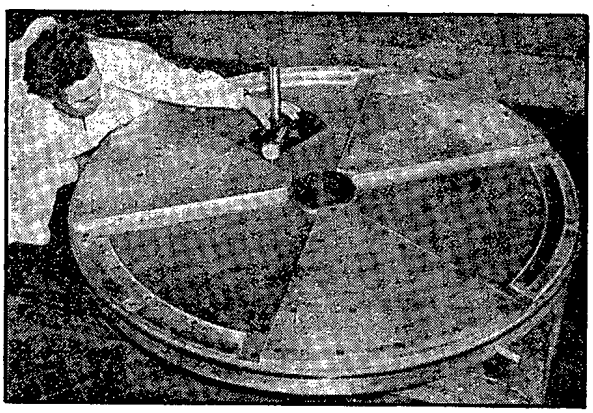

Fig. 8. View of lid of $1\frac{1}{2}$-meter cyclotron chamber.

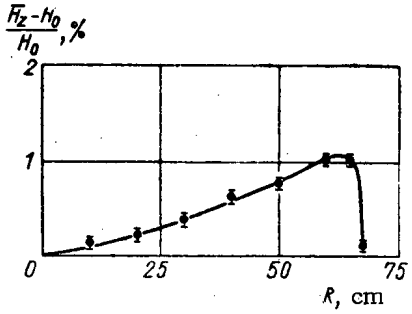

Fig. 9. The relationship $\bar{H}_z(R)$ for the $1\frac{1}{2}$-meter cyclotron ($H_0 = 14\,000$ oe).

At R> 110 mm there is a sharp drop in $\bar{H}_z(R)$, caused by edge effects; therefore to retain the necessary shape $\bar{H}_z(R)$ in the range of radii 110< R< 140 mm steel correcting elements were fitted.

Since the distribution of the mean value of the field intensity, obtained as a result of the measurements, was in good agreement with the expected distribution, from the modeling data lids were made for the chamber, sector covers and correcting elements for the $1\frac{1}{2}$-meter cyclotron. Figure 8 shows the lid of the $1\frac{1}{2}$-meter cyclotron chamber with azimuthal variation of the magnetic field. After final correction of the magnetic field, which was made by screws with an enlarged head, the required relationship of $\bar{H}_z(R)$ was obtained (Fig. 9). Measurements of the field intensity on the cyclotron magnet and on the model gave such close results that no adjustments were needed to the sectors, the central discs and the peripheral correcting elements.

LITERATURE CITED

1. A. Moussa and J. Lafoucriete. Compt. rend. 233, No. 2, 139 (1951).
2. L. Thomas. Phys. Rev. 54, 580 (1938).
3. R. A. Meshcherov et al., Atomnaya Énergiya 8, 3, 201, (1960).*
4. E. M. Moroz and M. S. Rabinovich, Pribory i Tekhnika Éksperimenta 1, 15, (1957).

*Original Russian pagination. See C. B. translation.

THE THERMOELASTIC STRESSES IN THE WALLS OF A REACTOR HOUSING WITH INTERNAL SOURCES OF HEAT IN NONSTATIONARY STATES

B. I. Maksimenko, K. N. Nikitin, and L. I. Bashkirov

Translated from Atomnaya Énergiya, Vol. 10, No. 2, pp. 131-137, February, 1961
Original article submitted February 18, 1960

In nonstationary processes, the thermoelastic stresses arising at various critical points and parts of a reactor, working over a wide range of change in heat load, can exceed the stresses arising under stationary conditions. Therefore, to ensure reliable operation with changing loads, the rate at which these processes takes place should be limited. The geometric form of a number of the critical points may be reduced to the two usual configurations of plane and cylindrical walls. By solving the nonstationary heat conduction problem for plane and cylindrical reactor walls with internal heat sources, comparative results have been obtained for the thermoelastic stresses arising in walls of this sort during transitional processes.

In order to calculate the thermoelastic stresses in the walls of a reactor operating under nonstationary conditions, it is necessary to solve the nonstationary heat conduction problem under the following conditions: 1) the internal heat sources are uniformly distributed throughout the material of the wall; 2) the coefficient of heat conduction of the material is independent of temperature; 3) the magnitude of the thermoelastic stress does not exceed the elastic limit of the material, and the form of the wall remains constant; 4) the temperature distribution is one-dimensional.

If there are internal heat sources, the maximum stresses, in the majority of cases, are found to be the tangential stresses at the surface of various parts. Therefore all the considerations which follow will be directed toward finding these stresses.

Plane Wall

The law governing the distribution of temperatures in a plane wall with internal heat sources (Fig. 1) is given by the well-known heat conduction equation [1]:

$$\frac{\partial t}{\partial \tau} = a \frac{\partial^2 t}{\partial y^2} + \frac{q_v}{c_p \gamma}. \tag{1}$$

We are solving this equation with the boundary conditions

$$\left.\frac{\partial t}{\partial y}\right|_{y=\pm\delta} = \pm h (t_\tau - t)$$

and the initial condition

$$t|_{\tau=0} = t_0.$$

Here $h = \alpha/\lambda$ is the ratio of the coefficients of heat production and thermal conductivity; $t_T = t_0 + c\tau$ (°C) is the temperature of the coolant; t_0 (°C) is the initial temperature of the medium surrounding the wall, and c is the rate of change of the coolant temperature.

We also assume that the temperature of the coolant varies linearly, while the strength of the internal heat sources remains constant with time (q_v = const). In this case the expression for the temperature at any point of the plane wall takes the form:

$$t = t_0 + c\tau - \frac{w\delta^2}{2a}\left(1 - \frac{y^2}{\delta^2} + \frac{2}{h\delta}\right) + \frac{w\delta^2}{a}\sum_{n=1}^{\infty} \frac{2\sin\beta_n \cos\left(\beta_n \frac{y}{\delta}\right)}{\beta_n^2 (\beta_n + \sin\beta_n \cos\beta_n)} \exp\left(-\beta_n \frac{a\tau}{\delta^2}\right). \tag{2}$$

With the same boundary conditions, but with the initial condition

$$t|_{\tau=0} = t_1 + \frac{q_0\delta^2}{2\lambda}\left(1 - \frac{y^2}{\delta^2} + \frac{2}{h\delta}\right),$$

which corresponds to a stationary working state of strength q_0 and at a coolant temperature

$$t_T = t_1 + c\tau, \text{ where } t_1 > t_0,$$

the solution of Eq. 1 will have the form

$$t = t_1 + c\tau - \frac{w\delta^2}{2a}\left(1 - \frac{y^2}{\delta^2} + \frac{2}{h\delta}\right) + \frac{\delta^2}{a}\left(w + \frac{q_0}{c_p\gamma}\right)\sum_{n=1}^{\infty} \frac{2\sin\beta_n \cos\left(\beta_n \frac{y}{\delta}\right)}{\beta_n^2(\beta_n + \sin\beta_n\cos\beta_n)} \exp\left(-\beta_n^2 \frac{a\tau}{\delta^2}\right), \quad (3)$$

where $w = c - (qv/c_p\gamma)$ is the rate of change of temperature at any point of the wall, in the stationary state, and in the presence of internal heat sources.

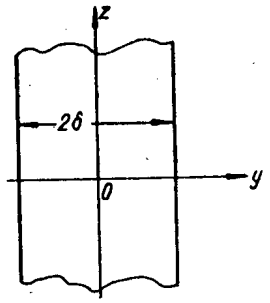

Fig. 1. Diagram of a plane wall with internal heat sources.

The tangential thermoelastic stresses on the surface of a plane wall, of infinite length and thickness 2δ, bathed by coolant on both sides, may be expressed by the equation

$$\sigma = \frac{\alpha_t E}{1-\mu}(t - \bar{t}). \quad (4)$$

The expression for the mean temperature of the wall will then have the following form:

1) for the initial condition $t|_{\tau=0} = t_0$

$$\bar{t} = t_0 + c\tau - \frac{w\delta^2}{2a}\left(\frac{2}{3} + \frac{2}{h\delta}\right) + \frac{w\delta^2}{a}\sum_{n=1}^{\infty} \frac{2\sin^2\beta_n}{\beta_n^3(\beta_n + \sin\beta_n\cos\beta_n)} \exp\left(-\beta_n^2 \frac{a\tau}{\delta^2}\right); \quad (5)$$

2) for the initial condition $t|_{\tau=0} = t_1 + \frac{q_0\delta^2}{2\lambda}\left(1 - \frac{y^2}{\delta^2} + \frac{2}{h\delta}\right)$

$$\bar{t} = t_1 + c\tau - \frac{w\delta^2}{2a}\left(\frac{2}{3} + \frac{2}{h\delta}\right) + \frac{\delta^2}{a}\left(w + \frac{q_0}{c_p\gamma}\right)\sum_{n=1}^{\infty} \frac{2\sin^2\beta_n}{\beta_n^3(\beta_n + \sin\beta_n\cos\beta_n)} \exp\left(-\beta_n^2 \frac{a\tau}{\delta^2}\right). \quad (6)$$

In these expressions, β_n is the nth root of the characteristic equation

$$\operatorname{ctg}\beta = \frac{\beta}{h\delta}.$$

Depending upon the initial conditions, the tangential stress will be equal to

1) $$\sigma = \frac{\alpha_t E}{1-\mu}\frac{w\delta^2}{a}\left[\frac{1}{2}\left(\frac{1}{3} - \frac{y^2}{\delta^2}\right) + (\bar{\Phi} - \Phi)\right]; \quad (7)$$

2) $$\sigma = \frac{\alpha_t E}{1-\mu}\left[\frac{w\delta^2}{2a}\left(\frac{1}{3} - \frac{y^2}{\delta^2}\right) + \frac{\delta^2}{a}\left(w + \frac{q_0}{c_p\gamma}\right)(\bar{\Phi} - \Phi)\right], \quad (8)$$

where

$$\bar{\Phi} = \sum_{n=1}^{\infty} \frac{2\sin^2\beta_n}{\beta_n^3(\beta_n + \sin\beta_n\cos\beta_n)} \exp\left(-\beta_n^2 \frac{a\tau}{\delta^2}\right); \quad (9)$$

$$\Phi = \sum_{n=1}^{\infty} \frac{2\sin\beta_n \cos\left(\beta_n \frac{y}{\delta}\right)}{\beta_n^2(\beta_n + \sin\beta_n\cos\beta_n)} \exp\left(-\beta_n^2 \frac{a\tau}{\delta^2}\right). \quad (10)$$

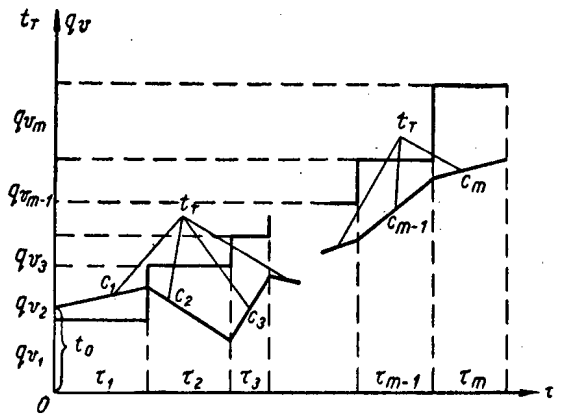

Fig. 2. Step-wise change in the coolant temperature, or in the strength of the internal heat sources.

It follows from Eqs. (7) and (8) that:

1) the thermoelastic stresses in the plane wall are directly proportional to the difference $w = c - (q_V/c_p\gamma)$ and the square of the half thickness of the wall, and are inversely proportional to the coefficient of thermal conductivity of the material;

2) the maximum absolute value of the stress occurs at the surface of the wall (at $y = \delta$);

3) with increasing time, the difference $(\bar{\Phi} - \Phi)$ decreases, and, accordingly, the absolute value of the stress at the surface increases.

For sufficiently long times, and in particular for $\tau \geq \geq [2 + (5/h\delta)](\delta^2/a)$, the difference $(\Phi - \Phi)$ becomes so small that it may be neglected. In this case, the so-called stationary state of the second kind supervenes, in which the maximum value of the tangential stresses, for either of the two initial conditions considered, is given by the formula

$$\sigma = \frac{\alpha_t E}{1-\mu} \frac{w\delta^2}{2a} \left(\frac{1}{3} - \frac{y^2}{\delta^2} \right). \tag{11}$$

This formula makes it possible to determine the thermoelastic stresses in a plane wall, with linear time variation of coolant temperature, and with internal heat sources of constant strength. However, for practical purposes, if the thermoelastic stresses are being investigaged in the transient state it is necessary to consider the change in coolant temperature under the condition that the strength of the internal sources changes too. This can be done, using the heat conduction equation (1), for a step-wise change in the coolant temperature, or in the strength of the internal heat sources (Fig. 2). Leaving out the intermediate steps, in a way similar to the solution of Eq. (1) for a plane wall with linear coolant temperature change and internal heat sources of constant strength, we can finally write for the case of step-wise heating or cooling.

$$t = t_0 + c\tau - \frac{w_m\delta^2}{2a}\left(1 - \frac{y^2}{\delta^2} + \frac{2}{h\delta}\right) + \frac{\delta^2}{a}\left[w_1\Phi_\tau + (w_2 - w_1)\Phi_{\tau-\tau_1} + \ldots + (w_m - w_{m-1})\Phi_{\tau - \sum_{i=1}^{m-1}\tau_i}\right], \tag{12}$$

where the value of Φ_τ is given by Eq. (10);

$$\Phi_{\tau-\tau_1} = \sum_{n=1}^{\infty} \frac{2\sin\beta_n \cos\left(\beta_n \frac{y}{\delta}\right)}{\beta_n^2(\beta_n + \sin\beta_n\cos\beta_n)} \exp\left[-\beta_n^2 \frac{a(\tau-\tau_1)}{\delta^2}\right];$$

$$\Phi_{\tau-\tau_1-\tau_2} = \sum_{n=1}^{\infty} \frac{2\sin\beta_n \cos\left(\beta_n \frac{y}{\delta}\right)}{\beta_n^2(\beta_n + \sin\beta_n\cos\beta_n} \exp\left[-\beta_n^2 \frac{a(\tau-\tau_1-\tau_2)}{\delta^2}\right] \text{ and so on.}$$

and m is the number of steps or intervals in the process.

The mean temperature across a section of the wall is given by the expression:

$$t = t_0 + c\tau - \frac{w_m\delta^2}{2a}\left(\frac{2}{3} + \frac{2}{h\delta}\right) + \frac{\delta^2}{a}\left[w_1\bar{\Phi}_\tau + (w_2 - w_1)\bar{\Phi}_{\tau-\tau_1} + \ldots + (w_m - w_{m-1})\bar{\Phi}_{\tau - \sum_{i=1}^{m-1}\tau_i}\right], \tag{13}$$

where the value of $\bar{\Phi}_\tau$ is given by Eq. (9), and

$$\bar{\Phi}_{\tau-\tau_1} = \sum_{n=1} \frac{2\sin^2\beta_n}{\beta_n^3(\beta_n + \sin\beta_n\cos\beta_n)} \exp\left[-\beta_n^2 \frac{a(\tau-\tau_1)}{\delta^2}\right];$$

$$\overline{\Phi}_{\tau-\tau_1-\tau_2}=\sum_{n=1}^{\infty}\frac{2\sin^2\beta_n}{\beta_n^2(\beta_n+\sin\beta_n\cos\beta_n)}\exp\left[-\beta_n^2\frac{a(\tau-\tau_1-\tau_2)}{\delta^2}\right]\text{ and so on.}$$

Substituting Eqs. (12) and (13) in Eq. (4), we obtain the expression for the thermoelastic stresses

$$\sigma_m=\frac{\alpha_l E}{1-\mu}\left\{\frac{w_m\delta^2}{2a}\left(\frac{1}{3}-\frac{y^2}{\delta^2}\right)+\frac{\delta^4}{a}\left[w_1(\overline{\Phi}_\tau-\Phi_\tau)+(w_2-w_1)(\overline{\Phi}_{\tau-\tau_1}-\Phi_{\tau-\tau_1})+\ldots\right.\right.$$
$$\left.\left.\ldots+(w_m-w_{m-1})(\overline{\Phi}_{\tau-\sum_{i=1}^{m-1}\tau_i}-\Phi_{\tau-\sum_{i=1}^{m-1}\tau_i})\right]\right\}. \qquad (14)$$

As in the preceding cases, for $\tau-\sum_{i=1}\tau_i\geqslant\left(2-\frac{5}{h\delta}\right)\frac{\delta^2}{a}$ all the differences $(\overline{\Phi}-\Phi)$ become so small with respect to the first term in the series that they can be neglected.

As a result, the stresses may be calculated from the expression

$$\sigma_m=\frac{\alpha_l E}{1-\mu}\frac{w_m\delta^2}{2a}\left(\frac{1}{3}-\frac{y^2}{\delta^2}\right), \qquad (15)$$

where, for the last step, $w_m=c_m-(q v_m/c_p\gamma)$.

Examination of Eq. (15) yields the following conclusion: on going over to each succeeding step, the stresses increase (or decrease) very rapidly, and at the end of the step, for sufficiently large values of τ_1, τ_2 etc. they remain constant with time.

From the general solution (14) it is not hard to find out how the maximum values of the stress vary at each step, for special cases involving various combinations of number of steps, change in strength of the internal sources, and rate of change of coolant temperature.

Cylindrical Wall

In cylindrical coordinates, the equation of heat conduction for a cylindrical wall of infinite length with internal heat sources takes the form:

$$\frac{\partial t}{\partial\tau}=a\left(\frac{\partial^2 t}{\partial r^2}+\frac{1}{r}\frac{\partial t}{\partial r}\right)+\frac{q_v}{c_p\gamma}. \qquad (16)$$

We shall solve Eq. (16) for two cases of heat removal.

Case I. Internal heat removal with linear variation in coolant temperature and insulated external surface (Fig. 3).

The boundary conditions are

$$\left.\frac{\partial t}{\partial r}\right|_{r=r_2}=0\ ,\quad \left.\frac{\partial t}{\partial r}\right|_{r=r_1}=-h(t_\tau-t);$$

the initial condition is

$$t|_{\tau=0}=t_0.$$

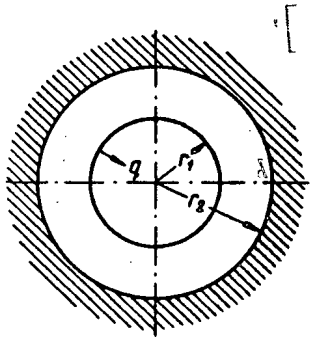

Fig. 3. Internal heat removal.

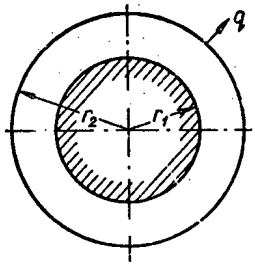

Fig. 4. External heat removal.

Here $t_T = t_0 + c\tau$. With these two sets of conditions, the solution of Eq. (16) takes the form:

$$t = t_0 + c\tau - \frac{wr_1^2}{4a}\left[1 + (k^2-1)\frac{2}{hr_1} - \varrho^2 + 2k^2 \ln \varrho\right] + \frac{wr_1^2}{a}\Phi\left(\frac{a\tau}{r_1^2};\ \varrho;\ hr_1;\ k\right), \tag{17}$$

where $k = r_2/r_1$; $\rho = r/r_1$, and r_2, r_1, and r are respectively the external and internal radii of the hollow cylinder and the variable radius of a point in between.

The mean temperature over the thickness of the wall is given by the expression:

$$\bar{t} = \frac{r^2 + r_1^2}{r^2(r_2^2 - r_1^2)}\int_{r_1}^{r_2} t r\, dr + \frac{1}{r^2}\int_{r_1}^{r} t r\, dr. \tag{18}$$

Substituting the values of the temperature from Eq. (17) into the above expression, we obtain:

$$\bar{t} = t_0 + c\tau - \frac{wr^2}{4a}\left[\frac{3}{4} - \frac{5}{4}k^2 - \frac{1}{4}\varrho^2 - \frac{1}{4}\frac{k^2}{\varrho^2} + \frac{k^4}{k^2-1}\left(1 + \frac{1}{\varrho^2}\right)\ln k + k^2 \ln \varrho + (k^2-1)\times\right.$$
$$\left.\times\frac{2}{hr_1}\right] + \frac{wr_1^2}{a}\bar{\Phi}\left(\frac{a\tau}{r_1^2};\ \varrho;\ k;\ hr_1\right). \tag{19}$$

Subtracting Eq. (17) from Eq. (19) finally gives the values of the temperature drops:

1) on the external surface of the cylinder ($r = r_2$ and $\rho = k$)

$$\Delta t^{\text{ext}} = \frac{wr_1^2}{4a}\left(\frac{1}{2}k^2 + \frac{1}{2} - \frac{2k^2}{k^2-1}\ln k\right) + \frac{wr_1^2}{a}(\bar{\Phi} - \Phi)^{\text{ext}}; \tag{20}$$

2) on the internal surface of the cylinder ($r = r_1$ and $\rho = 1$)

$$\Delta t^{\text{int}} = \frac{wr_1^2}{4a}\left(\frac{3}{2}k^2 - \frac{1}{2} - \frac{2k^4}{k^2-1}\ln k\right) + \frac{wr_1^2}{a}(\bar{\Phi} - \Phi)^{\text{int}}. \tag{21}$$

The thermoelastic stresses on the external and internal surfaces of the cylinder with internal heat transfer are equal respectively to:

$$\sigma_i^{\text{ext}} = \frac{\alpha_t E}{1-\mu}\frac{wr_1^2}{a}\left[\frac{1}{4}\left(\frac{1}{2}k^2 + \frac{1}{2} - \frac{2k^2}{k^2-1}\ln k\right) + (\bar{\Phi} - \Phi)^{\text{ext}}\right]; \tag{22}$$

$$\sigma_i^{\text{ext}} = \frac{\alpha_t E}{1-\mu}\frac{wr_1^2}{a}\left[\frac{1}{4}\left(\frac{3}{2}k^2 - \frac{1}{2} - \frac{2k^4}{k^2-1}\ln k\right) + (\bar{\Phi} - \Phi)^{\text{int}}\right]. \tag{23}$$

As in the case of the plane wall, the thermoelastic stresses produced by step-wise change in the strength of the internal sources, or coolant temperature may be represented in the form:

$$\sigma_m = \frac{\alpha_t E}{1-\mu}\frac{w_m r_1^2}{4a} f(k,\ \varrho) + \frac{\alpha_t E}{1-\mu}\frac{r_1^2}{a}\left[w_1(\bar{\Phi}_\tau - \Phi_\tau) + (w_2 - w_1)(\bar{\Phi}_{\tau-\tau_1} - \right.$$
$$\left. - \Phi_{\tau-\tau_1}) + \ldots + (w_m - w_{m-1})\left(\bar{\Phi}_{\tau - \sum_{i=1}^{m-1}\tau_i} - \Phi_{\tau - \sum_{i=1}^{m-1}\tau_i}\right)\right], \tag{24}$$

where m is the number of steps, or intervals, and

$$f(k,\ \varrho) = \frac{1}{4}(1-\varrho^2)\left(1 + \frac{k^2}{\varrho^2}\right) - \frac{k^4}{k^2-1}\left(1 + \frac{1}{\varrho^2}\right)\ln k + k^2 \ln \varrho + k^2 - \varrho^2.$$

Comparing Eq. (24) with Eq. (14), we can draw the following conclusions:

1) the changes in the thermoelastic stresses with multistep changes in the strength of the internal heat sources or coolant temperature occurring in the hollow cylinder are analogous to those which occur in the plane wall;

2) for sufficiently long time intervals, all the differences ($\bar{\Phi}$-Φ) become so small, that they do not have to be

taken into consideration, and then the maximum values of tangential stress on the external and internal surfaces at the end of each step are given by the equations:

$$\sigma_i^{ext} = \frac{\alpha_t E}{1-\mu}\frac{w_m r_1^2}{4a}\left(\frac{1}{2}k^2+\frac{1}{2}-\frac{2k^2}{k^2-1}\ln k\right); \quad (25)$$

$$\sigma_i^{int} = \frac{\alpha_t E}{1-\mu}\frac{w_m r_1^2}{4a}\left(\frac{3}{2}k^2-\frac{1}{2}-\frac{2k^4}{k^2-1}\ln k\right). \quad (26)$$

Case II. External heat removal with linear variation in coolant temperature and insulated internal surface (Fig. 4).

The boundary conditions are:

$$\left.\frac{\partial t}{\partial r}\right|_{r=r_1} = 0\,, \quad \left.\frac{\partial t}{\partial r}\right|_{r=r_2} = h(t_T - t);$$

the initial condition is:

$$t|_{\tau=0} = t_0.$$

Omitting the intermediate steps, we shall write the final equations for the thermoelastic stresses:

1) on the external surface of the cylinder

$$\sigma_e^{ext} = \frac{\alpha_t E}{1-\mu}\frac{wr_1^2}{a}\left[\frac{3}{8}-\frac{1}{8}k^2-\frac{1}{2}\frac{\ln k}{k^2-1}+(\overline{\Phi}-\Phi)^{ext}\right]; \quad (27)$$

2) on the internal surface of the cylinder

$$\sigma_e^{int} = \frac{\alpha_t E}{1-\mu}\frac{wr_1^2}{a}\left[\frac{1}{8}(k^2+1)-\frac{k^2\ln k}{2(k^2-1)}+(\overline{\Phi}-\Phi)^{int}\right]. \quad (28)$$

Experimental studies on the heating of a hollow cylinder, carried out in the Heating Laboratory of the Scientific-Investigational Tube Institute [2], have shown that a hollow cylinder can be considered as a rolled-up sheet of suitable wall thickness. This simplifies the calculation of the distribution of temperature and thermal stress in a hollow cylinder.

From Eqs. (22) amd (23) for internal heat removal, and Eqs. (27) and (28) for external heat removal, the maximum temperature drops entering into the expression for the thermoelastic stresses (4) are equal to:

$\Delta t_i^{ext} = m_1\frac{wr_1^2}{a}$, here $m_1 = \frac{1}{4}\left(\frac{1}{2}k^2+\frac{1}{2}-\frac{2k^2}{k^2-1}\ln k\right)$;

$\Delta t_i^{int} = m_2\frac{wr_1^2}{a}$, here $m_2 = \frac{1}{4}\left(\frac{3}{2}k^2-\frac{1}{2}-\frac{2k^4}{k^2-1}\ln k\right)$;

$\Delta t_e^{ext} = m_3\frac{wr_1^2}{a}$, here $m_3 = \frac{3}{8}-\frac{1}{8}k^2-\frac{1}{2(k^2-1)}\ln k$;

$\Delta t_e^{int} = m_4\frac{wr_1^2}{a}$, here $m_4 = \frac{1}{8}(k^2+1)-\frac{k^2}{2(k^2-1)}\ln k$.

If we consider the hollow cylinder as a rolled-up sheet with wall thickness

$$\delta = r_2 - r_1 = r_1(k-1),$$

then, as follows from the solution (15), the maximum temperature drops entering into the expression for the thermoelastic stresses (4) are equal to:

1) on the surface bathed by coolant

$$\Delta t_1 = n_1\frac{wr_1^2}{a}, \text{ here } n_1 = \frac{1}{3}(k-1)^2;$$

2) on the insulated surface

$$\Delta t_2 = n_2 \frac{wr_1^2}{a}, \text{ here } n_2 = \frac{1}{6}(k-1)^2.$$

The quantities m and n may be given the name "form coefficients." Comparing the expressions for the temperature differences in a hollow cylinder and a sheet, the conclusion can be drawn, that if the hollow cylinder is replaced by a rolled-up sheet, the thickness of the latter should be taken for calculational purposes to be

$$\delta_1 = \delta \sqrt{\frac{m}{n}}. \tag{29}$$

The values of the form coefficients m and n, and the ratio m/n, for different values of $k = r_2/r_1$, are given in the table.

Values of the Form Coefficients and Their Ratios

$m, n, \frac{m}{n}$	Values of $k = r_2/r_1$					
	1,1	1,15	1,2	1,25	1,3	1,5
m_1	0,0016832	0,0037355	0,00667	0,0104	0,01495	0,04171
$-m_2$	0,003476	0,008061	0,01461	0,0231	0,03373	0,1015
$-m_3$	0,003165	0,007013	0,01218	0,018662	0,026365	0,0684
m_4	0,001683	0,003735	0,00667	0,0104	0,01495	0,04171
$-n_1$	0,00333	0,00751	0,01333	0,0208	0,03	0,0833
$-n_2$	0,00167	0,00376	0,00666	0,0104	0,015	0,0416
$\frac{m_1}{n_2}$	~1,0	~1,0	~1,0	~1,0	~1,0	~1,0
$\frac{m_2}{n_1}$	1,041	1,075	1,095	1,11	1,123	1,218
$\frac{m_3}{n_1}$	0,952	0,934	0,914	0,897	0,877	0,822
$\frac{m_4}{n_2}$	~1,0	~1,0	~1,0	~1,0	~1,0	~1,0

CONCLUSIONS

1. The equations derived for thermoelastic stresses can be used for making calculations on heat generating elements, the reactor housing, and other points of interest during transitional states, as well as on starting and cooling off the reactor.

2. The thermoelastic stresses at the insulated surface of a hollow cylinder, within the practical range of ratios of radii (up to $\approx k \leq 1.5$), may be calculated from the formulas for a plane wall.

3. The thermoelastic stresses at the surface of a cylinder, bathed by a coolant, may also be calculated from the formulas for a plane sheet, but with the addition of a calculational wall thickness, given by Eq. (29).

LITERATURE CITED

1. A. V. Lykov, Theory of Heat Conduction. [in Russian], Moscow, Gostekhteorizdat (1952).
2. N. Yu. Taits, Technology of Steel Heating [in Russian], Moscow, Metallurgizdat (1950).

THE REACTION BETWEEN SOLID UO_2 AND MnO_2 IN A SULFURIC ACID SOLUTION

E. A. Kanevskii and V. A. Pchelkin

Translated from Atomnaya Énergiya, Vol. 10, No. 2, pp. 138-142, February, 1961
Original article submitted July 5, 1960

In connection with the extensive use of pyrolusite in the sulfuric acid leaching of uranium from ores, a study was made of the reaction between UO_2 and MnO_2 in a sulfuric acid solution, and possible mechanisms were discussed. The experimental data show that the reaction apparently occurs at the points of contact of the hydrated surface layers of UO_2 and MnO_2; the rate of the process is limited by steric hindrances. On this basis the role of iron ions was also considered in the reaction between a solid oxidizing agent (pyrolusite) and primary minerals of uranium in the acid leaching of uranium-containing ores.

The nature of the reaction between solid UO_2 and MnO_2 in sulfuric acid solution is of considerable interest. It is known that at the present time pyrolusite is used extensively in the sulfuric acid leaching of uranium from ores [1-3] and it undoubtedly plays the part of an oxidizing agent. Processes occurring in the ore pulp containing a solid phase of complex composition (ore) a second solid phase (pyrolusite) and a number of ions and compounds in the liquid phase are very complex. For this reason the first stage in the investigation should be the comparatively simpler process—reaction between UO_2 and MnO_2 in sulfuric acid solution. As yet this reaction has not been specially investigated, although there are some apparently correct ideas on the leaching of uranium from ores using MnO_2 (pyrolusite) in papers dealing with the technology of uranium leaching (for example see [3,4]).

Starting Materials and Experimental Method

Uranium dioxide was obtained from the mixed oxides which had first been subjected to peroxide purification by reducing with hydrogen at 900°C. The content of tetravalent uranium in the mixed oxide was 98% with respect to the sum of the tetravalent and hexavalent uranium. The MnO_2 used in the work was of the "pure" grade and was not subjected to further purification. The sulfuric acid was "chemically pure". The concentration of manganese in the solution after the completion of the process was determined colorimetrically [5]. The method for analyzing uranium was described in [6].

Possible Mechanisms

As far as we know, there are no references in the literature to the stoichiometry of the reaction between UO_2 and MnO_2, but this reaction is usually written in the form of the following equations:

$$UO_2 + MnO_2 + 2H_2SO_4 \rightarrow UO_2SO_4 + MnSO_4 + 2H_2O$$

or

$$UO_2 + MnO_2 + 4H^+ \rightarrow UO_2^{2+} + Mn^{2+} + 2H_2O.$$

Our experimental check of the correctness of this equation confirmed that the ratio of the number of UO_2 moles to the number of MnO_2 moles taking part in the reaction is equal to unity. For this reason in later work when considering possible mechanisms we used this equation.

It might be assumed that in an acid medium at first one of the oxides is dissolved and then there is a heterogeneous oxidation-reduction process. In this case the reaction of UO_2 and MnO_2 in acid medium is expressed by one of the following schemes:

$$\text{(I)}\quad \begin{cases} UO_{2(s)} + 4H^+_{(aq)} \rightarrow U^{4+}_{(aq)} + 2H_2O_{(l)}; & \text{(a)} \\ U^{4+}_{(aq)} + MnO_{2(T)} \rightarrow UO^{2+}_{2(aq)} + Mn^{2+}_{(aq)} & \text{(b)} \end{cases}$$

$$UO_{2(s)} + MnO_{2(s)} + 4H^+_{(aq)} \rightarrow UO^{2+}_{2(aq)} + Mn^{2+}_{(aq)} + 2H_2O_{(l)}$$

$$\text{(II)}\quad \begin{cases} MnO_{2(s)} + 4H^+_{(aq)} \rightarrow Mn^{4+}_{(aq)} + 2H_2O_{(l)}; & \text{(a)} \\ Mn^{4+}_{(aq)} + UO_{2(s)} \rightarrow Mn^{2+}_{(aq)} + UO^{2+}_{2(aq)}. & \text{(b)} \end{cases}$$

It can also be asumed that at first there is solution of UO_2 and MnO_2 and then homogeneous reaction of the tetravalent and hexavalent uranium in the solution:

$$(III)\begin{cases} UO_{2(s)} + 4H^+_{(aq)} \rightarrow U^{4+}_{(aq)} + 2H_2O_{(l)}; & (a) \\ MnO_{2(s)} + 4H^+_{(aq)} \rightarrow Mn^{4+}_{(aq)} + 2H_2O_{(l)}; & (b) \\ U^{4+}_{(aq)} + Mn^{4+}_{(aq)} + 2H_2O_{(l)} \rightarrow UO^{2+}_{2(aq)} + Mn^{2+}_{(aq)} + 4H^+_{(aq)}. & (c) \end{cases}$$

It should be emphasized that in the suggested schemes the separate stages are not shown, but only the successive reactions. The possibility is not ruled out therefore that, for example, one of the stages of the reaction (II, b) or (III, c) is the formation of trivalent manganese. However, this problem will not be discussed here.

A common feature of the schemes (I) and (II) is the fact that in not one of the successive reactions do the UO_2 and MnO_2 take part simultaneously. Because of this the rate of the total process should be in a linear relationship to the size of the UO_2 surface, if the (I, a) reaction is limiting. The size of the MnO_2 surface should not have any effect on the rate of the process. On the other hand, if reaction (II, a) limits the process, then its rate should be in a linear relationship only to the size of the MnO_2 surface.

To check the correctness of these conclusions a determination was made of the dependence of the rate of reaction for a constant amount of UO_2 on the excess of MnO_2 with respect to the stoichiometric calculation (figure, MnO_2/UO_2) and then the dependence of the rate of the process on the excess of UO_2 (see figure, UO_2/MnO_2)*. An appropriate correction was introduced because the "pure" grade of manganese dioxide contains MnO impurity.

However, the experimental data (see figure) show that the rate of the processes is affected by the size of both the UO_2 and MnO_2 surfaces. It should also be emphasized that the dependence of the rate of the process on the size of the UO_2 or MnO_2 surfaces is not linear. A similar shape of the curve presumably indicates that the UO_2 and MnO_2 play the same part in the reaction, i.e. they take part simultaneously in it.

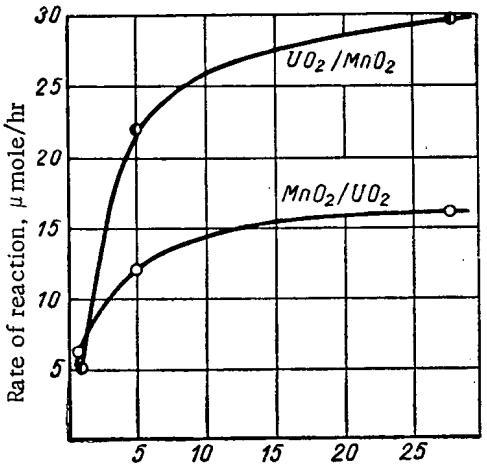

Rate of solution of UO_2 and MnO_2.

This proves that in the schemes considered above, not one of the stages can be considered limiting in any case. Furthermore, in the light of obtained experimental data the possibility cannot be excluded that the process could take place according to the following scheme, assuming "solid phase" reaction of the oxides:

$$(IV)\begin{cases} UO_{2(s)} + MnO_{2(s)} \rightarrow UO_{3(s)} + MnO_{(s)}; & (a) \\ UO_{3(s)} + 2H^+_{(aq)} \rightarrow UO^{2+}_{2(aq)} + H_2O_{(l)}; & (b) \\ MnO_{(s)} + 2H^+_{(aq)} \rightarrow Mn^{2+}_{(aq)} + H_2O_{(l)}. & (c) \end{cases}$$

The extensive use of MnO_2 to oxidize a number of substances in neutral organic oxidizing agents at room temperature [7] apparently supports this assumption.

It is obvious that in aqueous solutions the reaction between UO_2 and MnO_2, i.e., stage (IV, a), is not a solid phase, reaction in the sense in which it is understood in [8-10]. In a number of other papers it is assumed that the so-called solid phase reactions in most cases proceed with the decisive participation of gases or liquids or the same and others simultaneously [11]. When considering stage (IV, a) it should be remembered that MnO_2 in aqueous solution is undoubtedly hydrated [7], and on the surface of UO_2 in acid solutions a hydroxide forms [12]. Consequently, the solid phase process, shown schematically in the form of equation (IV, a), in practice is much more complex. It is important that according to this scheme for the reaction between UO_2 and MnO_2 in acid solution, not containing foreign ions, it is essential to have contact between the solid phases.

It is well known that UO_3 and MnO_2 in acid solutions dissolve rapidly; therefore all kinetic features of the total reaction, if the scheme (IV) is correct, are bound up with the reaction of UO_2 and MnO_2; more accurately with processes occurring at the points of contact of the hydrated layers of these components.

The observed dependence of the rate of the process on the size of the surface of UO_2 or MnO_2 will not be under-

* The method for determining the rate of reaction was described in detail by the authors in an article submitted to the journal "Neorganicheskaya Khimiya."

standable if the reaction proceeded according to schemes (I), (II) or (III) on the whole surface of UO_2 and MnO_2, since the rate of solution of solids in liquids is in a linear relationship to the size of the solid phase surface (for example see [13,14]). If the reaction occurs not on the whole surface of the UO_2 and MnO_2 particles, but only in a layer formed at the point of contact, it is obvious that the dependence of the rate of the process on the size of the surface of the reacting components should not be linear.

If the rate of the process is limited by the reaction (IV, a) then it should be expected that the concentration of hydrogen ions, not taking direct part in this stage of the process, should not affect the degree of reaction of UO_2 and MnO_2 in acid medium over a fixed length of time of the experiment. For a comparatively wide region of change in concentrations of sulfuric acid with an equimolar ratio of UO_2 and MnO_2 and 100 ml solution, this is confirmed by experimental data. The absence of an effect of sulfuric acid concentration on the degree of reaction of UO_2 and MnO_2 is difficult to reconcile with schemes (I), (II) or (III), since each of them includes the reaction of solution of oxides with the participation of hydrogen ions, these reactions depending to a large extent on the concentration of hydrogen ions [15,16].

The given experimental data agree most completely with scheme (IV). However, on their basis the possibility cannotbe excluded of the process occurring according to other schemes if the rate of the process can be effected in the same way by UO_2 and MnO_2 and the hydrogen ion concentration has no effect.

Some Features of the Process

We will consider at first the effect of preliminary grinding of UO_2 and MnO_2. Samples of UO_2 (1.0 g) and MnO_2 (0.37 g) were ground for an hour in a mechanical SMB mortar. After this for 4 hr at 20°C in 50 ml of 0.5 N H_2SO_4, oxides were dissolved, separately or ground together, and, in parallel, oxides were dissolved which had not been subjected to additional grinding. The grain size of the initial UO_2 and MnO_2 was 0.074 mm, their degree of reaction was determined from the concentration of uranium in the solution after the end of the experiment. The data on the reaction of UO_2 and MnO_2 are as follows:

Conditions for preparing specimens	Degree of reaction, %
UO_2 (initial)	0.3
$UO_2 + MnO_2$ (initial)	12
$UO_2 + MnO_2$ (ground separately)	45
$UO_2 + MnO_2$ (ground together)	83

These data show that the grinding of UO_2 and MnO_2 especially when they are ground together, has a very favorable effect on the reaction of these substances in sulfuric acid solution, which confirms the correctness of scheme (IV). However, an x-ray study showed that the solid-phase reaction during the grinding of dry oxide for several hours only occurs to a very small extent—less than 0.1%. Consequently, the role of grinding is mainly to facilitate the formation of pairs of UO_2 and MnO_2 particles in close contact.

Other assumptions can also be put forward for the mechanism of reaction of UO_2 and MnO_2 in sulfuric acid medium. For example, we will asume that the reaction occurs at the moment of fast impact of free particles of these dioxides and then these particles diverge. In this case the completeness of the reaction should depend on the number of impacts of particles and, consequently, should increase with decrease in the ratio S:L. The effect of this factor should therefore be studied.

Experiments were carried out at room temperature in glass test tubes fastened on a disc rotating at a speed of 60 rpm. The weight of UO_2 was 0.5 g, that of MnO_2 was 0.185 g. The oxides were ground together for an hour in a mortar. The H_2SO_4 concentration was 5 N, time of the experiments, 30 min. When calculating the ratio S:L the weight of the solid was taken as the total weight of UO_2 and MnO_2. The degree of reaction of UO_2 and MnO_2 in sulfuric acid solution in this case was determined by the concentration of uranium. The following data were obtained for the effect of the ratio S:L on the reaction of UO_2 and MnO_2:

S:L	Degree of reaction
1:1	22.6
1:2	21.0
1:3	21.5
1:4	21.5
1:5	23.8
1:10	21.2
1:15	21.2
1:20	21.0

The lack of dependence of the degree of reaction of components on the ratio S:L indicates that the reaction between UO_2 and MnO_2 in sulfuric acid solutions occurs not as a result of rapid reaction of the particles in brief contact with one another but probably occurs in the boundary layer which is strongly hydrated, forming at points of close and constant contact of UO_2 and MnO_2 particles.

The relative strength of these pairs of particles is also confirmed by results of experiments in which a study was made of the effect of the intensity of mixing. On changing the speed of the four-blade mixer from 50 to 500 rpm the degree of reaction of UO_2 and MnO_2 in 1 N or 5 N H_2SO_4 remains practically unchanged both in the stoichiometric ratio of these oxides and with a large excess of MnO_2.

From the combination of all experimental data it can therefore be assumed that the reaction of UO_2 and MnO_2 in sulfuric acid solution proceeds according to the scheme (IV) in the absence of foreign ions. At first there is reaction in the surface hydrated layers of the UO_2 and MnO_2 particles in close contact; then the reaction products are rapidly dissolved, reaction again occurs on the fresh surface of the particles, etc. However, it must not be assumed that the process cannot occur according to schemes (I), (II) or (III) if at separate stages of successive reactions, unstable, rapidly decomposed substances are formed. In this case, as when the process occurs according to scheme (IV) if there is not sufficient contact between the reacting substances the rate of the process is limited by steric hindrances.

The experimental data obtained in the present work throw more light on the role of iron ions during the sulfuric acid leaching of uranium from ores using pyrolusite. The assumption that iron is a direct oxidant and the process occurs according to the scheme

$$(V)\quad \begin{cases} UO_{2(s)} + 2Fe^{3+}_{(aq)} \rightarrow UO^{2+}_{2(aq)} + 2Fe^{2+}_{(aq)}; & (a) \\ 2Fe^{2+}_{(aq)} + MnO_{2(s)} + 4H^{+}_{(aq)} \rightarrow 2Fe^{3+}_{(aq)} + Mn^{2+}_{(aq)} + 2H_2O_{(l)} & (b) \end{cases}$$

at first glance is in contradiction to the higher oxidation-reduction potential of Mn^{2+}/MnO_2 compared with Fe^{2+}/Fe^{3+}:

$$Fe^{2+}_{(aq)} \rightleftarrows Fe^{3+}_{(aq)} + e^- \quad (E^0 = 0{,}77\text{v});$$

$$Mn^{2+}_{(aq)} + 2H_2O_{(l)} \rightleftarrows MnO_{2(s)} + 4H^{+}_{(aq)} + 2e^- \quad (E^0 = 1{,}22\text{v}).$$

Further, if we consider the necessity for contact between the two solid phases for oxidation of UO_2 by means of MnO_2 in pure solution and the absence of necessity for such contact in the presence of iron ions in the solution, then it becomes understandable why the sulfuric acid leaching of primary uranium mineral from ores, which almost always contain iron, occurs according to scheme (V).

SUMMARY

1. A study has been made of the effect of the intensity of mixing, the ratio UO_2:MnO_2, the H_2SO_4 concentration preliminary grinding of oxides and other factors on the reaction between UO_2 and MnO_2 in sulfuric acid solution.

2. On the basis of the obtained experimental data, possible schemes have been discussed.

3. It has been found that the occurrence of this reaction in which two solid phases take part is effected to a large extent by steric factors. In connection with this the problem was considered of the occurrence of the process with the presence in the solution of Fe^{2+} and Fe^{3+} ions, eliminating these steric hindrances.

In conclusion we would like to thank V. G. Romanova for taking part in the work and L. V. Zverev for his useful comments.

LITERATURE CITED

1. B. V. Nevskii, Atomnaya Énergiya 6, 1, 5 (1959).*
2. G. E. Kaplan, B. V. Nevskii, and B. N. Laskorin, Atomnaya Énergiya 6, 2, 113 (1959).*
3. J. Clegg and D. Foley, Uranium Ore Processing. Addison–Wesley Publ. Co., Reading, 1958.
4. A. Godin, Reports of the International Conference on the Peaceful Use of Atomic Energy (Geneva, 1955), Vol. 8, [in Russian] (Moscow, Metallurgy Press, 1958), p. 17.

*Original Russian pagination. See C. B. translation.

5. A. I. Ponomarev, Methods for the Chemical Analysis of Minerals and Rocks. Vol. 1, [in Russian] (Moscow, Acad. Sci. USSR Press, 1951), p. 158.
6. P. N. Paley, Reports of the International Conference on the Peaceful Use of Atomic Energy (Geneva, 1955), Vol. 8 [in Russian] (Moscow, Metallurgy Press, 1958), p. 268, 271.
7. R. Evans. Quart. Revs, 13, No. 1, 61 (1959).
8. W. Jost. Diffusion und chemische Reaktion in festen Stoffe, 1937.
9. J. Hedvall. Reaktionsfähigkeit der festen Stoffe, 1938.
10. J. Hedvall, and H. Jagitsch. Z. anorgan. und allgem. Chem. 262, 49 (1950).
11. A. M. Ginstling, Studies of the Mechanism and Kinetics of Reactions in Mixtures of Solids. Thesis [in Russian] (Leningrad, 1952).
12. J. MacKay and M. Wadsworth. Trans. ASME 212, 597 (1958).
13. D. A. Frank-Kamenetskii, Diffusion and Heat Transfer in Chemical Kinetics [in Russian] (Moscow Acad. Sci. USSR Press, 1947).
14. A. B. Zdanovskii, The Kinetics of Solution of Natural Salts under Conditions of Forced Convection [in Russian] (Leningrad State Chemistry Press, 1956).
15. E. Ya. Rode, Oxygen Compounds of Manganese [in Russian] (Moscow, Acad. Sci. USSR Press, 1952) p. 131.
16. V. I. Spitsyn, G. M. Nesmeyanova,and E. A. Kanevskii, Zhur. Neorg. Khim. 5, 9, 1938 (1960).

A STUDY OF THE PROPERTIES OF URANIUM HEXAFLUORIDE IN ORGANIC SOLVENTS

N. P. Galkin, B. N. Sudarikov, V. A. Zaitsev,

D. A. Vlasov, and V. G. Kosarev

Translated from Atomnaya Énergiya, Vol. 10, No. 2, pp. 143-148, February, 1961
Original article submitted April 14, 1960

Studies have been made of the solubility and kinetics of solution of uranium hexafluoride in carbon tetrachloride, chloroform, dichloromethane, asymmetrical dichloroethane, symmetrical tetrachloroethane, pentachloroethane, trifluorotrichloroethane, symmetrical trichloropropane, and tetrachloropropane. It has been shown that solutions of uranium hexafluoride in carbon tetrachloride, tetrachloroethane, pentachloroethane, and trifluorotrichloroethane are completely stable for two weeks at 20°C; at this temperature solutions of uranium hexafluoride in chloroform, dichloroethane, and dichloromethane are unstable. It has been shown that reactions of uranium hexafluoride with these studied organic solvents at 60-100°C occur in the following way: at first uranium pentafluoride is formed which is reduced at first to the intermediate uranium fluorides, containing a large amount of tetravalent uranium, and then to uranium tetrafluoride.

It is known that uranium hexafluoride is soluble in carbon tetrachloride, chloroform, symmetrical tetrachloroethane and other halogenated hydrocarbons [1,2]. In [3] the solubility of uranium hexafluoride was studied in carbon tetrachloride in the temperature range 5-35°C.

Solutions of uranium hexafluoride and chlorinated and fluorinated hydrocarbons have varying stability. For example, uranium hexafluoride forms a stable solution in symmetrical tetrachloroethane. The yellow solution loses its color on boiling; on cooling, the yellow color is restored. This change in color is explained by the formation of complex compounds of uranium hexafluoride with tetrachloroethane which becomes colorless on boiling. Solutions of uranium hexafluoride in pentachloroethane have a stability which is still greater than in symmetrical tetrachloroethane.

In addition to this uranium hexafluoride reacts with some organic solvents. For example, 1,2-difluoro-1,1,2,2-tetrachloroethane reacts fairly rapidly with uranium hexafluoride. Gases are liberated and as a result the whole of the uranium hexafluoride is reduced to uranium tetrafluoride [1]. Some organic solvents can be used to reduce uranium hexafluoride to the tetrafluoride at fairly low temperatures. The reduction of uranium hexafluoride by liquid trichloroethylene at ~80°C was described in [4].

On heating solutions of uranium hexafluoride in carbon tetrachloride up to temperatures of 150°C in an autoclave a reaction takes place, accompanied by an increase in pressure and temperature. The reaction products are uranium tetrafluoride, chlorine and a mixture of freons CCl_3F and $CFCl_3$. The equation of the reaction will have the following form:

$$UF_6 + 2CCl_4 \rightarrow UF_4 + Cl_2 + 2CCl_3F.$$

The aim of the present work is to determine the solubility of uranium hexafluoride in halogenated hydrocarbons which are the most stable to uranium hexafluoride, and to study the stability of the obtained solutions. Most of the selected solvents are readily available and cheap.

The solubility of uranium hexafluoride was determined in a quartz vessel with a seal. The sealing liquid was a mixture of completely fluorinated hydrocarbons with a boiling point of ~140°C. A fixed volume of the organic solvent was added to the vessel and solid uranium hexafluoride in an amount needed to form a saturated solution at the particular temperature. When mixing was complete and the liquid had been allowed to stand, a fixed volume of solution was removed for analysis. The uranium content in the organic phase was determined volumetrically. All the organic solvents used in the work were subjected to careful chemical purification and repeated fractional distillation.

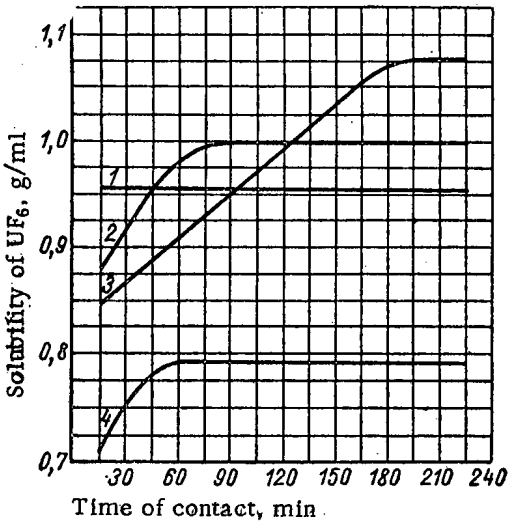

Fig. 1. The effect of time of mixing on the solubility of uranium hexafluoride at 25°C in halogenated hydrocarbons: 1) CH_2Cl_2; 2) $C_2Cl_3F_3$; 3) $CHCl_3$; 4) CCl_4.

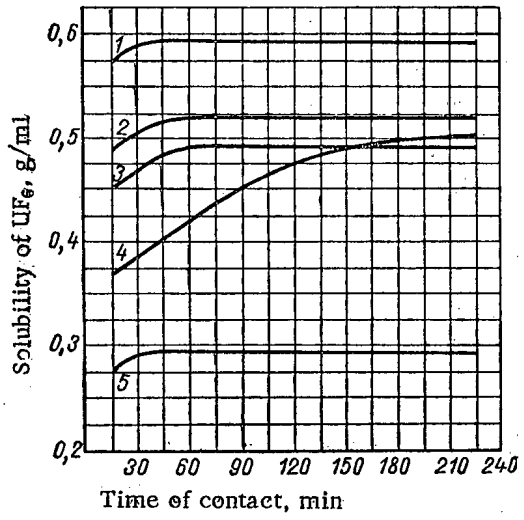

Fig. 2. Effect of time of mixing on the solubility of uranium hexafluoride at 25°C in halogenated hydrocarbons: 1) $C_3H_4Cl_4$; 2) $C_2H_2Cl_4$; 3) C_2HCl_5; 4) $C_3H_5Cl_3$; 5) $C_2H_4Cl_2$ (at 10°C).

The kinetics of solution of uranium hexafluoride in all organic solvents was studied at 25°C; experiments with dichloroethane were carried out at 10°C. Figures 1 and 2 give the solubilities of uranium hexafluoride in halogenated hydrocarbons for different times of mixing.

As can be seen from these data, equilibrium in the solution of uranium hexafluoride in most organic solvents is established in 1 hr. Only in chloroform and trichloropropane is the equilibrium established in 3 hr. The values are given below for the solubility of uranium hexafluoride in the investigated halogenated hydrocarbons at 25°C:

Organic solvent	Solubility of UF_6, g/ml
CH_2Cl_2	0.983
$CHCl_3$	1.095
CCl_4	0.799
$C_2H_4Cl_2$	0.626
$C_2H_2Cl_4$	0.520
C_2HCl_5	0.490
$C_2Cl_3F_3$	0.983
$C_3H_5Cl_3$	0.415
$C_3H_4Cl_4$	0.600

When studying the dependence of uranium hexafluoride solubility on temperature the time of mixing was 1 hr for all organic solvents; only for chloroform and trichloropropane was the time of mixing 3 hr. Figures 3 and 4 give the solubilities of uranium hexafluoride in halogenated hydrocarbons at different temperatures. In the investigated temperature range the solubility of uranium hexafluoride in all halogenated hydrocarbons increased with temperature. Chlorine derivatives of methane had greater dissolving capacity than the chlorine derivatives of ethane and propane.

A study was also made of uranium tetrafluoride solubility and that of uranyl fluoride in carbon tetrachloride and chloroform at 25°C. These studies were of interest because these compounds can be present in uranium hexafluoride in small amounts. A determination was also made of the solubility of the double salt $3NaF \cdot UF_6$ at 25°C. The results of the experiments are given in Table 1.

As can be seen from the data, the solubility of uranium tetrafluoride and uranyl fluoride in carbon tetrachloride and chloroform is very low (it is presumably of the same order in the other investigated solvents), the solubility of the double salt $3NaF \cdot UF_6$ is somewhat higher, which is possibly due to the presence in it of hexafluoride which was partially absorbed during the preparation of the salt.

Solutions of uranium hexafluoride in the studied halogenated hydrocarbons had different colors: green—in carbon tetrachloride, orange—in chloroform, yellow—in tetrachloroethane and pentachloroethane, cherry red—in dichloroethane, dichloromethane, tetrachloropropane and trichloropropane. An exception is the colorless solution of uranium hexafluoride in trifluorotrichloroethane. The intensity of the color of the solutions increases with the concentration of uranium hexafluoride. The formation of colored solutions is probably due to the formation of complex compounds of uranium hexafluoride with the organic solvents.

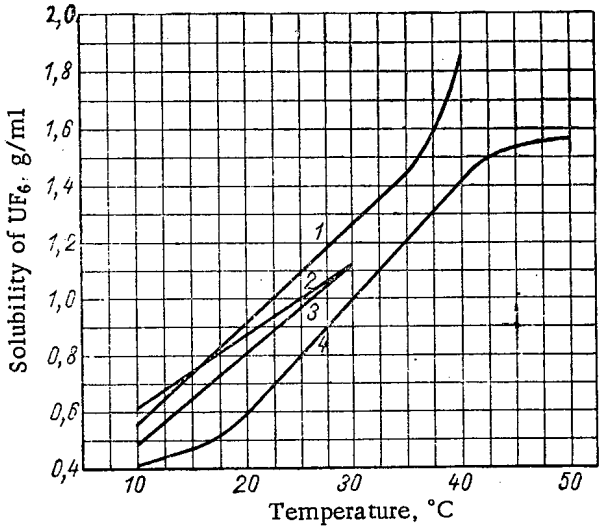

Fig. 3. The temperature dependence of the solubility of uranium hexafluoride in halogenated hydrocarbons: 1) $CHCl_3$; 2) $C_2Cl_3F_3$; 3) CH_2Cl_2; 4) CCl_4.

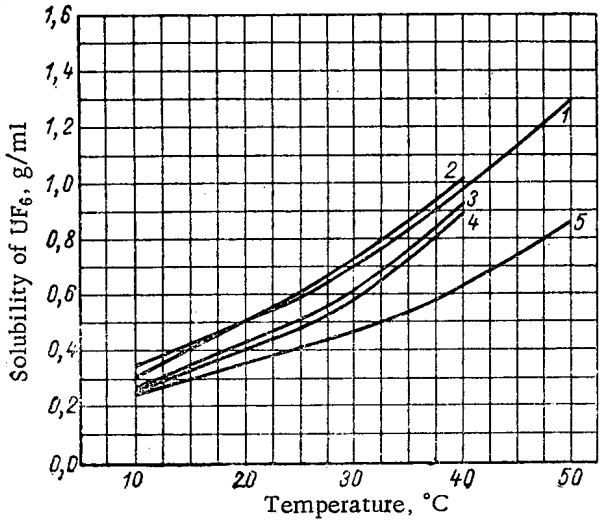

Fig. 4. The temperature dependence of the solubility of uranium hexafluoride in halogenated hydrocarbons: 1) $C_3H_4Cl_4$; 2) $C_2H_4Cl_2$; 3) $C_2H_2Cl_4$; 4) C_2HCl_5; 5) $C_3H_5Cl_3$.

TABLE 1. The Solubility of Uranium Tetrafluoride, Uranyl Fluoride and the Double Salt $3NaF \cdot UF_6$ in Carbon Tetrachloride and Chloroform at 25°C

Compound	Solubility mg/liter U	
	in CCl_4	in $CHCl_3$
UF_4	<15	15
UO_2F_2	<15	15
$3NaF \cdot UF_6$	72	—

TABLE 2. The Stability of Solutions of Uranium Hexafluoride in Organic Solvents as a Function of the Standing Time at 20°C

Organic solvent	Initial concentration of UF^6, g/ml	UF^6 concentration after 7 days standing, g/ml	UF^6 concentration after 14 days standing, g/ml
CCl_4	0,273 0,185	0,270 0,186	0,272 0,184
$C_2H_2Cl_4$ (symmetrical)	0,190 0,130	0,188 0,127	0,189 0,128
$C_2Cl_3F_3$	0,304 0,206	0,300 0,203	0,302 0,204

TABLE 3. Degree of Reduction of Uranium Hexafluoride during 30 Days at 20°C

Organic solvent	Initial content of U^{6+}, g	Content of U^{4+}, g	Degree of reduction of uranium, %
CCl_4	0,920	0,020	2,2
$C_2H_2Cl_4$ (symmetrical)	0,933	0,020	2,1
C_2HCl_5	0,995	0,021	2,0
$C_2Cl_3F_3$	0,630	0,019	3,2

The method for studying the stability of solutions at room temperature (20°C) was as follows. Solutions of uranium hexafluoride of known concentration in aluminum containers were placed in a desiccator. After certain intervals of time the contents of hexa- and tetravalent uranium in the solutions were determined volumetrically. No tetravalent uranium was found in any of the cases. The results of the experiments are given in Table 2.

The constancy of the uranium hexafluoride concentration, the absence of tetravalent uranium in the solution, the stability of the color of the solution and the absence of precipitates in them indicated that solutions of uranium hexafluoride in the studied organic solvents are completely stable at 20°C for two weeks.

A study was made of the stability of solutions of uranium hexafluoride in carbon tetrachloride, symmetrical tetrachloroethane, pentachloroethane and trifluorotrichloroethane with a standing time of about 30 days. The method

of investigation was as before, but in connection with the formation of precipitates the content of tetra- and hexavalent uranium was determined in the whole contents of the containers. In all cases the volume of the solutions was 5 ml. The results of the experiments are given in Table 3.

It can be seen from these data that regardless of the initial concentration of the uranium hexafluoride and the type of organic solvents, the tetravalent uranium content remains constant; this is probably due to the reaction of uranium hexafluoride with the material of the container.

A study was made of the stability of solutions of uranium hexafluoride in chloroform and asymmetrical dichloroethane at 20°C and a standing time of 7 days. In both cases precipitates were formed; the volume of the solution was 5 ml. The studies were carried out according to the above-described method. The results of the experiments are given in Table 4.

TABLE 4. Degree of Reduction of Uranium Hexafluoride during 30 Days at 20°C

Organic solvent	Initial content U^{6+}, g	Content U^{4+}, g	Degree of reduction of uranium, %
$CHCl_3$	0,603	0,162	27
$C_2H_4Cl_2$ (asymmetrical)	0,500	0,150	30

TABLE 5. Temperature Dependence of the Degree of Reduction of Uranium Hexafluoride by Dichloromethane

Temperature °C	Content of U^{4+} in solution, g	Total content of U^{4+}, g
10	0,021	0,048
20	0,012	0,059
25	0,009	0,066

TABLE 6. Degree of Reduction of Uranium Hexafluoride by Organic Solvents (in Percentages)

Organic solvent	Temperature, °C		
	60	80	100
CCl_4	0	0	57,5
$CHCl_3$	1,1	6	56,0
CH_2Cl_2	10,8	27,7	57,1
$C_2H_4Cl_2$	20,5	36,8	50,7
$C_2H_2Cl_4$	3,9	5,7	18,5
C_2HCl_5	2,1	2,1	2,4
$C_3H_5Cl_3$	2,5	29,9	57,7
$C_3H_4Cl_4$	47,5	70,8	82,7

It can be seen from these data that solution of uranium hexafluoride in chloroform and asymmetrical dichloromethane are less stable than in the previously studied organic solvents. Solutions of uranium hexafluoride in dichloromethane were also unstable. Partial reaction was observed as soon as the solid uranium hexafluoride was mixed with the solvent. The conditions of the experiments were as follows: the volume of solvent was 3 ml, UF_6 — 8 g; time of mixing was 30 min. The results of the experiments are given in Table 5.

The stability of solutions of uranium hexafluoride in some chlorinated derivatives of methane, ethane and propane at 60, 80 and 100°C were studied in the following way: solutions of uranium hexafluoride with the same concentration were placed in a steel bomb which was kept in a thermostat for 1 hr at a given temperature. After the completion of the experiment the total content of hexa- and tetravalent uranium were determined volumetrically in the obtained products.

In experiments in which the degree of reduction of uranium did not exceed 2.5% (for $CHCl_3$ at 60°C, for C_2HCl_5 at 60, 80 and 100°C, for $C_3H_5Cl_3$ at 60°C), the reaction products were a homogeneous organic phase. In view of the very low solubility of uranium tetrafluoride in organic solvents, the presence in the solution of tetravelent uranium was probably due to the solubility of the intermediate fluorides of uranium, formed during the reaction of uranium hexafluoride with organic solvents. In the other experiments precipitates were formed. Due to the reaction of uranium hexafluoride with chloroform and trichloropropane (at 80°C), dichloromethane and dichloroethane (at 60° and 80°C), tetrachloroethane (at 60, 80 and 100°C) and tetrachloropropane at (60°C) white compounds were obtained which disproportionated in air in 15-30 min and were almost instantaneously hydrolyzed in water with the formation of uranium tetrafluoride and uranyl fluoride. In the experiments the volumes of the solutions were 3 ml and the concentration of UF_6 was 0.48 g/ml. The results of the experiments are given in Table 6.

Under other conditions white products were obtained with a greenish hue of varying intensity (Table 7). These products were analyzed in the following way: the precipitates were separated from the organic phase on filter paper, washed with carbon tetrachloride and the content of hexa- and tetravalent uranium in them was determined.

TABLE 7. The Relationship of Hexa- and Tetravalent Uranium in the Obtained Products

Organic solvent	Ratio of U^{6+} to U^{4+}	Degree of reduction of uranium, %
$CHCl_3$	1,27	56,0
CH_2Cl_2	1,36	57,1
$C_3H_6Cl_3$	1,36	57,7
$C_3H_4Cl_4$	4,78	82,7

The investigations show that the reaction of uranium hexafluoride with various organic solvents occurs in the following way: initially uranium pentafluoride is formed which is first reduced to the intermediate fluoride of uranium containing a large amount of tetravalent uranium, and then to uranium tetrafluoride.

The following conclusions can be drawn from the study of the solubility of uranium hexafluoride in some halogen derivatives of methane, ethane and propane and a study of the stability of these solutions:

1. Chlorine derivatives of methane have a greater dissolving capacity than those of ethane and propane.

2. The solubility of uranium tetrafluoride and uranyl fluoride in carbon tetrachloride and chloroform is very low.

3. At 20°C solutions of uranium hexafluoride in carbon tetrachloride, tetrachloroethane, pentachloroethane and trifluorotrichloroethane are stable, and in chloroform, dichloromethane and dichloroethane they are unstable.

4. In the reaction of uranium hexafluoride with the studied organic solvents uranium pentafluoride is formed and is first reduced to intermediate fluorides of uranium and then to uranium tetrafluoride.

LITERATURE CITED

1. J. Katz and E. Rabinowicz, The Chemistry of Uranium, Vol. 1 [Russian translation] (Moscow, Foreign Literature Press, 1954) p. 356.
2. S. Smiley, Industr. and Engng Chem. 2, 147 (1959).
3. Nairn, Collins, and Taylor Transactions of the Second International Conference on the Peaceful Uses of Atomic Energy (Geneva, 1958). Selected Reports of Non-Soviet Scientists. Vol. 7. The Technology of Nuclear Raw Material [in Russian] (Moscow, Atomic Energy Press, 1959) p. 553.
4. Smiley and Brater, Transactions of the Second International Conference on the Peaceful Uses of Atomic Energy (Geneva, 1958). Selected Reports of Non-Soviet Scientists. Vol. 7. The Technology of Nuclear Raw Material [in Russian] (Moscow, Atomic Energy Press, 1959) p. 561.

METHODS OF REDUCING URANIUM HEXAFLUORIDE

N. P. Galkin, B. N. Sudarikov, and V. A. Zaitsev

Translated from Atomnaya Énergiya, Vol. 10, No. 2, pp. 149-155, February, 1961
Original article submitted February 8, 1960

On the basis of published material the present article gives brief characteristics of different methods for reducing smelting. Values are given for the free energy of some investigated reactions of the reduction of uranium hexafluoride. The effect of various factors is considered on the purity and the granular specific gravity of the obtained uranium tetrafluoride. The advantages and disadvantages of different schemes for reducing uranium hexafluoride are discussed.

Uranium hexafluoride is the most important product in the nuclear engineering industry since it is essential in the separation of uranium isotopes by the gaseous diffusion method.

Many papers have appeared recently on the fluoride method of treating irradiated nuclear fuel (the fluoride-vaporization process) with which the uranium in the form of uranium hexafluoride is separated from the active fission products [1-5]. Papers have also been published on the preparation of nuclear-pure uranium hexafluoride from uranium ore concentrates and rich uranium ores by the method of direct fluorination [6,7].

Uranium hexafluoride obtained by a given method should later be processed to metallic uranium or some of its compounds (uranium dioxide, uranium tetrafluoride, etc.), which have been used as nuclear fuel. In the conversion of uranium hexafluoride to the dioxide the most convenient methods will presumably be those based on the hydrolysis of uranium hexafluoride by water or by aqueous solutions with subsequent precipitation and roasting of the ammonium diuranate [8].

To prepare metallic uranium the chemical engineering conversion of uranium hexafluoride is carried out in two stages: at first the uranium hexafluoride is converted to uranium tetrafluoride, then the latter is subjected to reducing smelting. The reduction of uranium hexafluoride is therefore of considerable practical importance.

Various authors have studied the reduction of uranium hexafluoride to the tetrafluoride by hydrogen, hydrogen chloride, carbon tetrachloride, ammonia, ethylene, propane, trichloroethylene, sulfur dioxide, silicon tetrachloride, thionyl chloride and by other reducing agents. Some of the work was developed to pilot-plant and industrial scale. The most promising reducing agents for uranium hexafluoride from the point of view of obtaining uranium tetrafluoride suitable for reducing smelting are presumably hydrogen, carbon tetrachloride, hydrogen chloride, trichloroethylene and ammonia. Table 1 give the values of free energy for some of the investigated reduction reactions.

As can be seen from these data, in the series HCl, CCl_4, HBr, H_2 there is a reduction in the value of free energy for the reduction of uranium hexafluoride. In this direction the thermal effect of the reaction increases and the chemical affinity of the reacting substances increases. In connection with the large thermal effect (83.6 ± 2.5 kcal/mole UF_6 at a temperature of -30°C) it should be expected that the value of free energy in the reaction of uranium hexafluoride with ammonia will be lower than for the case of reduction of uranium hexafluoride by hydrogen.

Reduction of Uranium Hexafluoride by Hydrogen Chloride

In [9] there was a description of the reduction of uranium hexafluoride by hydrogen chloride; it was stated that at 200°C a mixture is obtained of brown, green and black products which become green on being degassed in a vacuum. The optimum temperature range of the reduction was 250–300°C.

An improved method for reducing uranium hexafluoride by hydrogen chloride was described in [10]. The reaction was carried out at 200–400°C in a vessel having the shape of an inverted cone. Vapors of uranium hexafluoride and hydrogen chloride were introduced tangentially into the chamber near its bottom where the stream of gases was relatively fast and had high turbulence. On reaching the upper part of the chamber where the area of cross section increased, the stream lost its speed and its turbulence was reduced, which helped the precipitation of uranium tetra-

TABLE 1. The Values of Free Energy for the Reduction of Uranium Hexafluoride

Reaction	Free energy, kcal/mole
$UF_{6(s)} + H_{2(g)} \rightarrow UF_{4(s)} + 2HF_{(g)}$	−68,9
$UF_{6(s)} + 2HBr_{(g)} \rightarrow UF_{4(s)} + 2HF_{(g)} + Br_{2(g)}$	−43,5
$UF_{6(s)} + 2CCl_{4(l)} \rightarrow UF_{4(s)} + Cl_{2(g)} + 2CCl_3F$ with a molar ratio $CCl_4 : UF_6 = 4:1$	−31,5
$UF_{6(s)} + 2HCl_{(g)} \rightarrow UF_{4(s)} + 2HF_{(g)} + Cl_{2(g)}$	−23,4

fluoride particles. The particle sizes of the product could be controlled by the volumetric rate of feed of the reagents. A 6-8-fold excess of hydrogen chloride in the mixture was used with different diluents. The granular weight of the uranium tetrafluoride varied within the limits of 1.6−2.0 g/cm^3. The authors of [10] state that the uranium tetrafluoride obtained in this way is suitable for direct reducing smelting in order to produce uranium.

Reduction of Uranium Hexafluoride by Hydrogen

Many papers have been devoted to the reduction of uranium hexafluoride by hydrogen. In [11] an account was given of the practically instantaneous reduction of uranium hexafluoride to the tetrafluoride by hydrogen at room temperature, however the experiments carried out in 1943 by Spencer-Palmer [12] did not confirm these data. At temperatures of 78−100°C uranium hexafluoride is practically unreactive with hydrogen. It is probable that the materials used in [12] contained impurities which were catalysts for this reaction.

The reduction of uranium hexafluoride by hydrogen was studied in greater detail in [12]. A study was made of the dependence of the degree of reduction of uranium hexafluoride by hydrogen on the temperature (Table 2) and the time of reaction (Fig. 1).

TABLE 2. Effect of Temperature on the Degree of Reduction of Uranium Hexafluoride by Hydrogen

Temperature of reaction, °C	226	250	275	285	292	295	305	312	330	331
Degree of reduction of uranium, %	3,8	22,3	40,1	42,5	44,3	44,8	50,5	52,2	58,6	59,1

Note. Time of process 30 min, molar ratio H_2: UF_6 = 5:1.

At a temperature of 121°C no reaction was observed between uranium hexafluoride and hydrogen; the reaction started in the temperature range 215−288°C. These data agree well with the results of the Spencer-Palmer work. Based on preliminary data, the authors observe that the reduction of uranium hexafluoride by hydrogen is a first order reaction and proceeds both in the gaseous phase and at the walls of the reactor. High activation energy is needed for it. This fact is mentioned in a number of other papers. It is mentioned that the reduction of uranium hexafluoride by hydrogen is accelerated catalytically in the presence of certain chlorides (hydrogen chloride, mercury monochloride, ferric chloride); however, in these cases also the reaction is comparatively slow [13].

At the Second Geneva Conference on the Peaceful Uses of Atomic Energy the US delegation presented a report [14] on the successful reduction of uranium hexafluoride by hydrogen on an industrial scale. Uranium hexafluoride was reduced by hydrogen according to the reaction $UF_{6(g)} + H_{2(g)} \rightarrow UF_{4(s)} + 2HF_{(g)} + 68.9$ kcal by two methods. In the first of them (the method of reactor with "hot" walls) the heat needed for the start of the reaction was communicated to the system through the wall of the reactor, in the second (the method of reactor with "cold" walls) the required heat was obtained by the reaction of hydrogen with elementary fluorine which was added together with the uranium hexafluoride.

The layout of the reactor with hot walls is shown in Fig. 2. The reactor (150-mm, with a tube of monel metal) was split up into five temperature zones; the wall temperature of the reactor varied within the limits 426−537°C. The feed rate of the uranium hexafluoride was 45.36 kg/hr, a 100% excess of hydrogen was used above the stoichiometric amount. The mean granular specific gravity of the obtained uranium tetrafluoride was 3.6 g/cm^3. The total of metallic impurities in the uranium tetrafluoride varied from $2.0 \cdot 10^{-4}$ to $1.3 \cdot 10^{-2}$%, averaging $4.0 \cdot 10^{-3}$%. The faults in this

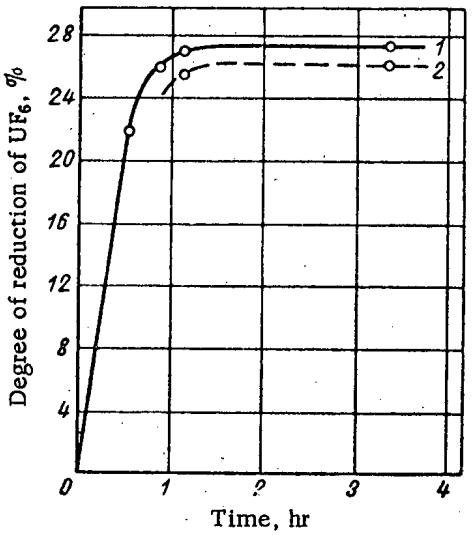

Fig. 1. Effect of Reaction time on the degree of reduction of uranium hexafluoride by hydrogen (at temperature 249–250°C). Molar ratio H_2:UF_6 equal to: 1) 6.0; 1.0; 2) 3.0: 1.0.

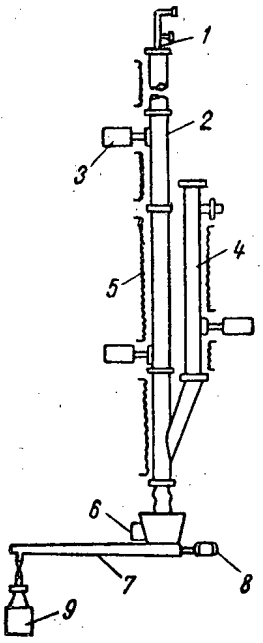

Fig. 2. Layout of reactor with hot walls: 1) nozzle; 2) reactor housing; 3) pneumatic vibrator; 4) Cottrell filter; 5) heater; 6) mechanical vibrator; 7) unloading worm; 8) motor; 9) receiver for UF_4.

method for reducing uranium hexafluoride, as shown by the authors themselves [14], are the considerable melting of the product on the reactor walls, especially in the upper zone and the formation of hardened material on the walls. After every 8 hr of operation the apparatus was stopped and the layer of fused uranium tetrafluoride was removed mechanically. Vibrating the reactor walls did not remove the fused product.

In the reduction of uranium hexafluoride in a reactor with cold walls an attempt was made to preheat the uranium hexafluoride and hydrogen to the required temperature; however, it was found that at 426°C the uranium hexafluoride reacts with the material of the tube (monel metal) forming solid crystalline products, presumably a mixture of intermediate uranium fluorides. The result was that the tubes choked up and the apparatus became unserviceable. Elementary fluorine was therefore added to the uranium hexafluoride to increase the temperature in the reaction zone. From the heat liberated during the reaction $F_2 + H_2 \rightarrow 2HF + 128$ kcal, the starting materials were heated to the required temperature. The reduction of uranium hexafluoride by hydrogen in this case proceeded entirely within the flame with

TABLE 3. Effect of the Gravimetric Ratio on the Granular Weight of UF_4

Gravimetric ratio F_2:UF_6	0,030	0,040	0,045	0,050	0,055	0,060	0,060	0,070	0,070	0,075	0,075
Granular density of UF_4, g/cm^3	2,18	2,59	2,68	2,99	2,89	3,08	2,99	3,08	3,58	3,71	3,48

the reactor walls at temperatures of 92-204°C. The layout of the apparatus is shown in Fig. 3. The gas rate at the nozzle varied from 15 to 40 m/sec with a rate of production of uranium hexafluoride of 4.53-11.34 kg/hr. The excess of hydrogen above the stoichiometric amount was 100-500%; the stream of fluorine was 0.05-0.08 kg F_2/UF_6.

For low flow coefficients with regard to fluorine the reduction of uranium hexafluoride was incomplete and the final product was contaminated with intermediate fluoride. The granular weight of the obtained uranium tetrafluoride was also determined by the gravimetric ratio of fluorine and uranium hexafluoride (Table 3). The thickness of the uranium tetrafluoride layer on the walls did not exceed 0.8 mm.

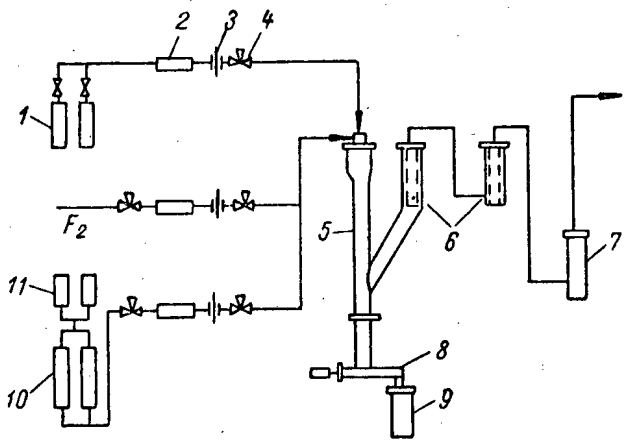

Fig. 3. Apparatus for reducing uranium hexafluoride by hydrogen using a reactor with cold walls: 1) H_2 cylinders; 2) receiver; 3) diaphragm; 4) control valve; 5) reactor; 6) porous filters; 7) traps; 8) unloading worm; 9) UF_4 receiver; 10) UF_6 cylinders; 11) container for UF_6.

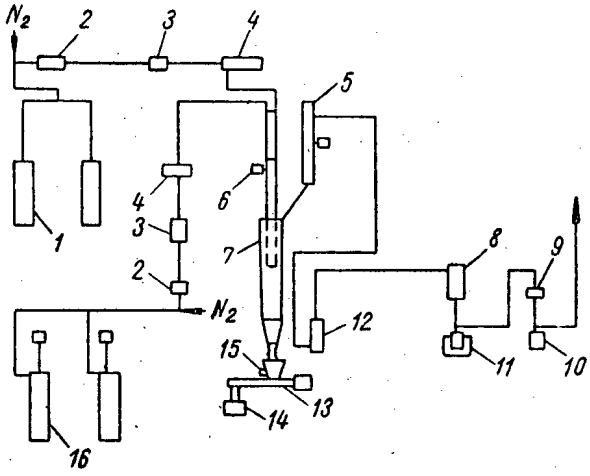

Fig. 4. Apparatus for reducing uranium hexafluoride with trichloroethylene: 1) UF_6 cylinders; 2) receivers; 3) mixers; 4) heaters; 5) Cottrell filter; 6) pneumatic vibrator; 7) reactor; 8) water-cooled condenser; 9) ice-cooled condenser; 10,11) receiver for freons; 12) porous filter; 13) unloading worm; 14) receiver for UF_4; 15) mechanical vibrator; 16) cylinders with C_2HCl_3.

With a certain modification the method of the reactor with cold walls was described in [15], where the energy needed for the start of the reaction was obtained by the recombination of atomic hydrogen:

$$2H \longrightarrow H_2 + 103 \text{ kcal.}$$

Reduction of Uranium Hexafluoride by Ammonia

It has been stated that uranium hexafluoride reacts with ammonia at a temperature of -72°C, forming a mixture of solid products.

At 300°C gaseous uranium hexafluoride reacts with ammonia in a reactor made of nickel and forms a mixture of ammonium uranium pentafluoride and ammonium fluoride (98% NH_4UF_5 + 5% NH_4F). X-ray structural analysis shows that there is no uranium tetrafluoride in this product. A product of this composition was obtained on fusing uranium tetrafluoride with ammonium bifluoride at 450°C [16]. The reaction of uranium hexafluoride with ammonia at 450°C also leads to the formation of ammonium uranium pentafluoride [15].

More detailed information on the reaction of uranium hexafluoride with ammonia is given in [17], where a study was made of the composition of products from the reaction of uranium hexafluoride with ammonia in the temperature range -50 to 200°C and the total equations are proposed for the reaction: for temperatures of -50 to -30°C

$$6UF_6 + (8 + 6n)NH_3 \longrightarrow 6UF_5 \cdot nNH_3 + 6NH_4F + N_2,$$

where n = 0.73;
for temperatures of 0-25°C

$$4UF_6 + 8NH_3 \longrightarrow 2UF_5 + 2NH_4UF_5 + 4NH_4F + N_2;$$

for temperatures of 100-200°C

$$3UF_6 + 8NH_3 \longrightarrow 3NH_4UF_5 + 3NH_4F + N_2.$$

The rate of reaction of solid uranium hexafluoride with gaseous ammonia was examined in the temperature range -20 to 20°C. The reaction rate decreased with decrease in temperature; however, even at -20°C the reaction was finished in 3-5 min. The reaction of uranium hexafluoride with ammonia occurred with a large evolution of heat even at low temperatures (Table 4). At 500°C ammonium uranium pentafluoride decomposed into uranium tetrafluoride and ammonium fluoride. The nitrogen content in the final product did not exceed 10^{-4}% [18-20].

TABLE 4. The Thermal Effect of the Reaction of Solid Uranium Hexafluoride with Liquid Ammonia

Temperature of reaction, °C	Thermal effect of reaction kcal/mole UF_6
—50	50,8±1,5
—40	67,0±2,0
—30	83,6±2,5

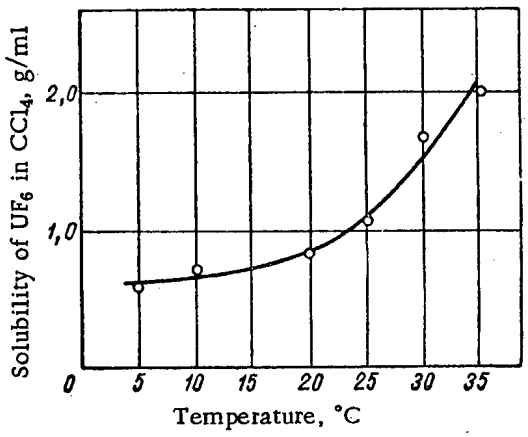

Fig. 5. Effect of temperature on the solubility of uranium hexafluoride in carbon tetrachloride.

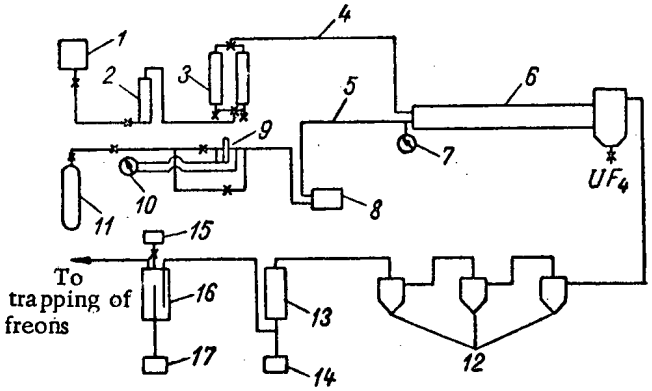

Fig. 6. Apparatus for reducing uranium hexafluoride by carbon tetrachloride: 1) CCl_4 cylinder; 2) rotameter; 3) vaporizer; 4) line of preliminary heating of CCl_4; 5) line of preliminary heating of UF_6; 6) rotary furnace; 7) manometer; 8) Kronberger flowmeter; 9) diaphragm; 10) differential manometer; 11) UF_6 cylinder; 12) cyclones; 13) condenser; 14) condensate receiver; 15) tank containing NaOH solution; 16) scrubber; 17) receiver for solution.

Reduction of Uranium Hexafluoride by Trichloroethylene

Trichloroethylene in the liquid and gas phases reacts with uranium hexafluoride according to [14,21]

$$UF_6 + CHCl = CCl_2 \rightarrow UF_4 + HF +$$
$$+ \text{ mixture of chlorofluorohydrocarbons}$$

The mixture of chlorofluorohydrocarbons is formed due to the reactions of addition, substitution, and polymerization and also to splitting of trichloroethylene molecules and subsequent formation of chlorofluoro derivatives of methane.

The reduction was carried out at 82°C in a spraying column and the uranium hexafluoride was first diluted by nitrogen. The resulting uranium tetrafluoride was collected as a slurry at the bottom of the column and separated from the excess trichloroethylene by a centrifuge. In [14] it was mentioned that during operation the gas nozzles became blocked and the separation of the solid and liquid phases was seriously hindered.

In the gas phase the reaction was carried out at 232°C with a molar ratio C_2HCl_3:UF_6 = 3:1 and the initial concentration of uranium hexaflouride was 0.5-3.5 mole %. The rate of flow of the uranium hexaflouride varied within the limits 0.9-2.3 kg/hr.

Under these conditions the uranium hexafluoride was completely reduced to uranium tetrafluoride with a granular weight of 0.22-1.6 g/cm^3. The granular weigh of uranium tetrafluoride was increased to 2.96 g/cm^3 on roasting its powder in an atmosphere of hydrogen fluoride at 900°C for 2 hr (Fig. 4).

The obtained uranium tetrafluoride was contaminated to a large extent with carbon,and to remove this the product was roasted in an atmosphere of nitrogen, hydrogen and oxygen. Only treatment of uranium tetrafluoride with oxygen led to a considerable reduction in the carbon content, however in this case to prevent the formation of uranyl fluoride it was essential to add hydrogen fluoride.

The described process was carried out on a pilot-plant scale. The gravimetric ratio of the trichloroethylene and uranium hexafluoride varied within the limits 0.7-3.25. The temperature of the gases at the input to the reactor varied within the range 82-304°C; the reactor temperature was 74-483°C. The density of the obtained uranium tetrafluoride did not exceed 1.6 g/cm^3. As regards the carbon content the product was below standard in all cases.

A serious fault of this method reducing uranium hexafluoride (apart from the low granular weight of uranium tetrafluoride and the high content of carbon in it) were the complications connected with the blocking of the tubes with readily condensing organic reaction products, especially hexachlorobenzene.

Reduction of Uranium Hexafluoride by Carbon Tetrachloride

It is known that uranium hexafluoride is readily soluble in carbon tetrachloride; the solution is stable at room temperature for several weeks (see page 356 of [13]). Figure 5 shows the solubility curve for uranium hexafluoride in carbon tetrachloride as a function of the temperature.

When a solution of uranium hexafluoride in carbon tetrachloride was heated in an autoclave to 150°C or when the vapors of uranium hexafluoride and carbon tetrachloride were reacted at 200°C and above, the uranium hexafluoride was reduced to the tetrafluoride according to the equation [22].

$$UF_6 + 2CCl_4 \rightarrow UF_4 + Cl_2 + 2CCl_3F.$$

It has been mentioned that in both cases this reaction proceeded stepwise: as well as the uranium tetrafluoride and elementary chlorine there were mixed chlorofluoro derivatives of methane, which underwent further change during the reaction.

Traces of uranium tetrafluoride had a catalytic effect on the reduction of uranium hexafluoride by carbon tetrachloride.

In the condensed phase the reaction was carried out in the following way: 1 liter of CCl_4 was added per 1 kg of UF_6 in an evacuated autoclave; the autoclave was then heated from outside to 150°C and further to 200°C from the heat of reaction. In 2 hr the pressure in the apparatus was raised to 25 atm, then the autoclave was cooled to 50°C, the gases were passed through alkaline scrubbers, where the chlorine was trapped, and then the gases were put into the atmosphere. There was 99.7% reduction of uranium hexafluoride to the tetrafluoride; the obtained uranium tetrafluoride was heated in a current of air at 120°C to remove chlorine and other adsorbed gases. When air was drawn in and when the vessel was poorly evacuated the reduction of uranium hexafluoride was accompanied by the formation of phosgene,

Uranium hexafluoride was quantitatively reduced by carbon tetrachloride with a molar ratio of components of 1:4 or with still greater excesses of carbon tetrachloride. A reduction in the excess of carbon tetrachloride led to an increase in the content of intermediate uranium fluorides in the reaction products.

In the gaseous phase there was continuous reduction of uranium hexafluoride by carbon tetrachloride at atmospheric pressure and temperatures of 200-400°C in a horizontal furnace of diameter 108 mm and length 1676.4 mm. The layout of the apparatus is shown in Fig. 6.

At 200°C for the quantitative reaction of uranium hexafluoride with carbon tetrachloride with the formation of solid nonvolatile products (intermediate uranium fluorides) the time needed is 2 min; the reduction of these products in a stream of carbon tetrachloride to uranium tetrafluoride is accomplished in 10 min.

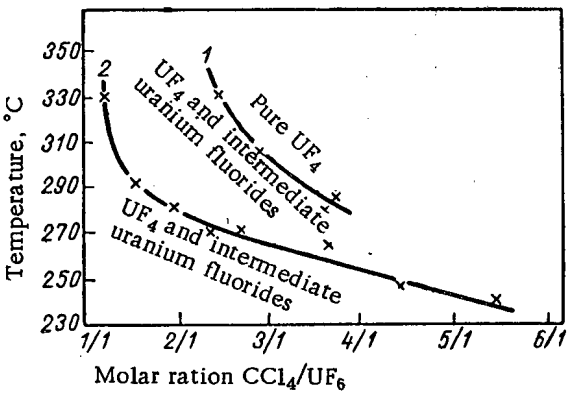

Fig. 7. The effect of temperature, rate of production and ratio of reagents on the degree of reduction of uranium hexafluoride by carbon tetrachloride. Rate of production: 1) 1 kg/hr uranium; 2) 0.6 kg/hr uranium.

Figure 7 shows the dependence of the degree of reduction of uranium hexafluoride by carbon tetrachloride on the reaction temperature, the rate of production and the ratio of the reagents.

By reducing uranium hexafluoride with carbon tetrachloride uranium tetrafluoride is obtained with a high granular weight and a content of impurities within the limits of the conditions.

LITERATURE CITED

1. W. Page et al., Report BNL-174 (March 1952).
2. G. Cather and R. Lenze, Nuclear Engineering and Science Congress, Ohio (December 1955).
3. R. Steunenberg et al., Report No. 539 presented by the USA to the Second International Conference on the Peaceful Uses of Atomic Energy (Geneva, 1958).
4. Steunenberg and Vogel, Transactions of the Second International Conference on the Peaceful Uses of Atomic Energy

(Geneva, 1958). Selected Reports of non-Soviet Scientists. Vol. 5. The Chemistry of Radioelements and Radiation Transformations [in Russian] (Moscow, Atomic Energy Press, 1959) p. 177.
5. V. Mecham et al., Atomnaya Teknika za Rubezhom 3, 48 (1958).
6. Lavroskii et al., Transactions of the Second International Conference on the Peaceful Uses of Atomic Energy (Geneva, 1958). Selected Reports of non-Soviet Scientists. Vol. 7. The Technology of Nuclear Raw Material [in Russian] (Moscow, Atomic Energy Press, 1959) p. 615.
7. Smiley and Brater, Transactions of the Second International Conference on the Peaceful Uses of Atomic Energy (Geneva, 1958). Selected Reports of non-Soviet Scientists. Vol. 7. The Technology of Nuclear Raw Material [in Russian] (Moscow, Atomic Energy Press, 1959) p. 587.
8. J. Murray et al., Report No. 439 Presented by the USA to the Second International Conference on the Peaceful Uses of Atomic Energy (Geneva, 1958).
9. E. Gladrow, and P. Chiotty. Report CK-1498 (1944).
10. K. David and G. Hugh. US patent No. 2 768 872 (1956).
11. O. Ruff and A. Heinzelmann. Z. anorgan. und allgem Chem. 72, 82 (1911).
12. J. Dawson et al. J. Chem. Soc., December, 1421 (1950).
13. J. Katz and E. Rabinowicz, The Chemistry of Uranium. Vol. 1 [Russian translation] (Moscow, Foreign Literature Press, 1954) p. 355.
14. Smiley and Brater, Transactions of theSecond International Conference on the Peaceful Use of Atomic Energy (Geneva, 1958). Selected Reports of non-Soviet Scientists. Vol. 7. The Technology of Nucear Raw Material [in Russian] (Moscow, Atomic Energy Press, 1959) p. 561.
15. R. Spenceley and F. Teetrel, US AEC, Report FMPC-400. National Lead Company of Ohio (May 6, 1953).
16. B. Ayers, Report CC-1504 (1944).
17. N. P. Galkin, B. N. Sudarikov,and V. A. Zaitsev, Atomnaya Énergiya 8, 6, 530 (1960).*
18. J. Van Impe, Chem. Engng Progr. 50, No. 5, 230 (1954).
19. A. Leah and R. Manney, US patent No. 2654 (1953).
20. H. Beruhardt et al.,Nucl. Sci. Abstrs, 10 792 (1956).
21. F. Martin,AERE C/R-1057 (1952).
22. Nairn, Collins, and Taylor,Transactions of the Second International Conference on the Peaceful Uses of Atomic Energy (Geneva, 1958). Selected Reports of non-Soviet Scientists. Vol. 7. The Technology of Nuclear Raw Material [in Russian] (Moscow, Atomic Energy Press, 1959) p. 553.

*Original Russian pagination. See C. B. translation.

LETTERS TO THE EDITOR

THE MECHANISM OF REACTION OF FAST NUCLEONS WITH NUCLEI

V. S. Barashenkov, V. M. Mal'tsev, and É. K. Mikhul

Translated from Atomnaya Énergiya, Vol. 10, No. 2, pp. 156-158, February, 1961
Original article submitted July 14, 1960

Several papers have been published on the experimental investigation of the mechanism of reaction of protons with energy of 9 Bev with nuclei (see bibliography in [1-5]). However, there is no single opinion on this problem: some are of the opinion that at energies of 9-10 Bev the mechanism of an intranuclear cascade, realized at lower energies [6], is replaced by a mechanism of simultaneous reaction with the whole "tube" of the nuclear material [4]; others consider that at an energy of 9 Bev the reaction of fast nucleons with nuclei occurs by means of intranuclear cascades [1,2].

In order to find which of the two discussed mechanisms is realized in the reaction of a nucleon with 9 Bev energy with a nucleus, we carried out calculations of an intranuclear cascade and compared them with experimental data. The calculations were made by the Monte Carlo method for the case of relativistic three-dimensional kinematics. Allowance was made for the multiple production of particles due to collision between fast particles and nucleons of the nucleus. The angular and energy distributions of the particles after elastic and inelastic (NN)- and (πN)-collisions were taken from experiments. A Fermi gas nuclear model was considered with the same parameters as those given in [6].

The results of the calculations and the known experimental data on shower and cascade particles* are given in Tables 1 and 2 and in Figs. 1-3 (the dotted line shows the experimental data of [1]).

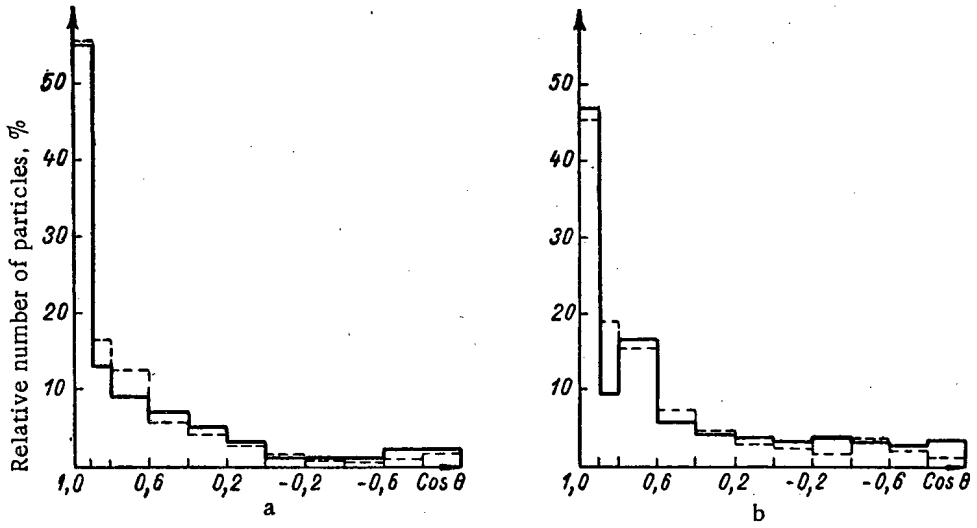

Fig. 1. Angular distribution of shower particles: a) group of light nuclei; b) group of heavy nuclei.

* We apply the term shower particles to nucleons with energies of 0.5-9 Bev and π-mesons with energies of 0.08-8 Bev. We use the term cascade particles for nucleons with energies of 0.03-0.05 Bev and π-mesons with energies of 0.15-0.08 Bev (for more details see [1]). All particles with lower energies will be referred to as evaporation particles.

TABLE 1. Mean Number of Particles Produced in One Act of Inelastic Nucleon-Nuclear Collision

Particles	Group of light nuclei		Group of heavy nuclei	
	calc.	exp[1,2]	calc.	exp[1,2]
Shower	2,9	3,0±0,2	4,1	3,5±0,3
Cascade	1,5	1,4±0,1	4,0	4,1±0,5
Evaporation	3,5	3,3±0,1	5--6	6,1±0,6

TABLE 2. Mean Kinetic Energy of Particles (in Bev), Produced in One Act of Inelastic Collision of a Proton with the Mean Nucleus of a Photoemulsion

Particles	Calculations	Experiment [1,2]
Shower protons	2,5	3,0±0,5
Shower pions	0,52	0,63±0,1 [5]
Cascade protons	0,15	0,120±0,012
Cascade pions	0,048	0,040±0,003

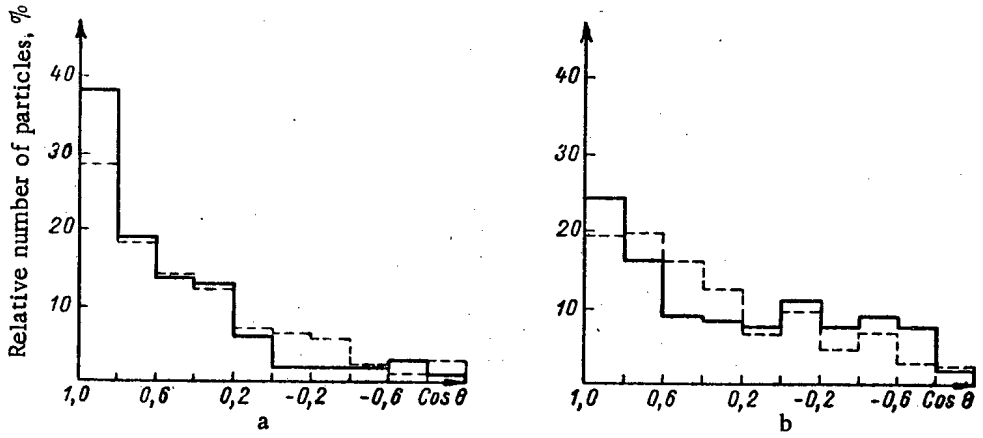

Fig. 2. Angular distribution of cascade particles: a) group of light nuclei; b) group of heavy nuclei.

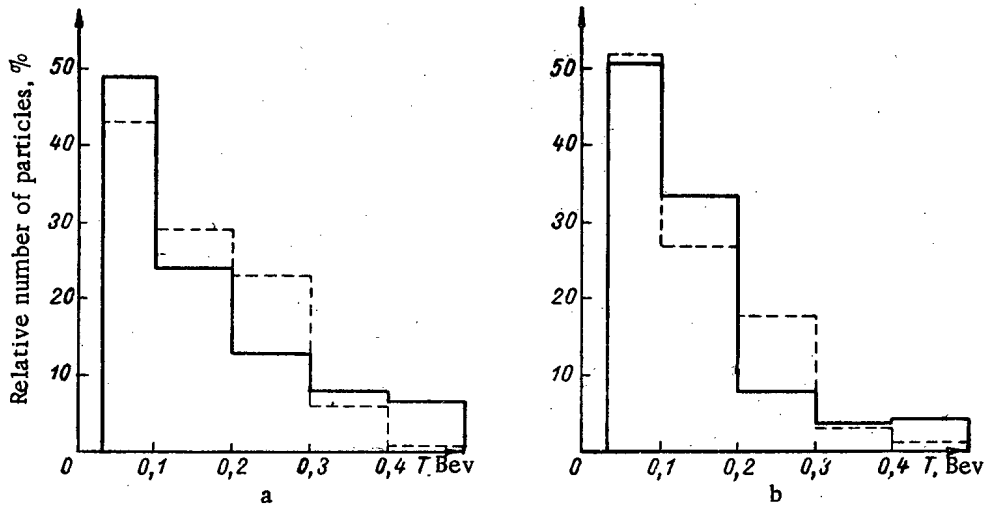

Fig. 3. Energy distribution of cascade particles (T is the kinetic energy): a) group of light nuclei; b) group of heavy nuclei.

As can be seen, the experimental and calculated data for the shower and cascade particles agree well; the experimental data for the evaporation particles with black traces can also agree with the calculated data; however,

the results of the calculations depend to a large extent on actual assumptions as to the model of the nucleus.

Together with arguments against the "mechanism of a tube" given in [1], the results of our calculations indicate that at an energy of 9 Bev and at lower energies a mechanism of intranuclear cascade is realized.

LITERATURE CITED

1. V. Barashenkov et al., Nucl. Phys. 14, 522 (1959/60).
2. V. S. Barashenkov, et al., Atomnaya Énergiya 7, 4, 376 (1959).
3. N. P. Bogachev et al., Zhur. Éksp. i Teoret. Fiz. 38, 432 (1960).
4. G. B. Zhdanov et al., Zhur. Éksp. i Teoret. Fiz. 37, 620 (1959).
5. Yu. T. Lukin et al., Zhur. Éksp. i Teoret. Fiz. 38, 1074 (1960).
6. N. Metropolis et al., Phys. Rev. 110, 185 204 (1958).

MEASURING THE RADIATION CAPTURE CROSS SECTIONS OF FAST NEUTRONS OF I^{127}

Yu. Ya. Stavisskii, V. A. Tolstikov, and V. N. Kononov

Translated from Atomnaya Énergiya, Vol. 10, No. 2, pp. 158-160, February, 1961
Original article submitted July 14, 1960

The isotope of iodine I^{127} can be used as a standard [1,2] when carrying out activation measurements. It has a convenient half life (25 min), a fairly high fast neutron radiation capture cross section and a known thermal neutron capture cross section.

However, until recently there were no data on fast neutron capture cross sections of I^{127} over a wide range of energies. Paper [3], the data of which were often used as a basis, is in sharp contradiction to the recently published data [4-6] and in all probability its results are erroneous. However, in [4-6] also, the range of energies of 0.01-2.5 Mev which is important in practical applications is not covered by measurements made with one method. The results of these papers also differ from one another.

In the present work, carried out in 1958-1959, the dependence of the radiation capture cross section of neutrons with energies of 0.02-2.5 Mev of I^{127} were determined by the activation method [7]. Specimens of iodine and a fission chamber with a layer of U^{235} were irradiated together by a stream of fast neutrons. The applied β-activity was measured by end-window beta-counters. The course of the cross section of radiation capture of I^{127} neutrons was calculated from the dependence of the fission cross section of U^{235} on the neutron energy. Mean values of the fission cross sections of U^{235} were used (see the continuous curve in [8]).

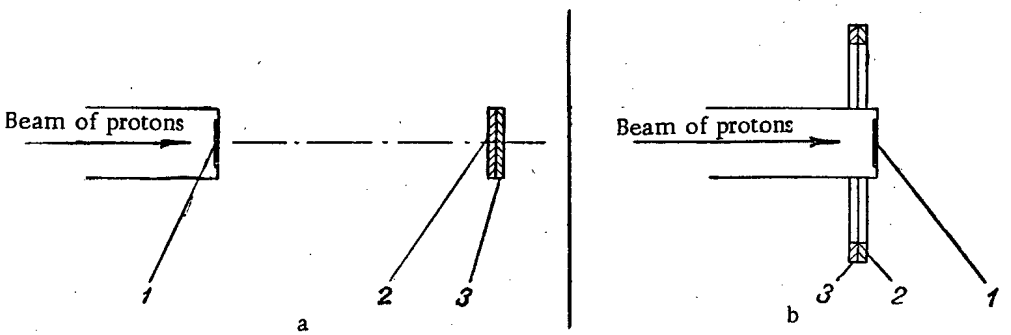

Fig. 1. Geometrical conditions under which the specimens and fission chamber were irradiated.

The source of fast neutrons was the reaction $T(p,n)He^3$, taking place in a Van de Graaf accelerator. A tritium target was used of 20 kev thickness.

The irradiation of neutrons with energies > 300 kev was carried out at an angle of 0° with respect to the direction of the beam of accelerated protons (Fig. 1a). The specimens were in the form of a disc of 20 mm diameter; they were placed at a distance of 45 mm from the center of the target close to the layer of U^{235}. Irradiation by neutrons with energies of < 300 kev were carried out at an angle of 100° with respect to the direction of the beam of accelerated protons (Fig. 1b). The specimens were in the form of rings of height 0.7 mm, external diameter 40 mm and internal diameter 28.5. The fission chamber was also in the form of a ring.

The measurements at angles of 0 and 100° with respect to the direction of the proton beam were carried out with a certain "overlapping" with regard to the neutron energy. The coincidence of cross sections in the overlapping regions of energies indicated the reliability of the measurements.

The effect from neutrons scattered by the walls of the container did not exceed 0.3%. It was determined from the deviation of the law of neutron flux decay with distance from the law $1/R^2$.

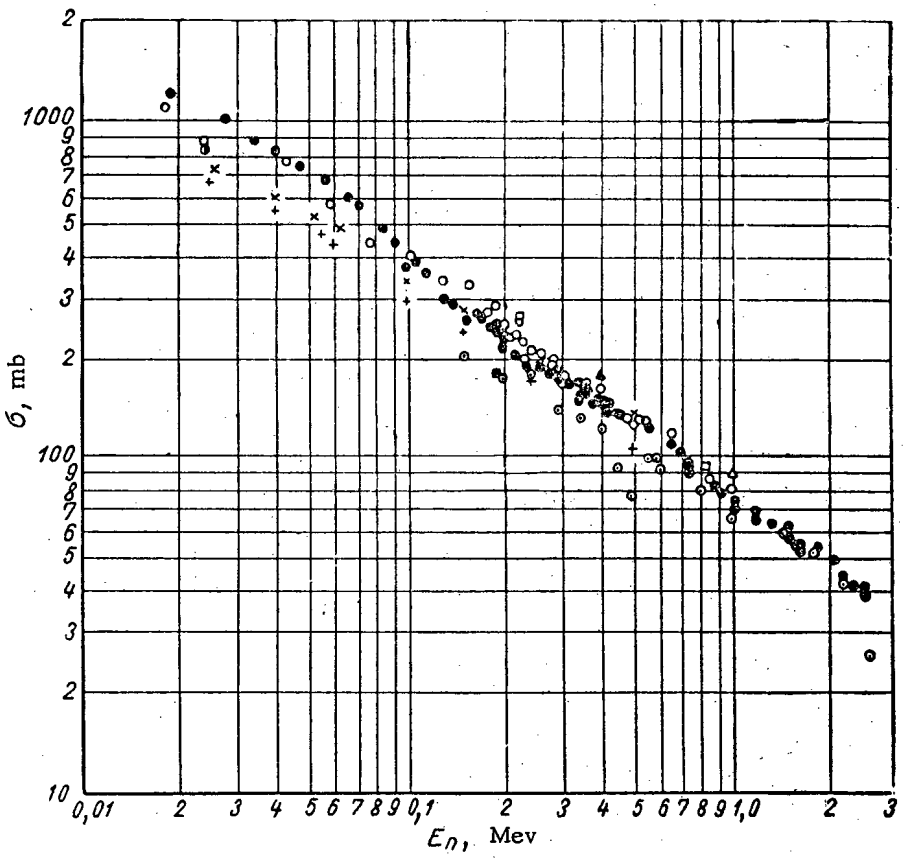

Fig. 2. The dependence of the neutron radiation capture cross section of I^{127} on the neutron energies. Data of particles: ●–the present; ◑–[1]; ⊙–[4]; ○–[15]; ×–[6]; △–[10]; □–[11]; +–[12]; ◙–[13]; ▲–[14].

The contribution of neutrons scattered in the target backing was found by calculation. The correction to the ratio $(A_{I127}/A_{U235})^b$ due to the scattered neutrons did not exceed several percent, which was confirmed by the coincidence of values of cross sections obtained in measurements at angles of 0-and 100°. Calibration measurements with thermal neutrons were carried out in the thermal neutrons was taken equal to 5.6 ± 0.3 b [8]. The fission cross section of U^{235} by thermal neutrons, equal to 582 ± 4 b, was taken from [9].

Errors in the obtained values of radiation capture cross sections of I^{127} neutrons were mainly determined by errors in the fission cross sections of U^{235}, which were ~25% for $E_n < 60$ kev, ~12% for $E_n = 60-150$ kev, ~8% for neutrons of higher energies [5].

The results of the measurements together with the data of other authors are given in Fig. 2.

In the investigated range of neutron energies the radiation capture cross section of I^{127} decays monotonously; within the limits of error in the measurement the experimental points lie on a curve of $E^{-0.7}$. The smooth dependence of the radiation capture cross section of I^{127} on the neutron energy is a very valuable factor when using this cross section as a standard in activation measurements. In the range of energies of 0.02-1 Mev our measurements agree well with the data of [5] within the limits. In the range of energies 0.15-1 Mev the values of the cross sections obtained in [4] are about 20% lower than our values, whereas in the region of energies 1-2.5 Mev they agree well.

The data of [10, 11] (the data of the last paper were obtained by the transmission method in spherical geometry) are also in good agreement with our work. For neutrons with energies of 0.01-0.2 Mev the cross sections given in [6, 12,13] are about 15-20% lower than the values obtained in the present work. These difference may be due to errors in the fission cross sections of U^{235} which in this region of energies are known with a relatively poor accuracy.

The authors would like to thank A. I. Leipunskii, O. D. Kazachkovskii,and V. S. Stavinskii for their interest in the work and for valuable discussions.

LITERATURE CITED

1. R. Macklin, N. Lazar, and W. Lyon. Phys. Rev. 107, 504 (1957).
2. A. I. Leipunskii et al., Transactions of the Second International Conference on the Peaceful Uses of Atomic Energy (Geneva, 1958). Reports of Soviet Scientists. Vol. 1. Nuclear Physics [in Russian] (Moscow, Atomic Energy Press, 1959) p. 136.
3. H. Martin and R. Taschek, Phys. Rev. 89, 1302 (1953).
4. A. Johnsrud, M. Silbert,and H. Barschall, Phys. Rev. 116, 927 (1959).
5. S. Bame and R. Cubitt, Phys. Rev. 113, 256 (1959).
6. F. Gabbard, R. Davis,and T. Bonner, Phys. Rev. 114, 201 (1959).
7. Yu. Ya. Stavisskii and V. A. Tolstikov, Atomnaya Énergiya 7, 3, 259 (1959).*
8. D. Hughes and R. Schwartz, Neutron Cross Sections, New York, 1958.
9. D. Hughes, Nucleonics 17, No. 1, 134 (1959).
10. D. Hughes, R. Gart, and D. Levin, Phys. Rev. 91, 1423 (1953).
11. T. S. Belanova, Atomnaya Énergiya 8, 6 549 (1960).*
12. Unpublished work of the Rice Institute, results given in [8].
13. W. Lyon and R. Macklin, Phys. Rev. 114, 1619 (1959).
14. B. Diven, Transactions of the Second International Conference on the Peaceful Uses of Atomic Energy (Geneva, 1958). Selected Reports of non-Soviet Scientists. Vol. 2. Neutron Physics [in Russian] (Moscow, Atomic Energy Press, 1959) p. 233.

*Original Russian pagination. See C. B. translation.

A BETA-SOURCE BASED ON Au^{198} FOR THE INVESTIGATION OF PHYSICAL PROPERTIES OF SUBSTANCES DURING IRRADIATION

M. A. Mokul'skii and Yu. S. Lazurkin

Translated from Atomnaya Énergiya, Vol. 10, No. 2, pp. 160-162, February, 1961
Original article submitted May 7, 1960

For investigations into the action of radiation on a substance in many cases it is sufficient to have an apparatus giving in a small volume (about 100 mm^3) an intensity of irradiation of the order of several hundred rads per second.

A working instrument of this type is described below (Fig. 1). The source of radiation is a gold tip of a bronze needle, in the form of a tube of gold foil with walls of 0.2 mm thickness, external diameter 0.85 mm and 10 mm length.

The needle with the gold tip 1 is fastened in an aluminum holder 2 and kept in a protective container of lead 3 weighing 14 kg.

The holder is fastened on the aluminum bar and is lowered into one of the channels of the reactor [1], where the thermal neutrons flux is $1.6 \cdot 10^{13}$ $cm^{-2} \cdot sec^{-1}$ (when operating at nominal power). After irradiation in this stream for 10^5 sec, $3 \cdot 10^{16}$ atoms of Au^{198} appear in the gold tip, decaying according to the reaction $Au^{198} \rightarrow \beta^- + Hg^{198}$ with a half life of 64.6 hr and maximum energy of the β-spectrum of 0.97 Mev. The decay is accompanied by γ-radiation with an energy of 0.411 Mev. The amount of Au^{198} obtained due to this irradiation in the reactor corresponds to an activity of ~2.5C.

Irradiation of Specimens in a Working Container. The specimens are in the form of a tube 4 (see Fig. 1) of diameter 1-2/5-8 mm of the investigated material into which the gold needle is inserted. For low-temperature irradiation the specimens are placed at the axis of a Dewar vessel of foam plastic 5, placed in a steel working container 6 with walls of thickness 8-100 mm. The protective container with the needle on a steel rod is placed on the working container and the needle is put into the specimen. Screw clamps 8 are used to hold the rod 7.

With an activity of the source of 2.5 C, in the gold itself and in the specimen due to retardation of the electrons the energy liberated is $5 \cdot 10^4$ $erg \cdot sec^{-1}$.

Electron Paramagnetic Resonance (EPR) in Irradiated Specimens. By means of a spectrometer similar to that described in [2] with high frequency modulation of the magnetic field measurements were made of the EPR spectra in specimens irradiated by the method described at room temperature and at 77°K [3]. The EPR spectra of polymethyl methacrylate, teflon and polyethylene, irradiated at a temperature of 20°C with different doses have the usual form.

Using the EPR, measurements were made of the dose distribution along the radii of the specimens. A strip of teflon of thickness 0.1 mm was coiled in a tube similar in dimensions to the usual specimens. After irradiation the strip was cut up into pieces corresponding to different layers and using EPR the number of peroxide radicals in each piece was measured. The number of radicals is proportional to the dose obtained by the material. This holds for doses (of the order of several megarad), which were used in our experiment. The dose distribution along the radius of the specimen is shown in Fig. 2. The path of the fastest β-electrons of Au^{198} in teflon does not exceed 2 mm [2]. Consequently, the layers of specimen at distances greater than 2 mm from the surface obtain a dose only from the γ-rays. The absolute value of the dose from γ-rays was measured by dosimetric instruments at distances (from the radiator) of 250 mm and more. Knowing the geometry of the source it is possible to calculate from these data the dose obtained from γ-rays by any layers of the specimen (see Fig. 2, broken curve) and also to obtain the absolute value of the dose, corresponding to the points of Fig. 2 lying between 2 and 3 mm. Consequently, it is possible to calculate the absolute value of the total dose in each layer (the continuous curve of Fig. 2).

It has been found that outside the source ~10% of the energy of β-electrons is liberated, i.e. a layer of speci-

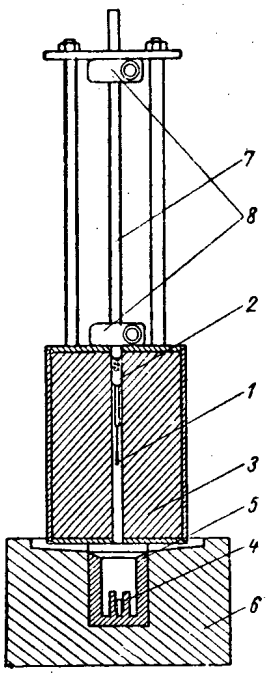

Fig. 1. Diagram of "gold needle" apparatus.

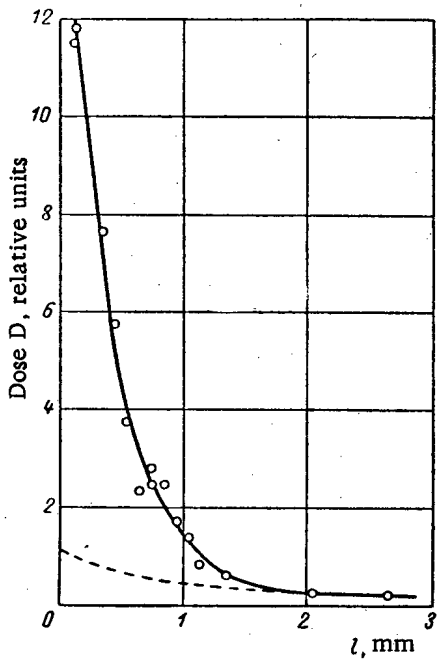

Fig. 2. Dose distribution along the radius of the teflon specimen irradiated by the gold needle. l) distance from the inside surface of specimen (tube); — total dose; - - - dose from γ -rays.

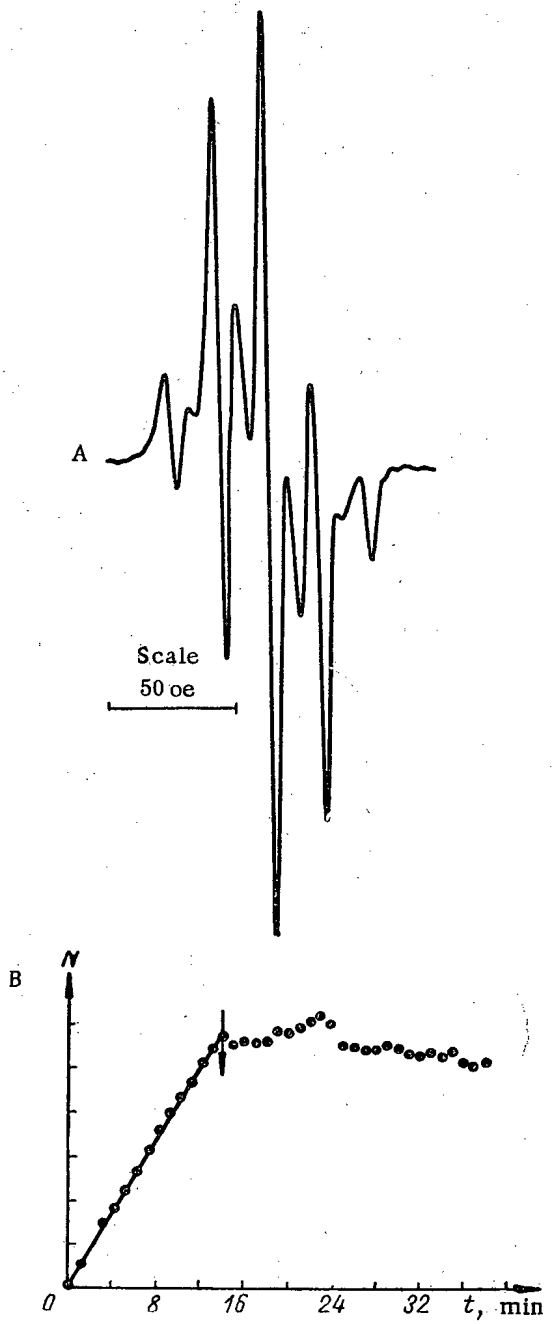

Fig. 3. EPR spectrum of polymethyl methacrylate during the irradiation process: A) spectrum; B) dependence of the value of the signal on time. The arrow indicates the instant of removal of the needle from the specimen.

men of thickness 1 mm obtains a mean dose of ~200-250 rad/sec. The contribution of the γ -rays to the total dose is ~16%. for the whole teflon specimen of the given thickness.

* Similar experiments were first conducted in the Institute of Chemical Physics, Academy of Sciences, USSR [4] using a linear electron accelerator at 1.6 Mev.

Observing EPR in the Process of Irradiation. The small dimensions of the source (gold needle) and the comparatively high intensity of irradiation make it possible to use this source to obtain EPR spectra in the irradiation of different materials*.

The specimen in the form of a tube was placed in a Dewar vessel in the resonator of the EPR-spectrometer. The needle on a long bar was placed inside the specimen. This led to a slight detuning of the resonator (no greater than on the introduction of ordinary specimens). Figure 3 shows the EPR spectrum in irradiated polymethyl methacrylate and the change in value of the signal during irradiation and after its completion.

Creep in Teflon Under Irradiation. In [3] there was a description of the reversible acceleration of relaxation processes in polymers under the action of irradiation in a reactor. It was of interest to find out whether this effect would be observed under the action of irradiation by light particles when the number of produced nuclear recoils is negligibly small compared with the case of irradiation in a reactor with high fast-neutron fluxes.

During irradiation by electrons the needle was placed parallel to the plane of the specimen at a distance of 1 mm from its center. The dose obtained by the specimen was distributed unevenly throughout its thickness and length. The mean dose rate throughout the volume of the specimen was 10-20 rad/sec. The needle was brought to the specimen periodically (six times in all). The tensile deformation of the specimen was recorded continuously* by the ÉPP-09 recording apparatus. The obtained curve is given in Fig. 4. Despite the certain number of random inflections on the curve (connected with friction in the instrument) the effect of reversible acceleration of creep can be clearly seen.

The described experiment was not intended to give quantitative results. However, it is fundamentally important and indicates that the reversible acceleration of relaxation processes in polymers is not connected with the specific action of heavy particles.

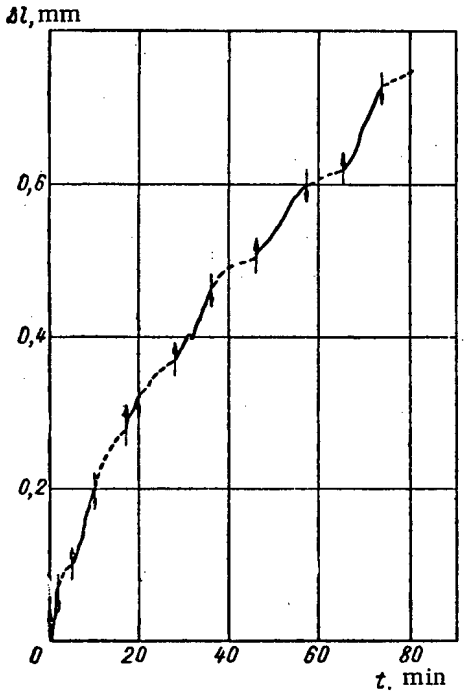

Fig. 4. Creep in teflon. Stress 0.35 kg/mm^2, temperature 18°C. The instants of switching on and switching off the irradiation are shown by arrows (top-switching on).

The small dimensions of the sources based on radioactive gold, the ease of protection from soft γ-radiation, the comparatively long half life and the large activation cross section make these sources very convenient for much work on the irradiation of materials. Using these sources it would presumably be possible to irradiate materials at the temperature of liquid helium simultaneously with the recording of the EPR spectra or with other measurements. The configuration of the radiators for many experiments should be different (gold disc, two parallel gold discs, thin-walled tube, etc.). The choice of the shape of the source is especially important in those cases where it is essential to have approximately the same dose rate throughout the whole volume of the specimen.

LITERATURE CITED

1. Yu. G. Nikolaev, Reactor Construction and the Theory of Reactors. Reports of the Soviet Delegation to the International Conference on the Peaceful Uses of Atomic Energy. (Geneva, 1955) [in Russian] (Moscow, Acad. Sci. USSR Press, 1955) p. 119.
2. A. G. Semenov and N. N. Bubnov, Pribory i Tekhnika Éksperimenta 1, 92 (1959).
3. A. G. Kiselov, M. A. Mokul'skii, and Yu. S. Lazurkin, Vysokomolekulyarnye Soedineniya 2, 11 (1960).
4. Yu. N. Molin et al., Doklady Akad. Nauk SSSR 123, 5, 882 (1959).
5. M. A. Mokul'skii, Yu. S. Lazurkin and M. B. Fiveiskii, Vysokomolekulyarnye Soedineniya, 2, 1, 110 (1960).

* The measurement was made by M. E. Fiveiskii on an instrument which he designed for the remote recording of creep curves.

A GENERATOR PRODUCING A HIGH FLUX OF 14 OR 2.5 Mev NEUTRONS

V. I. Petrov

Translated from Atomnaya Énergiya, Vol. 10, No. 2, pp. 163-166, February, 1961
Original article submitted September 1, 1960

High-voltage accelerators of 150–200 kev are generally used for the production of 14 and 2.5 Mev neutrons. In the majority of cases, the maximum D-T neutron flux is slightly more than 10^{10} n/sec. An increase in flux to 10^{11} n/sec and more (in the case of 2.5 Mev neutrons, to more than 10^9 n/sec) introduces certain technical difficulties which are associated both with the production of a sufficiently intense beam of deuterons in the accelerator tube and with the limiting thermal conditions for tritiated and deuterated targets.

In this letter a neutron generator is described which produces a D-T neutron flux greater than 10^{11} n/sec and a D-D neutron flux greater than 10^9 n/sec.

The construction of the generator is shown in the figure. A high-frequency-discharge ion source is used in the generator. The basic characteristics of the source are as follows: deuterium ion current, 9–11 ma; deuteron content, ~85%; deuterium consumption, ~53 cm^3/hr; length of ion extraction system channel, 10 mm; channel diameter, 3.5 mm; extraction voltage, 7–8 kv; high-frequency-generator power consumption, 500–600 w; generator frequency, 25 Mc. The power supply circuit for the source is assembled in a separate unit. Transmission line voltage to the unit is fed through four transformers which maintain the voltage at 250 kv (transformer ratio is 1:1). Operational control of the source is carried out from a control panel by adjustment of the voltages which are fed into the primary windings of the transformers. During operation, the ion source is continuously cooled by a stream of air from a fan.

The construction of the neutron generator acceleration chamber provides a minimum distance from ion source to target. That type of construction simplifies the problems of focussing and accelerating an intense ion beam. The chamber is made up of two sections in which the electrodes for the focussing and accelerating gaps are located. A porcelain cylinder serves as insulator for the focussing gap. The accelerating gap electrodes are located within an insulator made of a plastic similar to lucite. The shape and location of the electrodes keep scattered charged particles from striking the internal insulator surfaces.

High vacuum is produced in the accelerating chamber by a diffusion pump (pumping speed 1000 liters/sec) and a forepump. The diffusion pump is connected to the chamber through an angle valve on which an oil vapor trap cooled by liquid nitrogen is built. The 300-liter forevacuum tank is also used as a base for the acceleration chamber. The working vacuum in the chamber with an ion beam current of several milliamperes amounts to about 1×10^{-5} mm Hg.

An electromagnet which produces a transverse magnetic field across the path of the ion beam is placed at the exit of the acceleration chamber. The electromagnet winding is made of one layer of water-cooled copper tubing with a 5 x 3 mm bore. The need for the introduction of a magnet became apparent during the first experiments on ion beam acceleration. With an ion beam current of several milliamperes, the absence of a magnetic field led to the formation of an opposing electron current in the acceleration chamber comparable in magnitude to the ion current. The electron current upset the stable operation of the ion source; in a number of instances, it melted source walls, caused electrode heating, loss of vacuum, and high-voltage breakdown. The introduction of a transverse magnetic field very definitely removed the opposing electron current and associated phenomena. In addition, target operating conditions have been improved by the introduction of an electromagnet since, in the presence of a transverse field (of a particular strength), the target is freed from thermal loading by molecular ions in the beam, and is significantly less contaminated by deposits of organic vapors.

The accelerator high-voltage supply is obtained from two high-voltage devices: for the accelerating gap, from a 200 kv constant voltage generator at 20 ma load, and for the focussing gap, from a 30 kv, 20 ma rectifier. The high voltage generator is based on a one-stage voltage doubling circuit. The basic elements of the generator are a type

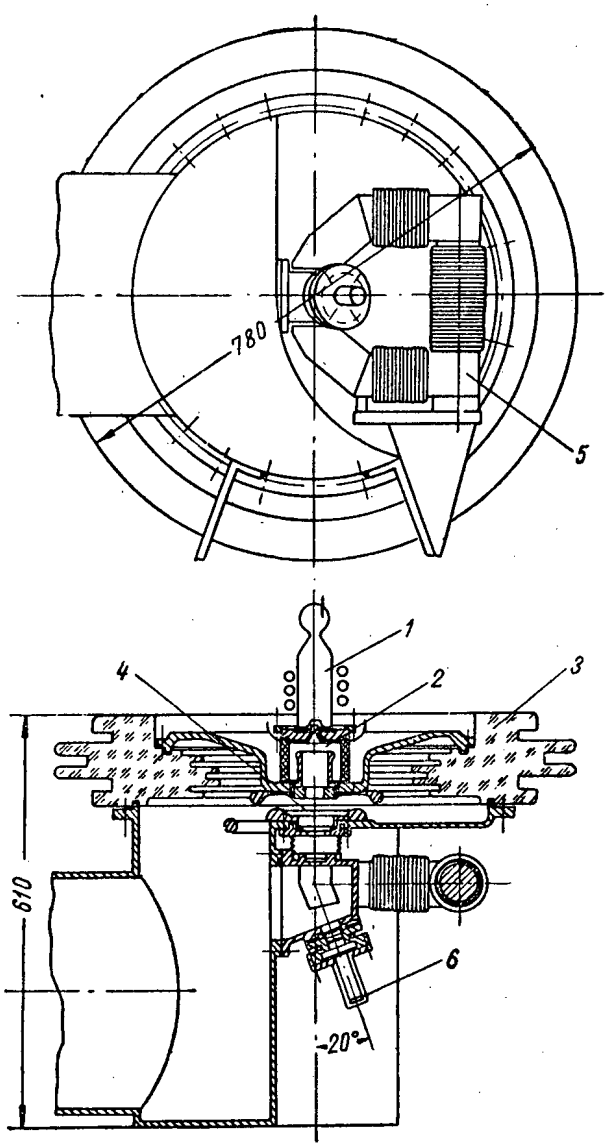

Construction of Neutron Generator (dimensions in millimeters): 1) Ion source; 2) focussing gap; 3) insulator; 4) accelerating gap; 5) electromagnet; 6) target.

IM-100-0.1 condenser, a KR-220 kenotron, and a type IOM-100/25 high voltage transformer. For the high-voltage supply of the focussing gap, a high-voltage rectifier based on a full-wave bridge circuit employing a KRMM-110 kenotron is used. Voltage to the rectifier is fed through a special 200 kv transformer. Under operating conditions, the voltage to the focussing gap electrodes is 23-25 kv, that to the accelerating gap electrodes is 170-180 kv. The ion source extraction voltage of 7-8 kv must be added to that.

Zirconium targets, saturated with tritium or deuterium on silver or copper backings 25 mm in diameter and 1.5-2 mm thick are used in the neutron generator. During operation, the targets are cooled by a stream of running water. Despite a satisfactorily high rate of cooling, the maximum permissiable ion current at the target at full accelerating voltage does not exceed 2.5-3 ma. An increase in the permissible current has been achieved by a circular displacement of the beam on the target through the use of a 4 kv, 5 kc, a.c. voltage. The voltage is fed, with phase shift, to two deflection plates located in a special exit structure. In this way, the permissible current at the target has been increased to 5 ma.

The neutron generator was placed in operation in 1959. Assembly and adjustment of the apparatus were carried out with the assistance of V. P. Zyuzin, R. N. Morozov, and V. P. Suslov. The following data, characteristic of machine operation, were obtained: maximum flux of 14 Mev neutrons, 5.3×10^{11} n/sec; maximum flux of 2.5 Mev neutrons, 5.0×10^{9} n/sec; operating deuteron current at the target, up to 5 ma; full accelerating voltage, 200-210 kv; maximum current of focussed deuterium ions at full accelerating voltage, 10 ma.

THE EFFECT OF RADIATION ON THE ELECTROCHEMICAL BEHAVIOR OF 1Kh18N9T STEEL

V. V. Gerasimov and V. N. Aleksandrova

Translated from Atomnaya Énergiya, Vol. 10, No. 2, pp. 164-166, February, 1961
Original article submitted September 1, 1960

The aim of this work was to study the electrochemical behavior of 1Kh18N9T steel during irradiation by thermal neutrons.

In the tests a special electrolytic glass cell was used (Fig. 1) of diameter 20 mm and height 400 mm. The thickness of the cell wall was ~1 mm. In the upper part of the cell there was a calomel electrode and an electrolytic switch. Tests were carried out on specimens of 1Kh18N9T steel. The specimen dimensions were 1 x 10 x 235 mm. The chemical composition of 1Kh18N9T steel is as follows: 0.07 weight% C; 1.23 weight.% Mn; 19.1 weight.% Cr; 10.5 weight.% Ni; 0.53 weight.% Ti.

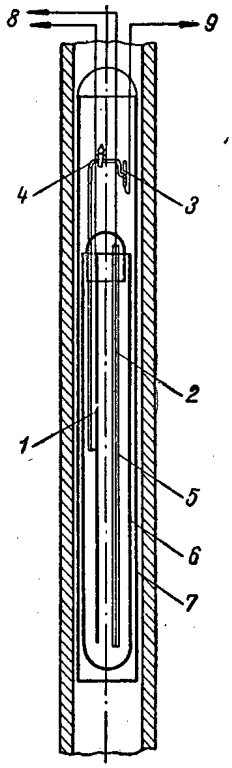

Fig. 1. Electrical cell: 1) Specimen; 2) auxilliary electrode; 3) calomel electrode; 4) electrolytic switch; 5) tube; 6) ampoule; 7) case; 8) to circuit; 9) to potentiometer.

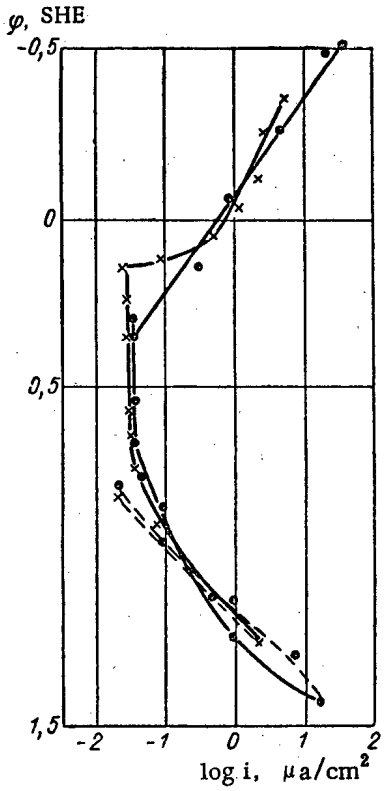

Fig. 2. Anodic and cathodic polarization of 1Kh18N9T steel in a 0.01 N solution of Na_2SO_4: —●—under conditions of irradiation at 80-90°C (——●—— curves taken under the same conditions in the reverse order; —x——without irradiation at 85°C (——x——curves taken under the same conditions in the reverse order).

Before the test the surface of the specimen was carefully cleaned with No. 180 polishing paper. The potential of the specimen was compared with that of a saturated calomel electrode. To avoid contamination of the investigated solution with potassium chloride the electrolytic switch (after drawing in potassium chloride) was washed with the working solution on the side of the specimen. The distance from the end of the electrolytic switch to the specimen in a given experiment does not affect the measured potential: with maximum removal of the end of the switch from the specimen (by ~5 mm) the potential decreases only by 0.015 v compared with the potential measured with minimum distance. The potential is practically unchanged along the length of the specimen: with a current of up to 100 μa the potential at the ends of the specimen is 0.02 v greater than the potential of the middle part.

The auxiliary specimen was a 1-mm diameter wire of 1Kh18N9T steel insulated from the investigated specimen by a 5-mm diameter glass tube. The investigations were carried out in a 0.01 N solution of sodium sulfate and a 0.01 N solution of sodium chloride. The volume of liquid poured into the cell was ~20 ml.

The current intensity was measured by the M-82 and M-91 milliammeters, the potential was measured by the LP-5 potentiometer. The current was provided by dry BAS-80 anode batteries. The electrolytic cell was protected from mechanical damage by a cover made of foil (1Kh18N9T steel) with wall thickness 0.1 mm. Between the cover and the wall of the cell near the middle part of the specimen there were the junctions of a chromel-copel thermocouple.

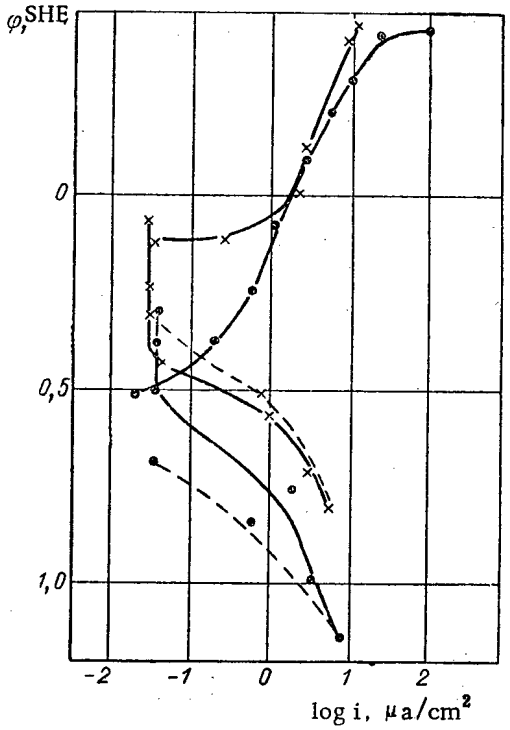

Fig. 3. Anodic and cathodic polarization of 1Kh18N9T steel in a 0.01 N solution of NaCl: —●— under conditions of irradiation at 80-90°C; —x— without irradiation at 85°C. (For the explanation of the broken curves see the caption to Fig. 2).

The Stationary Potential of 1Kh18N9T Steel at 80-90°C in Irradiated and Nonirradiated Solutions (Volts with Respect to a Standard Hydrogen Electrode (SHE))

Medium	Without irradiation		During irradiation	
	before polarization	3 hr after polarization	before polarization	3 hr after polarization
0,01 *N* solution Na_2SO_4	0,133	0,318	0,403	0,673
0,01 *N* solution NaCl	0,083	0,243	0,503	0,583

In order to study the electrochemical behavior of 1Kh18N9T steel during irradiation the cell was placed in the active zone of the reactor. The experiments were carried out with a flux of 10^{12} neutrons/cm^2·sec and a cell temperature of 80-90°C. Each experiment was performed twice. For comparison the experiments were repeated without irradiation in a thermostat at 85°C. The results of the measurements are given in the table.

The kinetics of the electrode processes were studied by the potentiostatic method. One hour after immersing the cell in the channel of the reactor the stationary potential was measured and the external current applied. The current potential and temperature were measured every 10 min. The current was assumed to be steady if, for a given value of the potential, it did not change in 1 hr. At first the cathode polarization curve was taken and then the anode polarization curve. Three to four hours after the end of polarization the stationary potential was again measured. The obtained polarization curves are shown in Figs. 2 and 3.

The irradiation did not change the kinetics of the anode process of 1Kh18N9T steel in a 0.01 N solution of sodium sulfate. The rate of the anode process in the passive region and in the region of superpassivation, the values of the breakdown potential during irradiation are the same as without irradiation.

In a 0.01 N solution of sodium chloride during irradiation the character of the anodic polarization curve of 1Kh18N9T steel is preserved. The rate of the anode process in the passive region is practically unchanged. However, the breakdown potential and the section of the anodic polarization curve corresponding to the superpassivation region are displaced toward the positive side by 100-150 mv.

In both tested solutions during irradiation the sections of the cathodic polarization curves corresponding to the ionization of oxygen were displaced toward the positive side. The latter fact points to an increase in the rate of the cathode process, which was caused by the presence in the solution of radiolysis products—short-lived radicals and hydrogen peroxide.

An increase in the rate of the cathode process leads to displacement of the stationary potential of steel toward the positive side (see table) due to which the region of the passive state decreases. In solutions where the region of the passive state is small, for example in chlorides and especially in the presence of tensile stresses in the metal, the displacement of the stationary potential toward the positive side under the action of irradiation can bring steel into the superpassivation region. The latter fact can lead to an increase in the effectiveness of the corrosion process. During irradiation in solutions of sodium sulfate a stationary potential is set up corresponding to the region of the passive state, in a solution of chlorides a stationary potential is set up close to the breakdown potential or corresponding to the region of superpassivation (see table and Figs. 2 and 3).

A METHOD OF INVESTIGATING PROCESSES OF RETARDATION OF FISSION FRAGMENTS IN METALS AND ALLOYS

N. A. Protopov, Yu. B. Shishkin, V. M. Kul'gavchuk, and V. I. Sobolev

Translated from Atomnaya Énergiya, Vol. 10, No. 2, pp. 166-168, February, 1961
Original article submitted November 21, 1959

The growing interest in the problem of making fuel elements, especially for the operation of nuclear reactors in energy-stressed systems and with deep combustion of the fissile isotope, requires a more detailed study of the elementary processes of retardation of fission fragments. Up to the present these processes have been insufficiently studied and it has only been established that there are regions of a thermal peak and their volume [1]. Some work was carried out in 1946 [2] with a noncollimated beam of fragments; in 1957 work was published [3] in which, using the mass spectrograph method for the separation of fragments, paths and retardation curves were determined for a number of metals such as aluminum, nickel and gold. To measure the energy of the fragments a CsI(Tl) scintillation counter was used, the sensitivity of which was determined by means of α-particles of polonium. However, the complexity of this method unfortunately limits its wide application when studying the retardation of fragments in a number of metals and alloys which are of the most interest for the technology of fuel element preparation.

In application to the metallurgy of nuclear fuel the problem of developing a similar method is considerably simplified if it is borne in mind that in this case considerable importance attaches to the duration of the regions of the thermal peak and the density of energy liberation, depending on specific losses in energy of the fragment, which in the final analysis characterize the scale of local damage in a solid and the rate of change in its physicomechanical properties. The difficulties belonging to problems of nuclear physics and connected with the identification of fragments by the masses and the nuclear charge are therefore eliminated since the specific losses in energy and paths of the fragments can be determined directly experimentally. Therefore, for the problems under consideration of considerable importance is the curve of specific losses in energy of the fragment as a function of its path.

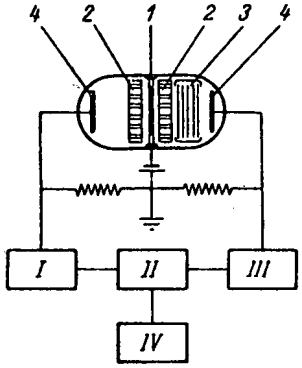

Fig. 1a. The main arrangement of the apparatus for studying the passage of U^{235} fission fragments in metals and alloys.

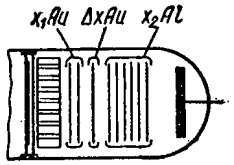

Fig. 1b. Arrangement of experiment for studying specific energy losses of fission fragments in metals by the method of substitution.

Figure 1a shows a scheme of experiments which demonstrate the essence of the method developed by the authors. The main part of the scheme is the ionization fission chamber. The impulses formed in both channels of the chamber are fed through amplifiers I and III to a circuit of double coincidences II with a resolving time of 0.5 μsec. The impulses are counted by the circuit IV with a mechanical counter. The fission chamber is made of brass and has a leakproof valve (not shown on the diagram) to evacuate the system and fill it with argon.

The chamber consists of the following elements (see Figs. 1a): 1—U_3O_8 preparation (~ 0.1 mg/cm^2, enriched up to 90% with U^{235}), applied to aluminum foil of thickness 0.4 mg/cm^2 and placed in the middle of the chamber; 2—collimators; 3—foil stack with variable thickness of the investigated metal; 4—collecting electrodes.

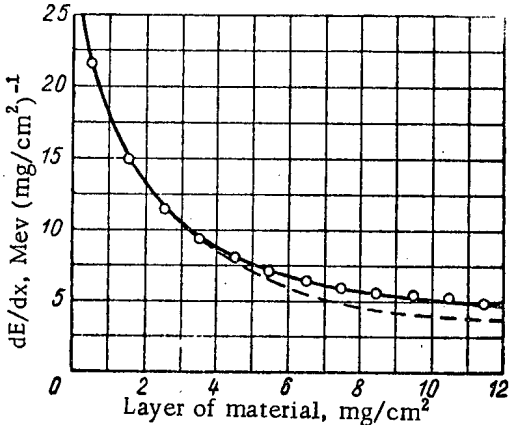

Fig. 2. Dependence of the specific losses of a light group of fission fragments on the path in gold: ——curve taken from [3]; ——data of authors.

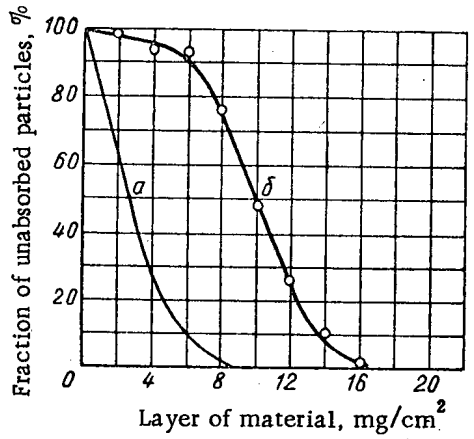

Fig. 3. Dependence of yield of fission fragments on the path in gold: a) curve taken from [2]; b) data of the authors.

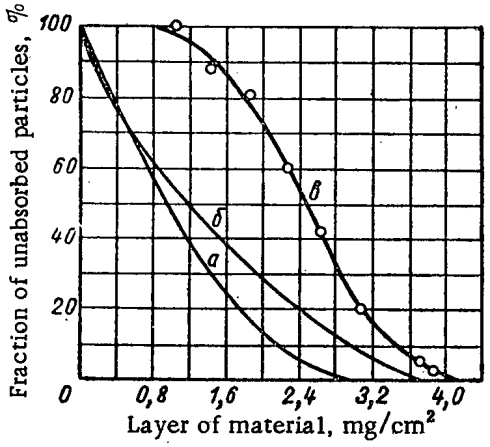

Fig. 4. Dependence of yield of fission fragments on the path in aluminum: a) curve taken from [2], plotted with an ionization fission chamber; b) curve taken from [2], plotted by radiochemical measurements; c) data of authors.

The thickness of the collimators and the pressure of the argon (~ 100 mm Hg) in the chamber are chosen so that the energy losses of the fragment on passing through the collimator can be neglected (~3-5 Mev). The use of a fission chamber and coincidence circuit eliminates errors connected with counting false impulses arising from the γ-quanta and the recoil nuclei. This means that all the measurements can be made in the nuclear reactor with a thermal neutron flux, changing according to the conditions of the experiments in the limits 10^6-10^8 neutrons/cm^2·sec.

We will illustrate the operation of the circuit with the example of liberation of fragments with the same path, we will determine their path and the specific energy losses. We will suppose that in each channel of the chamber behind the collimator there are foil stacks of the investigated material of the same thickness. We will designate the initial number of coinciding impulses by N_0 for zero thickness of the material. If d is increased the same in each channel then the number of coincidences will decrease. For a certain value $d = d_c$, the number of coincidences will be equal to zero or a very small part α of N_0, depending on the sensitivity of the circuit. In this case d_c will presumably characterize the total path of the considered fragments.

To measure the specific energy losses in this case we proceed in the following way. In both channels the same foil stacks are placed (with thickness $d = d_c$) of a material for which the curve of the dependence of specific energy losses on the path of the particles is known. Then in one of the channels all foils of the material with known losses, starting with the first, are successively replaced by foils of the investigated material (Fig. 1b); by selecting the thickness, constancy of the initial number of coincidences is obtained. Therefore, by the substitution method we determine the specific losses in the investigated material for the whole path of fragments. Throughout all measurements the second channel is kept unchanged.

To determine the path and specific losses of energy of the heavy and light groups of fragments separately, as in the previous case, we first determine N_0. Then in one of the channels the foil stack of the investigated material is dismantled until the number of coincidences becomes small compared with N_0. In this case the fragments with the maximum path will presumably be liverated. Depending on the selected value of the number of coincidences α the investigations are carried out for the same spectrum width of the fragment paths. Then, in the second channel of the chamber the foil stack of the investigated material is dismantled until the number of coincidences is reduced to zero. In this case the number of foils in the second channel characterized the total path of the corresponding heavy fragments. A similar substitution method is used to determine the specific energy losses of heavy and light groups of fragments separately, using known data on losses in any metal, for example, in aluminum.

Figure 2 shows the curve for specific energy losses during the retardation of fragments of a light group in gold, which we plotted with the described method. In these measurements $\alpha = 0.05$ and fragments were liberated with a maximum path, lying near the value 16.5 mg/cm^2. For comparison we give a curve of losses plotted by means of the graphic calculation of dE/dx from the energy-path curve taken from [3]. As can be seen, the results agree well.

Figure 3 shows a curve for the passage of fragments b, which we obtained for retardation in gold. For comparison a similar curve a is given, taken from [2]. As can be seen, the curves differ considerably. In the first place the maximum thickness of gold needed to absorb 100% of the fission fragments of U^{235} is not 9 mg/cm^2 (as in [2]) but 16.5 mg/cm^2. We notice that our measurements compare best with data of a later work [3], according to which the path for gold was equal to 13 mg/cm^2. The low value of the path in gold obtained in [2] is presumably due to the use of an insufficiently developed apparatus and method. On the other hand, our results agree with those of recently published work [4], from which it follows that the number of very light fragments with maximum paths is much greater than would be expected on the basis of earlier radiochemical measurements. In the second place, curve a is displaced some distance to the left. This is presumably due to the fact that in [2] an uncollimated beam of fragments was used.

Figure 4 gives a similar curve c for passage of fragments in aluminum and for comparison curves a and b are given, taken from [2]. The above remarks refer mainly to this case.

We notice that the curves for passage of a collimated beam of fragments take on a new importance. In fact, if the curve for passage in the material is determined by a certain function N = f(x), then the expression

$$L = N_0 l_{\min} + \int_{l_{\min}}^{l_{\max}} x f'(x)\, dx$$

(where $l_{\min}$ and $l_{\max}$ are the minimum and maximum paths of fragments in the substance respectively; N_0 is the total yield of fragments) is the total path taken by all fragments formed in unit time in unit volume of the solid. For a known value of the effective cross section S of the physical process accompanying the passage of a fragment, for example the process of homogenization of an alloy, as in [5], the product LS = dV/dt is the rate of homogenization of the alloy.

LITERATURE CITED

1. S. T. Konovbeevskii, Atomnaya Énergiya 2, 63 (1956).*
2. E. Segrè, and C. Wiegand, Phys. Rev. 70, 808 (1946).
3. B. Fulmer, Phys. Rev. 108, 1113 (1957).
4. B. S. Kovrigin and K. A. Petrzhak, Atomnaya Énergiya 4, 6, 547 (1958).*
5. S. T. Konovbeevskii et al. Atomnaya Énergiya 4, 1, 34 (1958).*

*Original Russian pagination. See C. B. translation.

THE MELTING POINT AND OTHER PROPERTIES OF THE LOWER OXIDES OF NIOBIUM

O. P. Kolchin and N. V. Sumarokova

Translated from Atomnaya Énergiya, Vol. 10, No. 2, pp. 168-170, February, 1961
Original article submitted October 4, 1960

Several lower oxides of niobium have been reported in the literature (Nb_4O, NbO, Nb_2O_2, Nb_2O_3, NbO_2, Nb_2O_4 and Nb_3O_7), although as a result of the investigations [1,2] the existence of only two of them has been established: the oxide NbO and the dioxide NbO_2. A knowledge of the properties of these oxides is essential both to determine their own possible applications and also to obtain an accurate conception of the processes taking place during the reduction of Nb_2O_5, in which the lower oxides occur as intermediate compounds, and of the processes for removing oxygen from niobium by vaporation in the form of lower oxides by heating the metal in vacuum. Yet contradictory and even inaccurate information about the properties of the lower oxides is frequently met with in the literature. For example, a "trioxide" of niobium, Nb_2O_3, with a melting point of 1772°C has been described [3], although in actuality this is not a separate oxide but a two-phase product.

Published data on the true lower oxides of niobium are very meager [2,4-8].

We have attempted to determine a number of properties of these lower oxides.

Initial Materials

Niobium dioxide was prepared by reducing the pentoxide with lamp black in vaccum at 1300 and 1700°C, and the oxide was prepared by the same method from the dioxide. The initial pentoxide contained (wt.-%): < 0.5 Ta_2O_5, 0.06 SiO_2, 0.1 TiO_2, and 0.04 Fe_2O_3; during reduction in vacuum the greater part of the iron, silicon, and titanium was removed. The three specimens of dioxide that were investigated contained (wt.-%): 0.02-0.04 C and 0.006 N; they had the compositions $NbO_{1.942}$, $NbO_{1.956}$, and $NbO_{1.986}$, which all lie within the homogeneous range of the dioxide [5]. X-ray analysis showed that the product was single-phase and had the parameters $a = 4.82 \pm 0.02$ kX and $c = 2.99 \pm 0.02$ kX, which agree with the values published in [2].

The specimens of niobium oxide contained (wt.-%): 0.04-0.06 C and 0.03 N and had the compositions $NbO_{0.95}$, $NbO_{1.01}$, and $NbO_{1.02}$, which all lie within the homogeneous range of the oxide [5].

Melting Point

The dioxide and oxide were ground to powder of particle size < 0.15 mm and compressed under a pressure of 1.5-2.0 tons/cm^2 into compacts 10 mm in diam and 10 mm high. Two compacts of the oxide or dioxide were placed, one on top of the other, in a container, 17 mm in diam and 100 mm high, made of niobium sheet. Then the container was placed inside the graphite heater of a vacuum (0.5-1.0 μ Hg) electric resistance furnace in such a way that the molten top portion of the upper compact was most strongly heated. By arranging the change in this way, it was possible to avoid interaction between the molten oxide and the metal and carbon heater. It also ensured suitable conditions for measuring the temperature of the molten oxide by means of a disappearing-filament optical pyrometer without the error [3] due to the unknown emissivity of the oxide, since the distance from the surface of the oxide to the top of the container was almost five times the diameter. To confirm that the true temperature was being measured, compacts of the oxide, lamp black, and graphite were placed in the same container and in separate experiments their temperature was measured in the region close to the melting point of the oxide. In spite of the considerable difference in the emissivities of carbon and niobium oxide, the difference between the measured temperatures did not exceed 10°C, i.e. it lay within the limits of experimental error of measurements made with the pyrometer. A correction was made in the pyrometer readings only for the light absorbed by the observation window in the vacuum furnace.

Under the conditions described, the melting point of the specimens of niobium oxide investigated was 1935°C, and that of the dioxide 2080°C. The approximate error in the temperature determination was 15°C.

Figure 1 shows a photomicrograph of the melted portion of the oxide compact, and from this it can be seen that there was no second phase present in the oxide whose melting point had been determined. The single-phase character was also confirmed by x-ray analysis. This showed that the product has a parameter $\underline{a} = 4.201$ kX. It is to be noted that even with a small excess of oxygen in the product it was possible to observe the presence of a second phase, niobium dioxide, which forms a eutectic with the oxide (Fig. 2); in the x-ray phase analysis, the sensitivity of which is ~1%, this phase was not observed.

Fig. 1. Structure of pure melted niobium oxide. Etched in $HF + HNO_3$ (3:1) for 3 sec. x200.

Fig. 2. Structure of melted niobium oxide containing niobium dioxide. Etched in $HF + HNO_3$ (3:1) for 3 sec. x 200.

The discrepancy between the values found for the melting point of the dioxide and those given in the literature [9] is no doubt due to the fact that in [9] the specimens of dioxide used contained niobium oxide as impurity, and hence the data obtained from them do not relate to the true melting point of the dioxide.

It is of interest to note that the melting point we have determined for niobium dioxide is close to the erroneous value determined in 1907 for metallic niobium (1950°C) [7] and for long regarded as reliable (see, for example, [10]). It is evident that the product of the reaction of niobium with oxygen was used to determine the melting point of the metal; this is quite possible since the melted oxide is very difficult to distinguish externally from the metal: it has a metallic luster and in external appearance is similar to an ingot of niobium, though very brittle.

Volatility. Composition of the Gaseous Phase

Weighing the upper compact after heating in vacuum (0.5-1 μ Hg) at various temperatures (accuracy of weighing = 0.0002 g) showed that the oxide and dioxide of niobium began to evaporate at a significant rate at 1700°C. At 1850°C the whole of the oxide and 45 wt.-% of the dioxide had evaporated after 4 hr, and the whole of the dioxide compact had evaporated after 8 hr.

A mass-spectroscopic investigation of the dioxide specimens we obtained showed [11] that the gaseous phase over the dioxide contained only NbO_2 molecules, i.e. there was neither dissociation nor association of the molecules.

Microhardness

The microhardness of various specimens of melted niobium oxide, the compositions of which lay within the limits of homogeneity of the oxide, was 1930 kg/mm^2 and the mean value of the microhardness of the eutectic (see Fig. 2) was 794 kg/mm^2 (load = 50 g). The microhardness of the dioxide was 1720 kg/mm^2, although this value may be inaccurate since small cracks appeared in the dioxide crystals during the microhardness determinations.

Character of the Electrical Conductivity

Niobium oxide is characterized by the electrical conductivity of metals, while the dioxide is a semiconductor.

Oxidation in Air

Studies were made of two specimens of dioxide, one of which was obtained at 1300°C and had a composition corresponding to the formula $NbO_{2.00}$, while the other was obtained at 1700°C and had the composition $NbO_{1.92}$. After grinding, both specimens formed black powders with a particle size 0.15 mm. A specimen of niobium oxide with the composition $NbO_{0.914}$ was obtained at 1700°C and ground to a gray powder haveing a metallic luster and a particle size of 0.15 mm. Samples of the oxide were heated in air at a temperature of 100-300°C. After this oxygen content was determined from the increase in weight on heating in air at 800°C; the accuracy of this method of determination is ~±0.1%. The oxygen content of niobium oxide did not change on heating for up to 6 hr at 100, 150, 200, 225, 250, and 275°C; the oxygen content of the dioxide increased slightly at 275°C. However, at a temperature as low as 150°C the surface of the particles of oxide and dioxide took on a yellowish tinge and at 200°C a bronze color. Both the oxide and the dioxide were completely oxidized to the pentoxide after 6 hr at 300°C.

The author wishes to thank L. V. Mel'nikova for carrying out the metallographic analysis of niobium oxide.

LITERATURE CITED

1. G. Brauer, Naturwissenschaften 28, 30 (1940).
2. S. I. Alyamovskii, G. P. Shveikin, and P. V. Gel'd, Zhur. Neorg. Khim. 3, No. 11, 2437 (1958).
3. "High-Temperature Techniques" (edited by Campbell) [Russian translation] (IL, 1959).
4. M. P. Morozova and L. L. Getskina, Zhur. Obshchei Khim. 29, No. 4, 1049 (1959).
5. G. Brauer, Z. anorgan. und allgem. Chem. 248, H. 1 (1941).
6. O. P. Kolchin, N. V. Sumarokova, and N. P. Chuveleva, Atomnaya Énergiya 3, No. 12, 515 (1957).*
7. G. Mellor, A Comprehensive Treatise on Inorganic and Theoretical Chem. V, IX (1933).
8. H. Schäfer and M. Jori, Z. anorgan. und allgem. Chem. 277, H. 6, 341 (1954).
9. R. Elliot, Metal Progr. 76, No. 10, 242, 248 (1959).
10. Atomics and Nucl. Energy 8, No. 9, 336 (1957).
11. S. A. Shchukarev, G. A. Semenov, and K. E. Frantiseva, Zhur. Neorg. Khim. 4, No. 11, 2638 (1959).

*Original Russian pagination. See C. B translation.

THE HARDNESS OF SOME NIOBIUM-BASE ALLOYS AT HIGH TEMPERATURES

I. I. Kornilov and R. S. Polyakova

Translated from Atomnaya Énergiya, Vol. 10, No. 2, pp. 170-172, February, 1961
Original article submitted June 18, 1960

One of the principal factors in raising the high-temperature strength of alloys is the formation of multicomponent solid solutions. On account of the complexity of the chemical composition of the solid solution, and increase takes place in the strength of the chemical bond between the atoms of the various elements.

The object of the present work was to investigate the change in hardness of niobium and its alloys with temperature. The "hot" hardness method described in [1] was used in the experiments.

As a result of these comparatively short-time hardness tests at high temperatures, estimates of high-temperature strength of the alloys were obtained which were in the same order as those obtained by long-time creep tests [2].

The capacity of niobium to form solid solutions is used in practice to strengthen it at high temperatures and to produce commercial alloys. For the investigation 2-to-6- component alloys were synthesized, the compositions being calculated to fall within the single-phase and supersaturated-solid-solution regions. The composition of these alloys (in wt.-%) are given in the table.

Nb	Mo	Zr	Si	Al	C
100	—	—	—	—	—
95	5	—	—	—	—
90	5	5	—	—	—
89	5	5	1	—	—
88	5	5	1	1	—
87,8	5	5	1	1	0,2

The alloys were made from the following materials: 99.2% metallic niobium, 99.9% molybdenum, 99.8% iodide zirconium, commercial silicon, 99.9% aluminum, and carbon. The alloys were melted in an arc furnace with a nonconsumable tungsten electrode and an argon atmosphere. To avoid metal losses the alloys were pressed into 20-g charges before melting. To obtain uniform ingots the specimens were turned over and remelted several times.

Cylinders 14 mm in diam and 5 mm high were machined from the specimens obtained. All the specimens were given a homogenizing anneal in a TVV-2 vacuum furnace at 1600°C for 10 hr. These conditions were sufficient to bring the specimens into an equilibrium state.

Microstructures of annealed alloys are given in Fig. 1.

Hardness measurements were carried out on a VIM-1 machine in vacuum at temperatures of 20, 100, 200, 300, 400, 500, 600, 700, 800, 900, and 1000°C. The diamond pyramid was under load for 1 min. Three impressions were made on each specimen at each temperature. The diagonal of the impression was measured on a PMT-3 microhardness machine.

Figure 2 gives curves showing the temperature dependence of the hardness of pure niobium, with a room-temperature hardness of 13.8 kg/mm^2. The hardness curve for niobium decreases linearly with rise of temperature to 400-600°C and then falls more steeply at 600-1000°C. At the latter temperature the hardness of niobium was 10 kg/mm^2. With greater complexity of chemical composition the hardness of the alloys increases, as can be clearly seen from curves 2-6. The course of curve 2shows that the introduction of a second element raises the hardness of the alloy, particularly at high temperatures. A similar change in hardness was observed in the three-component alloy. As the number of components in the alloys increased, the absolute value of the hardness rose markedly. However, the softening process proceeded somewhat more rapidly than in the case of binary and ternary alloys.

In order to demonstrate more clearly the part played by alloying in strengthening the alloys, a characteristic was introduced which indicates the degree of strengthening in relation to the composition of the alloy [3]. As a

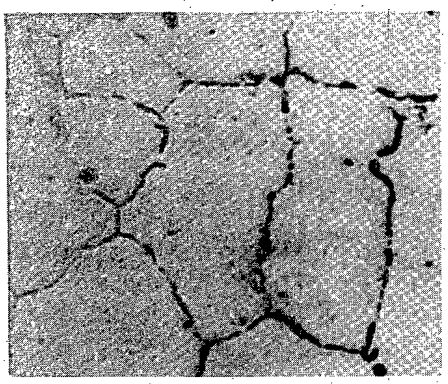

a

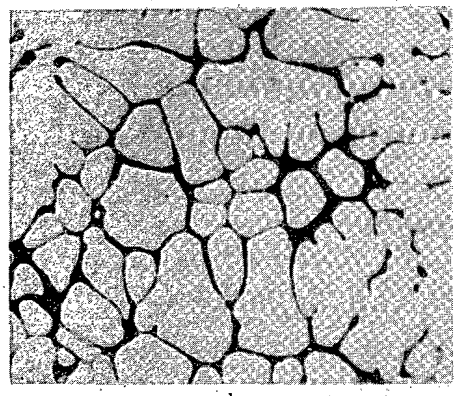

b

Fig. 1. Microstructures of annealed niobium-base alloys: a—90% niobium, 5% molybdenum, 5% zirconium (× 315); b—89% niobium, 5% molybdenum, 5% zirconium, 1% silicon (× 315).

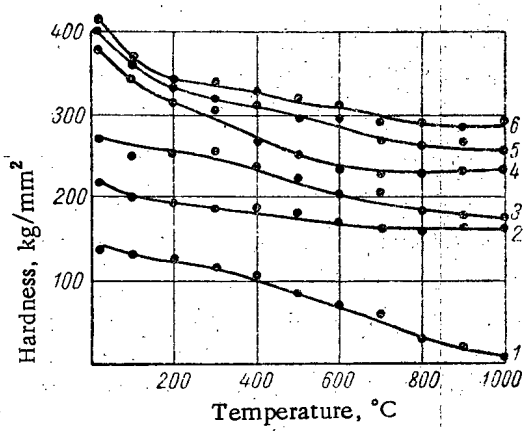

Fig. 2. Temperature dependence of the hardness of niobium alloys: 1) niobium; 2) two-component alloy; 3) three-component alloy; 4) four-component alloy; 5) five-component alloy; 6) six-component alloy.

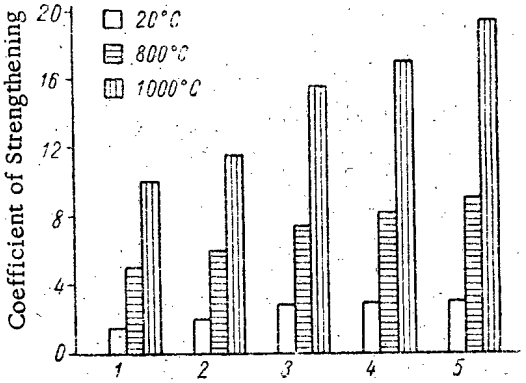

Fig. 3. Values of the coefficient of strengthening at 20, 800, and 1000°C. Alloys: 1) two-components; 2) three-component; 3) four-component; 4) five-component; 5) six-component.

measure of the degree of strengthening a coefficient was adopted, in the calculation of which the hardness of niobium was taken as unit at any temperature in the range from 20 to 1000°C.

Figure 3 shows the values of the coefficient of strengthening at 20, 800, and 1000°C. The two-component alloy had a coefficient 1.5 at room temperature (20°C), 5.0 at 800°C, and 10.8 at 1000°C. The coefficient increased with rise in the number of components in the alloy. Thus, the coefficient of a six-component alloy was 2.96 at 20°C and 19.3 at 1000°C, i.e. at 1000°C the six-component alloy was 19.3 times stronger than niobium.

From the foregoing the following conclusions may be drawn:

1) Niobium, like nickel, iron, and cobalt, can be strengthened by alloying with elements which enter into solid solution with it or form supersaturated solutions with separation of excess phase.

2. The "hot" hardness method enables the high-temperature strength of the alloys to be determined to a first approximation.

3. Multicomponent alloys having great hardness at 1000°C require further investigation and testing by the standard method.

LITERATURE CITED

1. M. G. Lozinskii, High-Temperature Metallography [in Russian] (Moscow, Mashgiz, 1956).
2. A. A. Bochvar, Izvest. Akad. Nauk SSSR, Otdel. Tekh. Nauk No. 10, 1369 (1947).
3. I. I. Kornilov, Izvest. Akad. Nauk SSSR, Otdel. Tekh. Nauk No. 1, 119 (1956).

THE CHARACTERISTICS OF IRRADIATED GLASSES*

Zdenek Spurný

Institute of Nuclear Studies, Czechoslovakia Academy of Sciences, Prague
Translated from Atomnaya Énergiya, Vol. 10, No. 2, pp. 172-173, February, 1961
Original article submitted September 22, 1960

In a number of papers [1-5] results have been given of investigations into the dependence of darkening of glass after irradiation with a certain dose on the composition of the glass, the effect of impurities in the glass on the formation of color centers, and descriptions have been given of the dosimetric properties of glasses of different compositions. To compare the action of ionizing radiation on glass of different types it is essential to determine certain indices. The use of Czech optical glasses for dosimetric purposes [6] has shown that the number of color centers forming in the glass during irradiation depends on the following factors: the dose of irradiation, the energy of the radiation, the chemical composition of the glass. If these factors are constant then the number of color centers forming in the glass also depends on the temperature, the dimensions of the glass and the time after irradiation.

In [7] four indices are suggested for the quantitative determination of the radiation effect in glasses: the index of stability of glass to the action of ionizing radiation K_s (the logarithm of the dose at which the light transparency is reduced by 5%), the index of saturation K_{sat} (the logarithm of the dose at which the glass is saturated with color centers), the minimum value of light transmission T_{min} (transmission in the region of saturation by color centers) and the coefficient of intensity of darkening Q (the ratio of the coefficient of light transmission before irradiation to the coefficient of transmission after irradiation at a dose of 10^6 r).

To measure these indices the following conditions must be satisfied:

1. The source of irradiation should be Co^{60} of about 100 r/min intensity in order to always observe the same conditions in measuring the energy and intensity of the source.

2. The temperature of the glass should be kept constant (20°C) in order to eliminate its effect.

3. The transmission of light should be measured not later than 10 min after irradiation, in order to eliminate the effect of fading (the dependence of "breakdown" of the color centers on the time after irradiation).

4. Glass specimens of the same thickness should always be used (preferably more than 1 mm) in order to eliminate the effect of scatter.

5. The light transmission should always be measured with a source of monochromatic light of a certain wavelength (for example $\lambda = 3500$ A).

The index K_s should be called the "threshold of noticeable changes" since it refers to the minimum measured number of color centers. This term is used in the literature and it should not be confused with the concept of stability of color centers. The index K_{sat} should be determined as the point of intersection of two tangents to the curve for dependence of light transmission on the dose of irradiation.

For the total quantitative characteristics of the radiation effect in glasses it is essential to introduce another very important constant, characterizing the stability of the color centers which form. It is well known that after formation, color centers "breakdown." Curves for the breakdown of color centers have been obtained experimentally for a number of optical glasses of different compositions. It has been found that the fading of glasses is best described by the empirical formula

$$\mu_\tau = \mu_T \frac{K_c}{K_c + \log \frac{\tau}{T}}, \qquad (1)$$

* This article was received from Czechoslovakia.

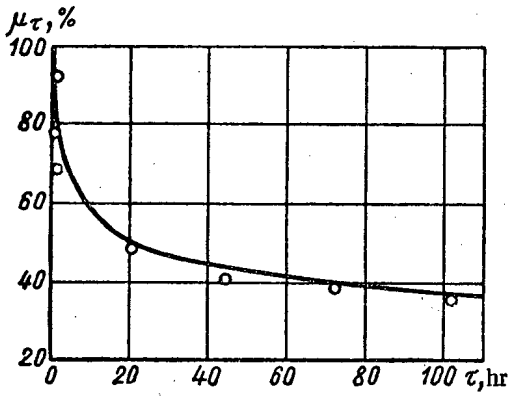

Curve for breakdown of color centers.

Indices of Czech Glasses After Irradiation

Type of glass	Indices					
	K_K	Q	K_H	T_{min}	K_c	T_c
SF-10	3,3	85	4,2	1	1,3	2
F-8	3,1	90	4,3	1	2,1	6
BK-12	3,4	19	4,4	1	3,4	25
Ordinary sodium	3,6	11	4,6	1	4,4	35
ZK-5	3,7	9	4,7	1	4,8	42
FK-5	4,4	3,6	5,4	1	5,5	120

where μ_T is the coefficient of the transmission of light, measured 1 hr after irradiation μ_τ is the same coefficient measured τ hours after irradiation ($T < \tau$; K_C is a constant).

The figure shows the curve for breakdown of color centers for ordinary sodium glass, obtained from formula (1), and experimental points. The constant K_C in formula (1) can sufficiently well characterize the stability of color centers (darkening of glass) which are more stable the greater the values of K_C; this stability can also be characterized by the time (in hours) needed to break down 25% of the formed centers (the constant T_C). Then, 100% of the number of color centers should be taken as the light transmission of glass after irradiation with a dose of 10^5r.

Observing the mentioned conditions of measurement, using a Co^{60} source we irradiated several types of Czech optical glasses of the standard Jena composition, we measured the indices of the author of [7] K_s, K_{sat}, Q, T_{min} and the author of the present work (K_C, T_C). The results of these measurements are given in the table. The measurements show that the indices suggested in [7] for glasses sensitive to radiation are apparently difficult to measure. A more accurate determination of these indices should therefore be given.

LITERATURE CITED

1. N. Kreidl and J. Hensler, J. Amer. Ceram. Soc. 38, No. 12, 423 (1955).
2. J. Schulman et al., Nucleonics 11, 52 (1953).
3. S. Davison et al., Nucleonics 14, 1 (1956).
4. J. Malsky et al., Trans. N. Y. Acad. Sci., November 17, 104 (1955).
5. S. M. Brekhovskikh, Steklo i Keramika 1, 3 (1958).
6. Z. Spurný. Jaderná energie 5, 163 (1960).
7. S. M. Brekhovskikh, Atomnaya Énergiya 8, 1, 37 (1960).*

*Original Russian pagination. See C. B. translation.

THE BUILD-UP FACTORS FOR HETEROGENEOUS SHIELDING

L. R. Kimel'

Translated from Atomnaya Énergiya, Vol. 10, No. 2, pp. 173-175, February, 1961
Original article submitted June 15, 1960

The energy build-up factors of γ-irradiation of Co^{60} in heterogeneous (double layer) shielding were determined for a plane-parallel beam normally incident on the shielding, the beam being provided by the method described in [1]. The detector was a halogen counter with filters [2]. The intensity was determined graphically by integrating its distribution before and after passing through the shielding barrier. The shielding materials were plates of lead, iron and aluminum measuring 75 x 75 cm. The build-up factors were determined for the combinations Pb + Al; Al + Pb; Pb + Fe; Fe + Pb; Fe + Al; Al + Fe. The material occurring first in the combination was nearer to the radiation source.

Tables 1, 2 and 3 give experimental values of the build-up factors (energy) for the given combination of materials.

TABLE 1. Build-up Factors for the Combinations Pb + Al (top values) and Al + Pb (bottom values) for $h\nu_0 = 1.25$ Mev

Thickness of material placed nearer to the source, μx	Thickness of material placed nearer to the detector, μx				
	1	2	3	4	5
1	2,3 2,1	3,2 2,7	4,4 3,0	5,4 3,3	6,6 3,4
2	3,0 2,7	4,1 3,1	5,4 3,3	6,9 3,6	8,4 3,8
3	3,7 3,0	5,0 3,4	6,7 3,7	8,5 3,8	10,3 4,0
4	4,4 3,2	6,0 3,6	8,0 3,9	10,2 4,0	12,5 4,3
5	5,3 3,4	7,0 3,8	9,4 4,1	12,0 4,3	14,6 4,6

TABLE 2. Build-up Factors for the Combinations Pb + Fe (top values) and Fe + Pb (bottom values) for $h\nu_0 = 1.25$ Mev

Thickness of material placed nearer to the source, μx	Thickness of material placed nearer to the detector, μx				
	1	2	3	4	5
1	2,3 1,8	2,8 2,0	3,5 2,2	4,4 2,5	5,1 2,8
2	2,7 2,0	3,5 2,3	4,3 2,6	5,2 3,0	6,3 3,3
3	3,3 2,5	4,2 2,8	5,2 3,2	6,3 3,5	7,4 3,8
4	3,8 3,1	5,0 3,4	6,1 3,7	7,5 4,1	8,8 4,4
5	4,3 3,6	5,8 4,0	7,1 4,3	8,7 4,6	10,2 5,0

TABLE 3. Build-up Factors for the Combinations Fe + Al (top values) and Al + Fe (bottom values) for $h\nu_0 = 1.25$ Mev

Thickness of material placed nearer to the source, μx	Thickness of material placed nearer to the detector, μx				
	1	2	3	4	5
1	2,6 2,5	3,4 3,4	4,5 4,3	5,5 5,1	6,8 6,0
2	3,3 3,3	4,1 4,1	5,4 5,2	6,6 6,0	7,0 6,9
3	4,2 4,2	5,3 5,3	6,5 6,3	7,7 7,2	9,3 8,0
4	5,3 5,3	6,5 6,4	7,8 7,4	9,1 8,2	10,7 9,0
5	6,7 6,4	8,0 7,5	9,3 8,5	10,6 9,4	12,2 10,3

From an analysis of the tables it can be seen that the build-up factor for Pb + Al combinations can be determined as the product of the build-up factors for lead and aluminum of the appropriate thicknesses (in μx). This determination of build-up factors for the cases where the light material follows the heavy material was recommended in [3]. For the combinations of Al + Pb the build-up factor is somewhat greater than for lead of a thickness (in μx) equal to the thickness of Al + Pb. For the combination Fe + Al and Al + Fe at small thickness the build-up factors almost coincide.

It can readily be shown that the build-up factor for double-layer shielding can be determined from the expression

$$B_{I,\,II} = B_{II}(\mu_0 x_{II}) + \frac{\int_0^{h\nu} J_I(h\nu)\, e^{-\mu_{II}(h\nu)\, x_{II}} B[h\nu, \mu_{II}(h\nu)\, x_{II}]\, dh\nu}{J_0 e^{-\mu_0 (x_I + x_{II})}}, \qquad (1)$$

TABLE 4. A Comparison of the Experimental (Upper) and Calculated (Lower) Values of the Energy Build-Up Factor for the Combination Pb + Al

Thickness of Pb, μx	Thickness of Al, μx		
	1	2	4
1	2,3 2,23	3,2 3,29	5,4 5,43
2	3,0 2,74	4,1 3,92	6,9 6,46

The expression (1) makes it possible (for cases where the spectrum of the scattered radiation is known after passing through the first barrier) to calculate the build-up factors. This calculation was performed for the combination Pb + Al, the spectra of radiation scattered after the lead being taken for an infinite medium [4]. With this selection the error is small, since the build-up factor for a barrier of thickness 1 μx is only 5% less than the build-up factor for an infinite medium at a depth 1 μx (for $h\nu = 1$ Mev) [5]. In the calculations no allowance was made for the angular distribution of radiation leaving the first layer, which is presumably not very large. In Table 4 the results of the calculation are compared with experimental data. The differences between the calculated and experimental data, mainly caused by the "rigid operation" of the detector in the region of soft energy, do not exceed ±15%. The good coincidence of experimental and calculated data for the combination 5μ xFe + 1.85 μ xPb is shown in [6]. From this work it can also be seen that the ratio of the energy build-up factors of radiation from a point isotropic source for the combination 1.85μ xPb + 5μ xFe and 5μ xFe + 1.85μ xPb is 1.5, which agrees well with our results (6.3 ÷ 4.0 = 1.58). The coincidence of the calculated and experimental data means that this method can be used to calculate build-up factors for arbitrary energies and material if the spectrum of scattered radiation is known.

The author would like to thank O. I. Leipunskii for his constant interest in the work.

LITERATURE CITED

1. F. Kirn, R. Kennedy, and H. Wyckoff, Radiology 63, (1), 94 (1954).
2. V. N. Sakharov, Atomnaya Energiya 3, 7,61 (1957).*
3. Reports of the Atomic Energy Commission, USA, Protection for Nuclear Reactors [Russian translation[(Moscow, Foreign Literature Press, 1958).
4. H. Goldstein and S. Wilkins. US AEC. Report NYO-3075 (1954).
5. M. Berger and J. Dogget, J. Res. Nat. Bur. Standards 56, No. 2 (1956).
6. S. G. Tsypin, V. I. Kukhtevich and Yu. A. Kazanskii, Atomnaya Energiya 2, 71 (1956).*

*Original Russian pagination. See C. B. translation.

SOLUTION OF THE KINETIC EQUATION FOR A MEDIUM WITH A POINT MONODIRECTIONAL SOURCE

E. B. Breshenkova and V. V. Orlov

Translated from Atomnaya Énergiya, Vol. 10, No. 2, pp. 175-177, February, 1961
Original article submitted August, 1960

The problem of the transmission of radiation in an infinite medium with various sources has been studied in many articles [1-3]. Point isotropic sources and infinite plane sources with various angular distribution of γ-radiation and neutron emission were studied. In such cases, due to the symmetry of the problem, the radiation flux depends only on three variables, which fact significantly simplifies the solution of the kinetic equation. The solution of this equation for a point monodirectional source is associated with five variables. The steady problem of the transmission of radiation through a medium with a point monodirectional source was examined in general form in [4], but the direct solution of this problem entails considerable mathematical difficulty due to the large number of variables. Satisfactory quantitative results have not been obtained.

In solving the single-velocity problem for a medium with point monodirectional source, I. I. Bondarenko used the reversibility of single-velocity diffusion and the problem was reduced to the solution of the kinetic equation for a medium with isotropic source.

The diffusion of radiation in a slowing medium (due to elastic and nonelastic collisions of neutrons with nuclei and Compton scattering of γ-rays by electrons) is an irreversible process. However in this case the problem may be solved by using a more general property of the kinetic equation, namely the reciprocity theorem [5,6].

In the present paper the solution of the kinetic equation for a medium with point monodirectional source is reduced with the aid of the reciprocity theorem to the solution of the conjugate kinetic equation for a medium with an isotropic source. This equation contains three independent variables and may be solved by the method of moments.

Suppose $G(\mathbf{r}, E, \Omega; \mathbf{r}_0, E_0, \Omega_0)$ is Green's function for the kinetic equation describing the flow of radiation with energy E and direction Ω at the point $\mathbf{r}$ (with the condition that at the point $\mathbf{r}_0$ there is a unit point source with energy E_0 and direction Ω_0). If the function $G^+(\mathbf{r}, E, E; \mathbf{r}_0, E_0, \Omega_0)$ is Green's function for the conjugate kinetic equation, then by the reciprocity theorem

$$G(\mathbf{r}, E, \Omega; \mathbf{r}_0, E_0, \Omega_0) = G^+(\mathbf{r}_0, E_0, \Omega_0, \mathbf{r}, E, \Omega).$$

Integrating this equation with respect to $d\Omega$, we obtain

$$G_0(\mathbf{r}, E; \mathbf{r}_0, E_0, \Omega_0) = G_0^+(\mathbf{r}_0, E_0, \Omega_0; \mathbf{r}, E), \tag{1}$$

where $G_0 = \int G d\Omega$.

Thus if we must know the distribution of total flux G_0 from a monodirectional point source, then it is sufficient to find the solution of the conjugate equation (including the angular distribution) for a medium with isotropic source.

In the case of γ-radiation the kinetic equation of a medium with a point monoenergetic monodirectional source has the following form:

$$\Omega \operatorname{grad} F(\mathbf{r}, \Omega, \lambda) = -\mu(\lambda) F(\mathbf{r}, \Omega, \lambda) + \int_{\lambda-2}^{\lambda} d\lambda' K(\lambda', \lambda) \int d\Omega' \frac{1}{2\pi} \delta(1 - \Omega\cdot\Omega' - \lambda + \lambda') \times$$

$$\times F(\mathbf{r}, \Omega', \lambda') + \delta(\mathbf{r} - \mathbf{r}_0)\,\delta(\Omega - \Omega_0)\,\delta(\lambda - \lambda_0),$$

where $F(\mathbf{r}, \Omega, \lambda)$ is the radiation flux at the point $\mathbf{r}$ with wavelength λ and direction of velocity Ω; $K(\lambda', \lambda) = nZ\pi r_0^2 (\lambda/\lambda')^2 \left[\frac{\lambda}{\lambda'} + \frac{\lambda'}{\lambda} - 2(\lambda' - \lambda) + (\lambda' - \lambda)^2\right]$ is the probability density of the Compton scattering with change

in wavelength from λ' to λ; $\mu(\lambda)$ is the coefficient of absorption. Together with this equation we may, corresponding to formula (1), solve the conjugate kinetic equation for a medium with isotropic source:

$$-\Omega \operatorname{grad} F^+(\mathbf{r}, \Omega, \lambda) = -\mu(\lambda) F^+(\mathbf{r}, \Omega, \lambda) + \int_{\lambda}^{\lambda+2} d\lambda'' K(\lambda, \lambda'') \int d\Omega'' F^+(\mathbf{r}, \Omega'', \lambda'') \frac{1}{2\pi} \times$$

$$\times \delta(1-\Omega\Omega''-\lambda''+\lambda)+\delta(\mathbf{r}-\mathbf{r}')\delta(\lambda-\lambda'). \tag{2}$$

In this the distribution of total γ-radiation flux in a medium with a point monodirectional source may be found with the formula

$$F_0(\mathbf{r}', \lambda') = F^+(\mathbf{r}_0, \Omega_0, \lambda_0).$$

Performing the substitution $\mathbf{r}-\mathbf{r}'=\mathbf{R}$ and considering the symmetry of the source, from which it follows that $F^+(\mathbf{R}, \Omega, \lambda) = F^+(R, \xi, \lambda)$, where $\xi = (\Omega R)/R$, we obtain together with formula (2), the following equation:

$$-\xi \frac{\partial F^+(R, \xi, \lambda)}{\partial R} - \frac{(1-\xi^2)}{R} \frac{\partial F^+(R, \xi, \lambda)}{\partial \xi} = -\mu(\lambda) F^+(R, \xi, \lambda) + \int_{\lambda}^{\lambda+2} d\lambda'' K(\lambda, \lambda'') \int d\Omega'' \times$$

$$\times F^+(R, \xi'', \lambda'') \frac{1}{2\pi} \delta(1-\Omega\Omega''-\lambda''+\lambda) + \frac{\delta(R)}{4\pi R^2} \delta(\lambda-\lambda'). \tag{3}$$

We expand the conjugate flux in a series of Legendre polynomials

$$F^+(R, \xi, \lambda) = \sum_{l=0}^{\infty} \frac{2l+1}{4\pi} F_l^+(R, \lambda) \mathcal{P}_l(\xi), \tag{4}$$

substitute formula (4) into equation (3), multiply the relation obtained by $\mathcal{P}_l(\xi)$ and integrate through by $d\Omega$. As a result we obtain an equation for $F_l^+(R, \lambda)$

$$-\frac{(l+1)}{2l+1}\left(\frac{l+2}{R}+\frac{\partial}{\partial R}\right) F_{l+1}^+(R, \lambda) + \frac{l}{2l+1}\left(\frac{l-1}{R}-\frac{\partial}{\partial R}\right) F_{l-1}^+(R, \lambda) =$$

$$= -\mu(\lambda) F_l^+(R, \lambda) + \int_{\lambda}^{\lambda+2} d\lambda'' K(\lambda, \lambda'') \mathcal{P}_l(1-\lambda''+\lambda) F_l^+(R, \lambda'') + \frac{\delta(R)}{R^2} \delta(\lambda-\lambda') \delta_{l_0}. \tag{5}$$

Multiplying equation (5) by R^n and integrating it over all of space, we obtain an equation for the moments $b_{l,n}(\lambda)$

$$-\frac{1}{2l+1}[(l+1)(l-n) b_{l+1, n-1}(\lambda) - l(l+n+1) \times b_{l-1, n-1}(\lambda)] = -\mu(\lambda) b_{l, n}(\lambda) +$$

$$+ \int_{\lambda}^{\lambda+2} d\lambda'' K(\lambda, \lambda'') \mathcal{P}_l(1-\lambda''+\lambda) b_{l, n}(\lambda) + 4\pi\delta(\lambda-\lambda') \delta_{l_0} \delta_{n_0}, \tag{6}$$

where

$$b_{l, n}(\lambda) = \int_0^{\infty} R^n F_l^+(R, \lambda) 4\pi R^2 dR.$$

It is easy to see that system (6) determines only the moments $b_{l,n}(\lambda)$, for which $l \leq n$ and the indices l and n have the same parity. We seek $F_{2l}^+(R, \lambda)$ and $F_{2l+1}^+(R, \lambda)$ in the following form:

$$F_{2l}^+(R, \lambda) = \frac{e^{-\mu R}}{4\pi R^2} \sum_{n=0}^{N} a_{2l, n}(\lambda) (\mu R)^n;$$

$$F^{+}_{2l+1}(R, \lambda)=\frac{e^{-\mu R}}{4\pi R^2}\sum_{n=0}^{N} c_{2l+1,\,n}(\lambda)(\mu R)^n,$$

where the coefficients $a_{2l,\,n}(\lambda)$ and $c_{2l+1,\,n}(\lambda)$ are solutions of the systems of N + 1 equations:

$$\left.\begin{aligned} b_{2l,\,2m}(\lambda)&=\sum_{n=0}^{N}\frac{(n+2m)!}{\mu^{2m+1}}a_{2l,\,n}(\lambda);\\ b_{2l+1,\,2m+1}(\lambda)&=\sum_{n=0}^{N}\frac{(n+2m+1)!}{\mu^{2m+2}}c_{2l+1,\,n}(\lambda)\end{aligned}\right\} \qquad (7)$$

for $m = l, l+1, l+2, \ldots, l+N$.

The solution of system (7) allows the expression of the coefficients $a_{2l,n}(\lambda)$ and $c_{2l+1,n}(\lambda)$ in terms of the even-even and odd-odd moments found from equation (6). It is easy to see that the number N is limited by the number of known moments. The more moments that are known, the more accurate may the quantity $F^{+}_{l}(R, \lambda)$ be calculated.

To solve the problem considered, it is useful to exclude the unscattered flux of radiation from the equation for moments (6), which may be done in the usual manner.

In conclusion the author expresses thanks to V. F. Turchin for many useful remarks in the preparation of this article, and to G. I. Marchuk and Sh. S. Nikolaishvili for fruitful discussions of the results.

LITERATURE CITED

1. H. Goldstein and J. Wilkins, US AEC, Report NYO-3075 (1954).
2. R. Aronson, J. Certaine, and H. Goldstein US AEC, Report NYO-6269 (1954).
3. R. Aronson et al., US AEC, Report NYO-6267 (1954).
4. V. Spencer and U. Fano, J. Res. 46, 446 (1951).
5. B. B. Kadomtsev, Doklady Akad. Nauk SSSR 113, No. 3, 541 (1957).
6. G. I. Marchuk, B. B. Orlov, Collection "Neutron Physics" [in Russian], A. I. Leipunskii, Editor (Moscow, Atomizdat, 1961) (in press).

THE EFFECT OF INELASTIC SCATTER OF NEUTRONS IN URANIUM ON THE MODERATION LENGTH IN WATER

B. A. Levin, E. V. Marchenko, and D. V. Timoshuk

Translated from Atomnaya Énergiya, Vol. 10, No. 2, pp. 177-179, February, 1961
Original article submitted July 7, 1960

In the calculation of uranium-water reactors an important part is played by the moderation length of the neutrons in the lattice. Measurements and calculations [1-3] of the moderation length, performed for different concentrations of uranium and different diameters of blocks in the lattices, show that the moderation length is considerably affected by the inelastic scatter of neutrons in uranium. The values of the neutron ages [$\tau = 1/6\bar{r}^2$] determined in assemblies using a thin source (convector) and in exponential experiments in subcritical systems, differ greatly. Besides certain reasons, this difference can be explained by the fact that in experiments of the first type there is practically no inelastic scatter in the source, whereas in experiments of the second type the inelastic scatter in the "parent" block can noticeably change the primary energy of the neutrons.

In the present work direct measurements were made of the effect of inelastic neutron scatter in uranium on the moderation length in pure water. For the most complete exclusion of the effect of elastic scatter the measurements were made in spherical-symmetrical geometry. The source of diameter 16 mm, imitating the spectrum of fission neutrons, was surrounded concentrically by spherical layers (of thickness 2 cm) of metallic uranium depleted with U^{235} isotope.

The mean square of the distance traveled by the neutrons from the point isotropic source on moderation to an energy of, for example, 1.46 ev is determined by the expression

$$\overline{r_{\text{In}}^2} = \frac{\int_0^\infty A(r)\, r^4 dr}{\int_0^\infty A(r)\, r^2 dr}, \qquad (1)$$

where A(r) is the activity of the indicator (indium foil in a cadmium can) as a function of the distance r from the source. The application of expression (1) to the distribution of moderation density in this particular case gives a value of $\bar{r}^2$ which is determined not only by the energy spectrum of the fast neutrons, but also by the dimensions of the cavity formed by the sphere in the moderator. In order to exclude the effect of dimensions of the cavity the measurements of $\bar{r}^2$ were performed with uranium layers of different radius a at a constant thickness of the layer. By extrapolating the relationship $\bar{r}^2(a)$ to $a = 0$ the value of $\bar{r}^2$ was determined corresponding to a point surce of neutrons. To study the effect of dimensions of the cavity on the value of $\bar{r}^2$ with change in a over wider limits and to obtain $\bar{r}_0^2$ for neutrons of the initial spectrum, measurements were made with thin-walled hollow spheres.

The measurements were made in a water-filled tank of diameter 100 cm and height 110 cm. The spheres were suspended on two steel wires of diameter 0.5 mm along which was lowered a light plexiglas holder until it was arrested by the sphere; the holder had grooves for locating the casettes with indium foils (at a given distance from the surface of the sphere). The casettes were sealed with wax. The foils of thickness 70 mg/cm^2 had a working surface diameter of 1.7 and 2.5 cm. Suspending the foils in the neutron field showed that the activities of indicators of the same diameter differed from the mean value by not more than 0.5%. As a rule, the targets were exposed in two pieces with a distance between them of not less than 8 cm. The activity of the foils was measured simultaneously from both sides by two scintillation counters (FÉU-29 with a crystal of stilbene of diameter 32 mm and thickness 1 mm) in lead shielding. The sensitivity of the apparatus was checked by a preparation of Sr^{90} and was kept at one level with an accuracy of ± 0.5%. The measurements at all distances were repeated from two to six times. At distances up to 15 cm from the surface of the uranium sphere the measurements were made by small targets, at distances of 10-21 cm by large targets in cadmium (thickness 0.5 mm) casettes and at distances of 15-31 cm by large targets in aluminum cassettes. In order to obtain the density distribution of moderation of the neutrons to an energy of 1.46 ev over the

whole range of distances, separate sections of the curve were placed together at the points where the measurements overlapped. In measurements with thin-walled spheres small targets in cadmium casettes were used. In addition, for a cavity with a = 3.3 cm, measurements were made with targets of different diameters in cadmium and aluminum cassettes. In both cases within the limits of error in the measurements (1.2%) the same values of $\bar{r}^2$ were obtained.

The values of $\bar{r}^2$ obtained from relationship (1) from the space distributions A(r) are shown in the figure and in the table. Integration of the curves of A(r) r^2 and A(r)r^4 at distances greater than r-a = 15 cm was performed analytically. In accordance with the results of the measurements it was assumed that the decrease in A(r)r^2, starting with r-a = 15 cm, becomes exponential with a relaxation length of 7.11 ± 0.08 cm for hollow spheres and 6.52 ± 0.06 cm for uranium. The relaxation lengths were determined by the method of least squares.

The Values of $\bar{r}^2$ Measured at Different Radii a of the Cavity in Water

	Cavity					With uranium			With lead	
a, cm	0,8	3,3	5,0	7,0	11,15	3,59	5,80	6,80	3,56	6,81
$\bar{r}^2(a)$, cm²	200,3±±2,6	244,8±±1,9	272,6±±5,3	311,2±±4,4	416,2±±7,9	206,3±±1,8	234,1±±1,8	255,1±±2,1	242,6±±3,2	305,2±±3,8
K*	0,588±0,006					0,480±0,027			0,582±0,039	
$\bar{r}_0^2$, cm²	187,1±1,1					161,5±4,0			182,8±5,7	

* k – coefficient for a in equation (2).

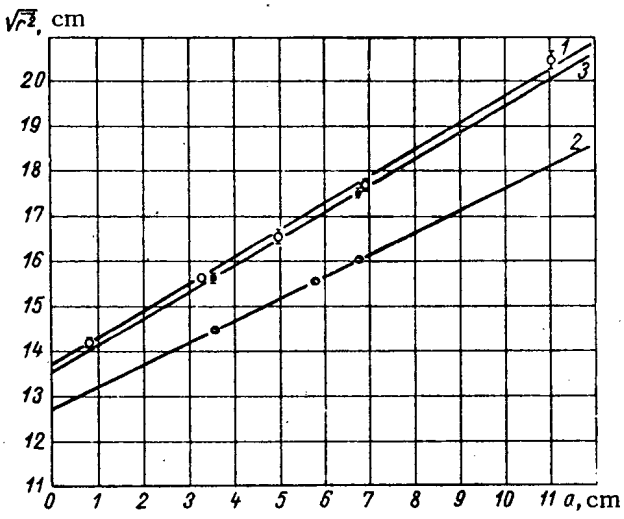

Dependence of $\sqrt{\bar{r}^2}$ on the radius a of a spherical cavity in water: 1) (○)–without scatterer; 2) (●)–with uranium; 3) (□)–with lead.

The neutron density was assumed to be constant within the spheres. As can be seen from the figure, $\sqrt{\bar{r}^2}$ is well approximated by a linear dependence on a

$$\sqrt{\bar{r}^2} = \sqrt{\bar{r}_0^2} + ka, \qquad (2)$$

which permits reliable extrapolation of the value $\sqrt{\bar{r}^2}$ and a = 0. From the curve 1 for neutrons of the imitating source which we used, $\bar{r}_0^2$ is equal to 187.1 ± 1.1 cm².

The results of measurements with layers of uranium are shown by curve 2. The difference in the slopes of curves 1 and 2 is presumably connected with the softening of the spectrum with inelastic reaction of neutrons with uranium nuclei. The correction for capture of the resonance neutrons in uranium was determined by comparing the course of density of neutrons with an energy of 1.46 ev near the uranium and hollow spheres on the assumption that the distributions of densities in the absence of resonance absorption are similar. The correction is 0.5% of the value of $\bar{r}^2$. The linear extrapolation of curve 2 to a = 0 gives r_0^2 = 161.5 ± 4.0 cm².

Measurements with lead (see curve 3 of the figure) were made to find the effect of elastic scatter in a spherical layer on the moderation length. As shown by the measurements made by another method, inelastic scatter of fast neutrons is very small for the source which we used in lead. A comparison of curves 1 and 3 shows that the difference in the values of $\bar{r}^2$ obtained with spherical layers of lead and hollow spheres is very small and is within the limits of error of the experiment. Consequently, the observed reduction in $\bar{r}^2$ for uranium is not connected with elastic scatter of neutrons in the spherical layer.

In measurements with uranium there was a 9% increase in the number of neutrons connected with the fission of uranium mainly by fast neutrons (the uranium and lead spheres were in cadmium cans). Since the mean paths of fission neutrons and neutrons of the surce in uranium are close, in view of the closeness of the mean energies the effect of inelastic scatter will be approximately the same and the addition of fission neutrons is equivalent to an increase in source strength. A decrease in $\bar{r}^2$ due to fission neutrons which have not undergone inelastic scatter in uranium due to the difference in the ages of the fission neutrons (28 cm^2, see below) and neutrons of the source which we used (31 cm^2) is 1%. Therefore, allowing for this correction the inelastic scatter of neutrons in a layer of metallic uranium of thickness 2.0 cm leads to an increase in $\bar{r}^2$ of (12.7 ± 2.2)%.

On the basis of known cross sections, estimating the fraction α of inelastically scattered neutrons in a 2.0 cm thick layer of uranium as being equal to 0.21 and using the relationship $\bar{r}^2 = \alpha \bar{r}^2_{inel.} + (1-\alpha)\bar{r}^2_0$, we find that for inelastically scattered neutrons the second spatial moment $\bar{r}^2_{inel}$ is equal to 64 cm^2. From the relationship $\tau(E)$ [4] the mean energy of inelastically scattered neutrons in uranium is ~0.5 Mev.

Curve 1 (see figure) gives a quantitative allowance for the effect of dimensions of the source on τ, obtained in [5], for fission neutrons.

If we assume the end of the cylindrical tube with converter (U^{235}) to be a sphere of the same radius, then for τ we obtain the value 28 ± 1.5 cm^2, which is closer to the theoretical value $\tau_{theor.} = 26 \pm 0.5$ cm^2 [4] for neutrons of the fission spectrum in water.

The results of this work show that in uranium-water systems with blocks of sufficiently large dimensions a decrease in the moderation length of fission neutrons due to inelastic scatter in uranium is considerable and should be allowed for in reactor calculations.

We would like to thank G. A. Bat' for discussing certain theoretical problems, L. E. Morozova, G. S. Stolyarova, and L. A. Serdyukova for helping with the measurements and calculations.

LITERATURE CITED

1. S. M. Feinberg, Session of the Academy of Sciences, USSR, on the Peaceful Uses of Atomic Energy (Meeting of the physical and Mathematical Sciences Section) [in Russian] (Moscow, Acad. Sci. USSR Press, 1955), p. 185.
2. G. Coates et al., Reports of the International Conference on the Peaceful Uses of Atomic Energy (Geneva, 1955) Vol. 5 [in Russian] (Moscow, Acad. Sci. USSR Press, 1958) p. 223.
3. L. M. Barkov, A. P. Venediktov, and K. N. Mukhin, Atomnaya Énergiya 3, 40 (1956).*
4. H. Goldstein, P. Zweifel, and D. Foster, Transactions of the Second International Conference on the Peaceful Uses of Atomic Energy (Geneva, 1958). Selected Reports of non-Soviet Scientists. Vol. 2. Neutron Physics [in Russian] (Moscow, Atomic Energy Press, 1959) p. 688.
5. L. M. Barkov and K. N. Mukhin, Atomnaya Énergiya 3, 31 (1956).*

*Original Russian pagination. See C. B. translation.

NEWS OF SCIENCE AND TECHNOLOGY

INTERNATIONAL CONFERENCE ON RADIOISOTOPE APPLICATIONS IN THE PHYSICAL SCIENCES AND IN INDUSTRY

V. V. Bochkarev and A. S. Shtan'
Translated from Atomnaya Énergiya, Vol. 10, No. 2,
pp. 180-185, February, 1961

An international conference on radioisotope applications in the physical sciences and industry, organized by the International Atomic Energy Agency (IAEA) in collaboration with UNESCO, met in session from September 6 to September 16, 1960, in Copenhagen. Participants at the conference included over 550 persons from 40 nations and 11 international bodies; the number of reports heard was 150 (including two evening lectures), 20 of which were delivered by Soviet scientists.

The reports submitted to the conference can be grouped according to subject matter under 12 different headings. Below, we endeavor to make a brief summary of the most interesting papers, from our viewpoint, and the scientific and engineering data contained therein, grouping them under several broad headings.

Radioisotopes in Geophysics and Meteorology

Fifteen reports presented in these fields took up problems related to meteorite studies, propagation and migration of radioisotopes in the atmosphere and in the sea, carbon-14 dating, and applications for nuclear-geophysical techniques in mineral exploration and research on underground waters.

At the first session of the conference, papers presented by Soviet scientists were "Carbon-14 Dating" by A. P. Vinogradov, and "Liquid Scintillators for Radiocarbon Dating in Archeology" by I. E. Starik and colleagues. These papers made available data on a carbon-14 measurement procedure worked out in the Soviet Union for ascertaining the amount of C^{14} present in archeological and geological specimens, and information on age determination of numerous geological and archeological objects in the USSR.

A paper presented by O. A. Schaeffer and associates (USA), "Meteorites as interplanetary space samples, for studying cosmic rays," proved that the solar component of the cosmic radiation exerts no discernible effect on the composition of meteoritic matter, on the basis of a study of radioactive isotopes of different half-lives found in meteorites. K. Govel and P. Schmidlin of CERN presented a wealth of empirical data on determinations of the "cosmic" age of meteorites, i.e. the duration of their irradiation in cosmic space. The values derived ranged from 2 to 200 million years. W. Gehr et al. (West Germany) presented data on an application of the Re/Os-technique to age determinations of iron meteorites. Although the data reported by the authors on the age of iron meteorites, 5.6 to 8.7 10^9 years, is acknowledged to be of preliminary and tentative character, they are of great interest, since determination of the age of iron meteorites by other methods has been hampered by great difficulties. G. Wilson and A. Mac Near (Britain) presented findings on a determination of the half-life of Rb^{87}, reported as $(5.25 \pm 0.1) \cdot 10^{10}$ years, is the first value derived by the direct method; it is of great importance for calculations of the absolute age by the Rb/Sr method.

It is fitting to mention (bearing the foregoing discussion in mind) that papers on studies of the content of radioisotopes in meteorites are viewed as highly significant from the standpoint of age studies and the elaboration of theories bearing on the formation of the matter comprising the planetary system. This question, aside from its value as added knowledge, is of direct practical significance in that the conquest of outer space necessitates a knowledge of the changes produced by cosmic radiation in matter found in outer space; and some idea of the intensity of the cosmic radiation proper is also highly desirable.

Interesting and highly useful data on the irregular latitude distribution of C^{14} over the earth's surface obtained on the basis of four years of measurements (1956-1959) by G. Tauber (Denmark) and generalizations of the findings reported by other workers were made available in Tauber's paper entitled "The effect of geographic latitude on the migration of radioactive carbon from the stratosphere to the troposphere." The author in particular demonstrated that the pathways of migration and the mechanism allowing access from the stratosphere to the troposphere for fallout isotopes resulting from nuclear bomb explosions may be traced by determining the C^{14} content in contemporary flora specimens collected in various sites. This is of great interest both for prognoses of radiation hazards applicable to dif-

ferent regions and in relation to utilization of the radiocarbon method for determining absolute age. The author's recommendations on the feasibility of measurements of C^{14} content in atmospheric carbon dioxide at a large number of sampling stations in order to determine C^{14} transport from stratosphere to troposphere also merits attention. This report and two review papers presented by the World Meterological Organization showed the feasibility of utilizing radioisotopes to estimate displacement and the character of the transport of air and water masses over the earth's surface. This avenue of research unquestionably holds great promise not only for the solution of purely meterological aerological, and hydrological problems, but, as has already been stated, is also useful for prognoses regarding radioactive fallout levels.

Problems related to the use of tritium as a research tool in underground water studies were discussed in papers by Soviet (F. A. Alekseev et al.) and Netherlands (E. Kupper and H. Hout) authors.

A report by Yu. P. Bulashevich et al. (USSR) "Nuclear geophysics in exploration of ore and coal deposits," in which practical techniques for radioactive logging which have found many applications in ore and coal fields throughout the Soviet Union, was met with deep interest.

Radioisotopes in metallurgy and solid state physics

These areas were the subject of 15 papers presented. A paper by L. Lacombe et al. (France) discussed the question, associated with severe technical difficulties, of the separation and separate investigation of self-diffusion within grain boundaries and between grain boundaries. The paper demonstrated the fact that the formula derived by the Soviet scientist P. L. Gruzin can be extended and that, by measuring the total activity in iron specimens, the fractions of activity associated with self-diffusion within and between grain boundaries can be successfully distinguished.

A paper by C. Besnar and J. Talbot (France) discussed the use of isotopes in studying sulfur penetration in to iron when the iron has absorbed hydrogen from a cathode. The authors found an intensive penetration of the sulfur into the bulk phase of hydrogen-saturated iron, with the sulfur following a path along rain boundaries. This paper was of considerable practical interest.

A report by P. Albert and J. Betti (France) was devoted to the elaboration of techniques for determining trace impurities in high-purity materials (metallic and nonmetallic alike) for those instances where determination of such impurities by chemical and spectral analyses is not feasible. The possibility of determining traces of 45 elements (the number may be extended to 60 as more experience is acquired) was demonstrated by the example of neutron-irradiated aluminum and iron.

J. Crawford and J. Cleland (USA) explained the results of detailed investigations of thermal neutron effects on germanium and its properties (magnitude and mode of germanium conductivity). It was shown that of five germanium isotopes, three isotopes are transformed to chemical impurities (Ga^{71}, As^{75}, Se^{77}) which, upon forming in the germanium lattice, effect a change in the electrical properties of germanium. Data on the number of atoms of the isotopes formed and their half-lives are presented. A similar investigation was also carried out with respect to silicon and indium. The use of this method holds great promise for the study of numerous complex semiconductors (intermetallic and chemical compounds) which present great hindrances to the introduction of certain interesting impurities by the chemical pathway.

A paper by E. G. Miselyuk et al. (USSR) communicated findings of a study using radioactive isotopes Ag^{110}, Fe^{59}, Cd^{115}, Te^{127}, and Ta^{182} of diffusion and solubility of the corresponding isotope species in germanium. The interest placed in diffusion and solubility studies of these elements is particularly due to the fact that their impurity centers in germanium are electrically active and capable of affecting both conductivity and charge carrier recombination, by greatly increasing the rate of recombination. Soviet scientists also submitted papers dealing with diffusion, recrystallization, and phase transformations (S. Z. Bokshtein et al.), measurement of self-diffusion constants of cations in silicate melts with Na^{24}, K^{42}, and Ca^{45} employed as tracers (V. I. Malkin and B. M. Morgunov), determination of the thermodynamic activity of antimony in α-iron (I. A. Tomilin). Tomilin advanced a new method based on a study of the distribution of antimony between two phases, liquid lead and solid iron. The gist of this method is that a specimen of thin iron foil 10-30 microns thick and weighing about 0.1 g is contacted with molten lead containing a predetermined concentration of Sb^{124} tagged antimony. On being left to stand at a preset temperature, the antimony diffuses into the iron, ending up evenly distributed throughout the entire thickness of the foil. Use of the radioactive antimony isotope has made it possible to accurately measure the concentration of that element in specimens weighing less than 0.1 g. Quantitative determination of the composition of such tiny weights by straightforward chemical analysis is extremely difficult.

The study of lattice imperfections is one of the most burning problems in solid state physics. Methods widely used in such studies are the method of chemical additives and radiation effects on the lattice structure. A paper by G. Lambe (USA) discussed several possible uses of radioactive disintegration for bringing about imperfections in solids. The possibility of using this method for the above purpose was demonstrated by the author with tritium and krypton as examples. The method advanced may find a wide range of applications in obtaining and investigating free radicals in organic substances which exhibit reasonably high stability to radiation effects.

Radiation Detectors, Monitoring and Measuring Instruments, Activation Analysis Techniques

Under this heading, one paper of interest with respect to technique used is a communication by P. Keukelsbergs and associates (Belgium) in which data are given on specially selected counter gas mixtures allowing the possibility of measuring tritium in methyl chloride in a Geiger counter with an excellent plateau (length 1300 v, slope 2%). In a paper presented by D. Sprecklen and G. Stevens (Britain) on the use of autoradiography for quantitative analysis of radioactive specimens, a novel technique is advanced for preparing sample preparations with the use of post-scoring techniques, as well as a technique for recording many specimens on a single film. L. Wiesner and associates (West Germany) described an ingenious modification of the procedure of vapor chromatographic analysis using pure argon flow counters operating at reduced pressure in the region between ionization chamber and counter modes of operation.

Papers on activation analysis, especially several contributions devoted to the use of a new technique for carrying on activation analysis, are of some interest.

A paper presented by K. Lungren (Sweden) described a method of activation analysis which allows identification of isotopes in a complex mixture of radioactive substances without prior chemical separation, an accomplishment of enormous value for rapid execution of a large number of analyses. The paper presents a theory to explain the method and cites examples of the determination of several elements in mixtures. An arrangement consisting of a dual-channel facility with NaI-crystal scintillation counters. The channels are included in a triple-coincidence unit, at the output of which is an electronic circuit which determines the amplitude of the incoming signal.

A report by B. Carr (USA) is devoted to the use of pulsed neutron sources (based on the T (d, n) He reaction) in activation analysis. Miniature accelerators developed by the authors produce neutrons at 14 Mev energy and at an intensity adequate for the formation of the required numbers of short-lived radioisotopes in the test samples. A report by W. Meinke (USA) wad devoted to the use of a thermal neutron generator, producing a flux of 10^8 to 10^9 neutrons/ /cm^2·sec, for the same purpose, and to the use of pneumatic devices on reactors with a flux of 10^{12} neutrons/cm^2·sec.

It is worth noting that sources of that type may be found applicable in stationary facilities for neutron production and in portable instruments, particularly when the latter are used for well logging. The use of generators such as those proposed by Meinke broadens the field of applications for activation analysis, bringing it to the level of a routine industrial method, and the use of a pneumatic rabbit makes it possible to carry out an analysis for short-lived isotopes and in combination with high-speed spectrometers, i.e. makes it possible to shorten the time required and to enhance the sensitivity of the method.

The report submitted by W. Kuykendall and R. Wainerdi (USA) is highly interesting in this light. They developed system of automated activation analysis incorporating an anticoincidence gamma-ray spectrometer with a 256-channel analyzer and an IBM-704 electronic computer. This automatic counting arrangement takes into account the character of the gamma-ray spectrum and the decay time of the spectral components, and allows high-speed processing of the data for specimens containing a considerable number of different isotopes. At the present time, it takes 15 min to analyze a specimen containing 15 components. Kuykendall and Wainerdi worked out routines for qualitative and quantitative automatic analysis of specimens containing as many as 25 unknown constituents.

Radioisotopes and Chemistry

Almost one third of the reports read at the conference (49 reports) were devoted to the use of radioisotopes in chemistry. Solutions of analysis problems facilitated by the use of various radioisotope techniques furnished the subject matter for a large grouping of reports.

K. Evans and J. Harrington (Britain) described an interesting procedure followed in determining hydrogen content in metals by isotopic dilution with tritium. Experimental data on hydrogen content in beryllium, aluminum, and uranium specimens were reported.

A paper submitted by D. Ulen and S. Ziegler (USA) dealt with a determination of the composition of matter in the form of a gas or a solution containing compounds with reducing and oxidative properties, by binary chemical ex-

change. The method consists in evolving the radioactive gas Kr^{85} from Kr^{85} quinolate, and the content of the unknown compound is calculated from the amount of gas evolved. The method is interesting, novel, and may be found useful in industry. The authors employed this method for a meterological analysis of ozone in the upper layers of the atmosphere and for an analysis of air pollution by sulfur dioxide gas.

A. Schrodt (USA) proposed a variant of the radiometric method of chemical analysis based on measurements of the radioactivity of an excess of titrating reagent. This method results in fairly high accuracy, is simple in its experimental procedure, lends itself readily to automating adaptations, and is expected to meet with a wide variety of practical applications.

Modifications of the isotope dilution method devised to facilitate identification and quantitative estimating of small amounts of chemical substances were also interesting as described in several reports. In particular, a paper presented by R. Bailey (Britain), devoted to the use of isotope dilution in protein analysis, offers some new approaches in methods for determining racemization of amino acids. H. Phillips and W. Criddle (Britain), with the aid of a combination of paper chromatography and isotope dilution techniques, identified and evaluated the amount of decomposition products (labeled with C^{14} isotope) of gamma-irradiated saccharides. In a report by J. Carroll et al. (Britain), a highly sensitive microanalysis method using F^{18} in fluorine analysis was described; the method is based on the effect of absorption of the fluorine ion by a glass surface.

Several interesting papers were devoted to applications of radioisotopes in organic chemistry.

In a paper presented by T. Pratt and R. Wolfgang (USA), a theoretical investigation of the process of tritium-labeling of methane based on exchange between gaseous tritium and methane, induced by radiation, is presented, and a treatment of the reaction mechanism is given. Together with the paper by K. Wilzbach (USA) which takes up gamma radiation effects on tritium-labeled toluene, this paper may be viewed as a serious attempt to study the elementary events brought about in the molecules of various organic compounds by exchange between hydrogen and gaseous tritium.

In papers presented by H. Simon and D. Palme (West Germany), E. Hondett and R. Rowton (USA), G. Ropp (USA), D. Marinsky and D. Krasner (USA), G. I. Avdulov, N. K. Semenova, and I. F. Tupitsyn (USSR), the use of isotope effects of hydrogen and carbon in studying the mechanisms of organic reactions is described. The study of thermodynamic and kinetic isotope effects of hydrogen in isotope exchange of hydrocarbons dissolved in liquid hydrogen bromide and liquid ammonia reported by the authors of the last-mentioned paper aids in promoting a correct choice of methods for producing tagged (deuterated and tritiated) aromatic hydrocarbons and for bringing about isotope exchange conditions.

A paper presented by L. de Boekner and associates (Belgium) gives findings of measurements of the diffusion rate of a polymer solution through a semipermeable membrane and of adsorption of the polymer on the surface of the membrane. The paper shows that the possibilities inherent in tracer studies of the properties of polymeric systems have been greatly underestimated, and that tracer methods enjoy unquestionable advantages over the conventional and much less sensitive (e.g., gravimetric) methods.

A large group of papers were devoted to the various applications of isotopes in physical chemistry (investigations of kinetics and reaction mechanisms, of the structure of complexes, ion and isotope exchange, adsorptive phenomena, radiolysis, solubility, corrosion, etc.). Many of these papers hold considerable theoretical and methodical interest for specialists working in those fields.

For example, a paper by H. Lawrence and D. Stranks (Britain) expounds a new method for studying reactions of halide atoms, using the nuclear reaction (n,γ) to produce radioactive atoms, which thereupon enter into a reaction with the substrate. Values were obtained for the rate constants and energy of activation for exchange between iodine and methyl iodide ions. A paper by E. Kereszk et al. (Hungary) also took up exchange between iodinated organic molecules and the element iodine, particularly the effect of solvents on isotope exchange rate. Studies of this kind have paved the way for evaluating the strength of iodine atom bonds in molecules, and may harbor practical significance for production of tagged organic (iodinated) compounds through the isotope exchange method.

An investigation of the structure of complex compounds through exchange of radioisotopes was discussed in a paper by B. Jazowska-Zebiatowska and J. Czolkowski (Poland). In this work, isotope exchange methods were successfully combined with other physical-chemical techniques. Data on exchange rates for carbon isotopes in the $K_3Mn(CN_6) + KC^{14}N$ and $K_3Mn(CN)_5NO + KC^{14}N$ systems allowed the authors to present justification for their view on the electronic structure of complexes, and to prove the associative character of the exchange process. The fact of the effect of visible light on exchange rate will be found interesting.

A paper by R. Dietz and associates (USA) presented data characterizing the process of extraction of In^+ and Ga^+ ions from aqueous HCl solutions by dichloroethyl ether. The extraction coefficients were derived radiometrically. In addition to new results referable to the ionization constants of HCl and HBr in an organic phase and the instability constants of $InCl_4^-$ and $InBr_4^-$, the paper present such practical value as, for example, elaboration of ore extraction technology for trivalent metals.

Radioisotopes in Industry

Over 300 papers were presented on the subject of industrial isotope applications. These papers took up both tracer applications and various arrangements for utilizing the penetrating power, absorption, and scattering of radiation.

Such problems as friction, wear, and lubrication were also treated. Reports submitted by the USSR, Great Britain, USA, Czechoslovakia, Japan, Canada, France shed quite a bit of light on new methods using radioisotopes to probe processes responsible for wear of materials, and to reveal the laws governing those processes. A large share of the attention was given to problems related to the operating mechanism of lubricants, rate at which lubricants are used up in practice, etc. Under this heading, the only papers by foreign scientists which presented any fundamentally new data were those by R. Campbell and L. Gruenberg (Britain). Two papers, by G. Cartledge (USA) and A. Findeis (Britain) were review papers on the subject, while the remaining papers offered either concrete cases of applications for already familiar radioisotope techniques to the solution of particular problems, or failed to present adequate proof that the methods suggested in the papers are superior to methods now in use. In particular, one of the papers by Campbell and Gruenberg presented experimental data on engine wear obtained by the method of radioactive inserts. These data, along with findings from numerous other investigations resulting from use of the method of radioactive inserts practiced in the USSR, place in doubt the feasibility of employing the method of activating large-size diesel engine cylinder sleeves, a technique evolved in the USA, especially in the light of a comparison of the simplicity and ease of activation of inserts as against the complexity of shielded irradiation arrangements.

Much interest was evoked by a paper submitted by Yu. S. Zaslavskii and G. I. Shor (USSR) on the use of tracer methods to evaluate the performance properties of lubricating oils. Data were presented on a radiometric method for investigating electrokinetic processes and sedimentation in oils with additives to which tagged carbon black had been introduced. The technique is based on the use of beta counters performing the double function of detectors and electrodes establishing the electric field, an arrangement which makes it possible to automatically record the rate of displacement of tagged carbon black in oils with additives in response to electric and gravitational fields. The method is suitable for investigating various disperse systems having a labeled disperse phase. The authors also render an account of a complex research method which they worked out for probing multicomponent antiseize compounds with highly efficient action against scoring, in the absence of corrosive attack.

An interesting point appearing in papers by Campbell and Gruenberg is the use of pulsating current to achieve local heating of surfaces. The experimental data obtained are of interest to the oil refining industry. Kol, Kopecky, and Frynda (Czechoslovakia) explain an interesting and simple procedure for investigating wear on large turbogenerator parts, in the paper they presented.

W. Grimes (USA) and colleagues presented experimental data on the corrosive action of fluorine-containing compounds on metals. A report by G. Cartledge (USA) devoted to a study of corrosive attack on metals and ways of coping with it attracted the interest of specialists in several branches of industry, even though the paper was intended as a survey.

J. Cameron and P. Berry (Britain) explained their method for checking the leaktightness of vessels by using Kr^{85} which, in the view of the authors, is eminently suitable for leak detection, superior in that respect to other radioactive gases. There are two variants to the method. In the first variant, the gas is admitted inside the vessel and outleakage is measured. In the second variant, the gas is allowed to surround the component to be measured. The technique may be used in industry for automatic monitoring of small vacuum volumes, although contamination difficulties may turn out to be a problem (e.g., occlusion of the gas by the test component).

Several papers were devoted to uses of beta-excited x-rays in the solution of various problems. Among these, we may note the report by R. Pegg and D. Pollack (Britain) dealing with use of a tritium source for continuous analysis of sulfur in hydrocarbon media and gases. The authors developed a device in which absorption of x-radiation emenating from tritium is put to use. The instrument may be incorporated into a process control loop. The sensitivity of the instrument is 0.1% of the sulfur present to an accuracy of 0.03% in a gas and 0.5% of the sulfur present to an accuracy of 0.04% in kerosene. The instrument will bring in sizable economic returns according to the authors' estimates.

Several reports took up the application of radioistopes in thickness gaging and weighing of the outside skin or jacketing of various industrial products. A paper presented by Soviet authors B. N. Vasil'ev and V. K. Latyshev et al. on radioactive thickness gaging of hot-rolled sheet product (5-50 mm thickness) was heard with great interest.

Let us mention, finally, the paper by J. Gregory devoted to the latest achievements in isotope applications in Australia. This paper presents a description of research efforts completed during the past two years. The isotope I^{131} was employed to label a small quantity of hot water at the intake of the cooling pond of an electric power generating station, and the movement of this water was traced till it was completely mixed with the water in the pond. Scintillation counters placed below water level recorded the radiation. A recording scintillation detector mounted in the pump house of the power station measured the rate of water transport shown by the labeled water returning to the station pond. The paper also contains a description of an investigation employing Br^{82} isotope to probe the flow paths in a raw-sugar tank. An application of P^{32}-tagged lubricant to uncover the reasons for the troublesome appearance of oil spots on valuable railway cargo was described, as well as the performance of a high-precision liquid density gage measuring fluid flow in concrete piping.

Production of Isotopes and Radiation Sources and Synthesis of Labeled Compounds

These questions were discussed in 27 papers embracing various aspects of the problem of radioactive preparation fabrication.

Several interesting reports dealt with methods and production technology relating to pile production of radioisotopes and the use of accelerators in isotope production. The report by J. Roy (Canada) devoted to production of the isotope Be^7 was found highly valuable and stimulating. This paper traces the development of the concept of producing radioactive isotopes by using double reactions and successive reactions of the (T, n) and (T, p) types, where tritons are first produced by irradiation of lithium using pile neutrons in the reaction Li^7 (n, p)T. At present, this method is the one used to produce F^{18} and other isotopes. The authors studied four different nuclear reactions and made an evaluation of the efficiency of alternate pathways in Be^7 production. Their suggestion is to produce Be^7 via a double reaction on protons and deuterons obtained through recoil when targets are irradiated by fast neutrons. The reactions are $Li^7(p,n)Be^7$, $B^{10}(p,\alpha)Be^7$, $Li^7(\alpha,n)Be^7$, and $Be^9(n,3n)Be^7$. The authors for instance demonstrated the fact that the reaction $Li^7(p,n)Be^7$ has practical significance in isotope production when LiOH is used as target: 1 gram of LiOH subjected to 20 days bombardment in a neutron flux of $2 \cdot 10^{11}$ neutrons/cm^2 sec intensity, yields several microcuries of Be^7. This paper is particularly important from a fundamental standpoint, since it demonstrates the feasibility of seeking out ways of producing isotopes through double reactions.

The short-lived isotope Fr^{223}, which may be produced from actinium via a paper chromatograph technique, may hold great promise for medical applications (paper by J. Fouarge and V. Meinke, Belgium). The same applies to isotope P^{33}. The development of a method proposed earlier for producing P^{33} via neutron bombardment of enriched S^{33} isotope was discussed in a report by S. Forberg and T. Vestermark (Sweden).

Under this heading, we also take note of a Belgian paper (J. Goste and A. Demildt) on cyclotron production of carrier-free Ta^{182} through deuteron irradiation of tungsten, and on the possibility of producing short-lived isotopes Ta^{184} (deuteron energy 12 Mev and higher) and Ta^{183} (deuteron energy 22 Mev) at satisfactory yields. H. Morinaga told of a new technique elaborated in Japan for producing radioisotopes of high specific activity on an internal betatron target by means of 25 Mev bremsstrahlung and at a dose rate of $\sim 10^4$ r/min. Eight new radioactive isotopes were obtained in this way: Co^{53}, Ga^{75}, As^{81}, In^{121}, In^{123}, Tm^{173}, Tm^{175}, Ac^{231}.

Considerable interest was stimulated by a paper presented by T. Butler, E. Lamb, and A. Rapp (USA) on new technological radioisotope production processes at Oak Ridge. These new processes are similar to techniques developed in the USSR. A shift to solvent extraction for separating out fission products is characteristic and significant in that solvent extraction was not used for those purposes previously in the USA. It is noteworthy that the processes recently developed in the USA have already been put into practice and are being utilized to produce isotopes having activities ranging high into the kilocurie range (Cs^{137}, Ce^{144}, Pm^{147}, Sr^{90}, Tc^{99}). It is particularly fitting to note the scaled-up pilot production of Pm^{147} and Tc^{99} and the high purity and specific activity reported for Pm^{147} (425 curies per gram of oxide, which is one half the highest theoretical computed activity).

Reports by I. Filosofo et al. (USA) and J. Cameron and J. Rhodes (Britain) on the production and investigation of beta-excited soft x-ray sources are of considerable interest. In these papers, data on the spectra and photon yields are determined experimentally and computed theoretically as functions of energy of beta radiation, thickness and atomic number of the target material; the design of four different types of sources is shown (target in front, reflecting

target, target formed of layers, and a source where the radioactive substance and target material are mixed). The papers present data for H^3, Kr^{85}, $Sr^{90}+Y^{90}$, Tl^{204}, and Pm^{147} targets, and describe a high level Pm^{147} source for industrial radiographic work.

J. Puig and J. Sandier (France) presented a paper on the preparation of solid Kr^{85} sources. A team of Soviet scientists (N. I. Bogdanov and others) submitted a report on a thermal method for preparing Sr^{90}-base sources.

Several reports read by scientists from various countries (USA, Italy, UAR, Belgium, West Germany) on the subject of synthesis of labeled compounds by various physical-chemical techniques (in an electric-arc discharge, under exposure to radiation and ultraviolet light) were heard at the conference. All of these papers offer only the underlying principles and possibilities inherent in the methods, with no concrete synthesizing techniques, since most of the workers failed to carry out adequate separation and purification of the substances containing radioisotopes, and therefore failed to adduce any data on contaminations of the basic product. It should also be mentioned here that these efforts constitute a novel and promising trend in the production of labeled molecules.

Soviet scientists presented several reports on research efforst using the energy of recoil nuclei to obtain radioactive preparations.

In a report by L. N. Kurchatova and B. V. Kurchatov, the production of concentrated Cl^{36} and Br^{82} preparations (with increased specific activity) via the method of recoil nuclei under irradiation in high-density neutron fields was discussed. The authors suggested and tried out an ingenious method for producing concentrated preparations of radiohalogens based on a modification of the Szilard-Chalmers effect. As a result, Br^{82} preparations were produced with specific activity reaching 15 mC/mg, and Cl^{36} preparations with specific activity to 0.23 mC/g.

A. N. Nesmeyanov et al. discussed the results of an investigation of interaction between tritium recoil atoms (obtained from irradiation of lithium) and some organic compounds. The authors studied the effect of tritium recoil atoms on cyclohexane, methyl cyclohexane, cyclohexanol, cyclohexylamine, benzene, cyclohexadienes, and demonstrated the possibility of producing tritiated cyclic hydrocarbons via "hot synthesis" with rather high yields. A report by B. G. Dzantiev and N. M. Barkalov entitled "Synthesis of radiosulfur-labeled compounds as a result of reactions between hot S^{35} atoms and cyclic hydrocarbons" summarized the results of many years' work by the authors on synthesizing sulfur-tagged open-chain and cyclic mercaptans and sulfides.

The role of vapor chromatography in the synthesis of labeled organic compounds was stressed in a paper submitted by Pichat et al. (France). A paper by R. Henri et al. (France) described methods for synthesizing some organic iodine-containing compounds by the isotope exchange approach.

A paper by Soviet authors O. I. Andreeva and G. T. Kostikova discussed carbon isotope exchange reactions between potassium cyanide and lithium carbonate, sodium carbonate, potassium carbonate, and barium carbonate.* The authors worked out a new method for synthesizing C^{14}-tagged potassium cyanide, which is the basic building block in the synthesis of many organic C^{14} compounds via isotope exchange $BaC^{14}O_3 \rightarrow KCN$ with subsequent separation of the potassium cyanide from the carbonate by ammonia liquid extraction. Labeled KCN is obtained in up to 90% yield and containing up to 96% basic material. Finally, we take note of the fact that work is being pursued in other lands on development of biosynthesis approaches to the production of labeled compounds. Interesting data on biosynthesis of three important S^{35}-labeled amino acids are to be found in a report by P. Chapeville et al. (France). S. A. Barker and associates (Britain) described the synthesis of two complex compounds (cyclic derivatives of C^{14}-tagged saccharides) based on biosynthesis by microorganisms.

Other papers described methods of synthesis involving the use of various labeled organic compounds.

The proceedings of the conference will be made available in printed form by the International Atomic Energy Agency early in 1961.

* Translators note "boron carbonate" in text. $BaCO_3$ is probably intended, and is mentioned in next sentence. Boron does not form a stable carbonate, as far as I know.

Translated from Atomnaya Energiya, Vol. 10, No. 2, pp. 190-191, February, 1961

USSR. The first steam turbine for the Novo-Voronezh nuclear power station has come off the line at the Kirov factory in Kharkov. The installation has a power rating of 70,000 kw. The turbine, designed for 3000 rpm, will be operated on saturated steam at 29 atmos pressure. The turbine will be automatically controlled.

USSR. The IV All-Union Conference on Physico-Chemical Analysis met in Moscow, December 6-10, 1960. Reports dealing with physico-chemical analysis of metals used in nuclear engineering, and with new problems in physico-chemical analysis related to nuclear radiation effects on materials were discussed at the plenary sessions. Panel sessions took up uranium metals and rare (refractory and rare-earth) metals.

BIBLIOGRAPHY

NEW LITERATURE

Translated from Atomnaya Énergiya, Vol. 10, No. 2, pp. 192-200

Books and Symposia

I. E. Irodov. Compendium of Problems in Atomic Physics. 2nd edition. Moscow, Atomizdat, 1960, 252 pages. 50 kopeks.*

This compendium contains about 850 problems and fairly adequate hints for the solution of the most complex and tough ones.

Each chapter begins with a brief review of the basic concepts and relationships needed to solve the problems dealt with in the chapter; the book terminates with a reference appendix of physical constants and useful tabulated data.

The number of problems has been increased 50% over the number in the first edition of the book, and illustrations have tripled in number. Three new chapters have been introduced: the Schroedinger equation, Characteristics of the atomic nucleus, and Elementary particles. The appendix has been supplemented with new tables.

This problem and answer book may be used as a textbook for a general course in atomic physics, for students majoring in physics.

G. N. Balasanov. Fundamentals of Process Control in the Hydrometallurgy of Rare and Radioactive Metals. Edited by Academician B. N. Petrov. Moscow, Atomizdat, 1960, 313 pages. 1 ruble, 41 kopeks.*

This book makes a presentation of the basic information on technical means of automatic control, and describes up-to-date techniques in design work and calculations for automatic checking, monitoring, and control systems applicable to technological processes in the hydrometallurgy of rate and radioactive metals.

The fundamental tenets of linear automatic control theory are presented, and some of the techniques are approached on the basis of concrete examples in setting up control loops and studying their stability. Some of the methods employed in studying nonlinear automatic control systems are entered into briefly. Process control variables of interest in hydrometallurgy are discussed, and recommendations are offered on the choice and adjustment of automatic controllers and on the design of control components.

Particular aspects of information on the design of systems subjected to random distrubances and adaptive control systems are outlined in concise form.

Recommended reference literature is listed at the end of the book.

The book is written to reach engineering and technical workers engaged in hydrometallurgical production, but may also be found useful by students in advanced institutes specializing in the field of hydrometallurgical process control.

M. Curie. Radioactivité. Translated from the French, 2nd edition. Moscow, Fizmatgiz, 1960. 516+xvi pages. 2 rubles, 2 kopeks.

This book is a classical monograph written on the basis of a lecture course which the author taught for many years at the Sorbonne. The first section of the monograph offers brief information on gaseous ions, electrons, and

* Prices are in terms of the new "heavy" ruble.

rays formed in rarefied gases as electric current is passed through them. The second and principal section of the monograph is devoted to naturally radioactive elements and their emitted radiations.

The book is written both for practicing scientific workers (physicists and chemists) and for students.

A. H. Vapstra, G. I. Hiech, R. Van Lishut. Nuclear Spectroscopy Tables. Translated from the English. Moscow, Atomizdat, 1960. 178 pages. 85 kopeks.

The book contains reference material dealing for the most part with alpha, beta and gamma ray spectroscopy.

Most of the data is presented in the form of graphs and tables, and only a small portion appears in textual form as concise explanations included in each section. The experimental data appearing in the book are accompanied by information of a theoretical nature. Particularly interesting from this standpoint are sections VIII and IX, which are devoted to angular distribution problems, correlations, and nuclear models.

The book may be used as a reference handbook in nuclear physics labs.

Plutonium Recycling in Thermal Reactors. Translated from the English. Moscow, Foreign Literature Press, 1960. 112 pages, 40 kopeks.

Problems involving plutonium recycling in nuclear reactor systems had to crop up sooner or later in nuclear engineering discussions. These problems form the subject of one of the 13-volume USAEC publications.

This volume embraces a rather wide range of questions, starting with physical problems related to plutonium utilization, and ending in reactor design for plutonium-burning reactors. It is generally known that one such reactor (PRTR) is under construction in the USA, and is expected to go into operation in the not too distant future. The problems of plutonium reactor physics are considered in this book in their relation to the PRTR reactor. Data of possible use in reactor neutron physics calculations are presented. However, the lion's share of the attention is given to plutonium fuel cycling, which is approached from the vantage point of maximizing savings in fuel costs and consequently optimizing the over-all economics of the reactor plant as a whole.

In discussing the problem of determining plutonium costs, we are led to the conclusion that this cost can be arrived at by assuming the plutonium to be a source of heat required for the generation of electric power, in other words through a comparison between plutonium and uranium as neutron sources.

The second large grouping of questions relates to plutonium technology with plutonium approached as a fuel. In this section, the design of fuel elements, plutonium alloys and their properties, plutonium ceramics, the fabrication of plutonium fuel and plutonium fuel elements, and data on pile testing of plutonium fuel are discussed. Methods used in chemical reprocessing of plutonium fuel elements are described.

The third section is devoted to the design of facilities for handing plutonium or using plutonium. In particular, a pilot plant for fabricating plutonium fuel and a plutonium recycle test reactor are described. A report on this reactor was presented to the second Geneva conference in 1958 and appeared in Russian translation.*

On the whole, the book may prove highly useful to specialists in power reactor design, since it sheds light on problems directly related to the perspectives of nuclear power development.

Articles from the Periodical Literature

I. Nuclear Power Physics

Neutron physics and reactor physics. Hot plasma physics and controlled fusion. Physics of acceleration of charged particles.

* Proceedings of the Second International Conference on the Peaceful Uses of Atomic Energy, Geneva 1958. Selected papers by foreign scientists. Vol. 4. Nuclear reactors and nuclear power engineering (in Russian). Moscow, Atomizdat, 1959, page 352.

Vestnik akad. nauk SSSR XXX, No. 10 (1960)

I. E. Tamm, p. 10-22. The current situation in the problem of the elementary particles.

——, 106-08. Low-energy and medium-energy nuclear reactions. Review of papers presented at the Second All-Union Conference on Low-Energy and Medium-Energy Nuclear Reactions. Moscow, July 21-28, 1960.

Doklady akad. nauk SSSR 134, No. 2 (1960)

F. A. Korolev et al., 314-17. Experimental research on electron oscillations in cyclic accelerators.

Zhur. tekhn. fiz. XXX, No. 10 (1960)

V. S. Vasil'evskii et al., 1137-44. The Tokamak-2 strong-field toroidal facility.

V. V. Matveev, A. D. Sokolov., 1145-51. Investigation of hard x-rays emitted by the Tokamak-2 toroidal machine.

E. P. Gorbunov et al., 1152-64. Investigation of a toroidal discharge in a strong magnetic field.

N. L. Tsintsadze, A. D. Pataraya, 1178-85. Cerenkov generation of hydromagnetic and magnetoacoustic waves in a rarefied anisotropic plasma.

L. M. Kovrizhnykh, 1186-92. On the instability of longitudinal oscillations in an electron-ion plasma placed in an external electric field.

Zhur. éksptl. i teoret. fiz. 39, No. 4 (1960)

V. S. Nikolaev, et al., 905-14. Investigation of equilibrium charge distribution in a beam of high-energy ions.

I. E. Nakhutin et al., 991-92. Production of the radioactive isotope Kr^{85} and studies of its gamma emission.

S. P. Kapitsa et al., 997-1000. A large-current microtron.

R. V. Polovin, 1005-1007. On the progress of shock waves traveling along magnetic field lines.

M. V. Kazarnovskii, A. V. Stepanov, 1039-41. Elastic resonant scattering of slow neutrons in crystals.

L. M. Kovrizhnykh, 1042-45. On shock waves in relativistic magnetohydrodynamics.

V. V. Vladimirskii, 1062-70. Magnetic mirrors, magnetic channels, and magnetic bottles for cold neutrons.

V. A. Karnaykhov, N. I. Tarantin, 1106-11. On the possibility of proton decay in nuclei.

Izvestiya akad. nauk SSSR, seriya fiz. 24, No. 9 (1960)

S. A. Baranov et al., 1035-40. Investigation of the fine structure of alpha emission by U^{234} and U^{235} (report submitted to the X All-Union Conference on Nuclear Spectroscopy, January 1960).

A. A. Vorob'ev et al., 1092-98. Study of alpha decay of U^{235} using an ionization alpha spectroscopy, January 1960).

Smena No. 19 (1960)

M. A. Leontovich, 22-23. People will one day burn their own sun here on earth (article dealing with the problem of building a thermonuclear electric power station.

Uspekhi fiz. nauk LXXII, No. 2 (1960)

A. I. Baz' et al., 211-34. Undiscovered isotopes of light nuclei.

Atomwirtschaft V, No. 10 (1960)

K. Franz, 458-60. Pulse analyzers for spectroscopy.

H. Wirtz, 461-62. Electronic paramagnetic resonance and nuclear magnetic resonance, new frontiers in spectrometry.

G. Horlitz, 479-81. Problems related to high-energy physics measurements.

Kerntechnik 2, No. 10 (1960)

J. Kalus, M. Pollermann, 319-22. Compensation ionization chamber for measuring thermal neutron flux.

Nucl. Energy No. 149 (1960)

J. Turner, 476, 484. Epoxy compound plastics used as a synchrotron material.

Nucl. Engng. 5, No. 54 (1960)

———, 523. The second accelerator conference, Amsterdam, October 4-6, 1960.

Nucl. Sci. andEngng. 8, No. 3 (1960)

R. Caldwell et al., 173-82. Gamma radiation from inelastic scattering of 14-Mev neutrons by the common earth elements.

H. Møller et al., 183-92. Low-energy neutron resonances in erbium and gadolinium.

Yadernyi sintez 1, No. 1 (1960) (Fusion research)

I. Bernstein, S. Trehan, 3-41. Plasma oscillations. I.

T. Green, G. Niblett, 42-46. Rayleigh-Taylor instability in a plasma accelerated in a magnetic field.

C. Mercier, 47-53. A necessary criterion of hydromagnetic stability applicable to an axisymmetric plasma.

H. Bodin et al., 54-61. Fast compression of a heated plasma in a linear z-pinch.

W. Faust, E. Harris, 62-63. Energy distribution of thermonuclear neutrons.

II. Nuclear Power Engineering

Theory of nuclear reactors an reactor calculations. Reactor design. Performance of nuclear reactions and of nuclear electric power generating stations

Vodosnabzhenie i san. tekhnika No. 9 (1960)

Z. B. Kipnis, 39-40. Nuclear power for space heating (outside the USSR).

Nauka i tekhnika No. 1 (1960)

Z. Peleke, W. Ulmanis, 4-7. Salaspils, our Latvian Dubna.

Atomkernenergie 5, No. 9 (1960)

H. Grümm, F. Putz, 309-312. Calculations for a water-moderated highly-enriched-fuel reactor.

J. Schmidt. 313-23. Studied of infinite, unmoderated, homogeneous critical systems.

W. Kliefoth, 344-49. Development of nuclear power in the German Democratic Republic [East Germany].

Atomkernenergie 5, No. 10 (1960)

N. Papmehl 357-360. A simple method for determining neutron Fermi age in light water.

D. Smidt, 361-66. Design of gas-cooled maritime-propulsion reactors.

H. Daldrup, 366-71. Circulation problems for saturated-steam cycles in an organic-cooled, organic-moderated maritime reactor.

H. Grümm, F. Putz, 371-79. Calculations for a water-moderated highly-enriched-fuel reactor. II.

Atompraxis 6, No. 10/11 (1960)

W. Zumach, 397-404. Nuclear instrumentation for reactors. Report 2. Personnel dosimetry, and instruments for monitoring fuel elements and neutron flux.

Atomwirtschaft V, No. 9 (1960)

H. Daldrup, 393-95. The atomic icecutter LENIN.

---, 396-97. Development of fuel element production. Based on proceedings of the IEAE conference, Vienna, May 1960.

R. Nass, 399-408. Materials and welding in reactor design.

Atomwirtschaft V, No. 10 (1960)

H. Braun, 434-37. Control problems in nuclear power reactor operation.

E. Schrüfer, 441-44. Instruments for physical measurements in nuclear reactors.

E. Schrüfer, 445-48. Applications for conventional measuring devices in nuclear reactor operation.

Kerntechnik 2, No. 9 (1960)

M. Pollermann, W. Marth, 265-67. Irradiation techniques used in the Munich research reactor.

W. Mialki, 282. Uses of boiling metals innuclear reactors.

A. Mareske, 283-84. Thermodynamic problems in maritime reactors. II. Engineering problems.

Kerntechnik 2, No. 19 (1960)

D. Bünemann, 297-300. Nuclear reactor control problems.

U. Kaczmarek, 300-301. Simulation of dynamical behavior of nuclear reactors.

W. Havranek, 307-12. Analog simulation applications in reactor work.

P. Dosch, E. Schneider, 313-18. Measuring equipment for the FR-2 research reactor at Karlsruhe.

---, 330. Neutron detectors for reactor design applications.

Nucl. Energy No. 149 (1960)

W. Shoupp, 458-61. In-pile direct conversion.

---, 477-78. Over-all building siting plan for the DRAGON reactor project.

Nucl. Energy No. 150 (1960)

---, 533-35. The Winfrith Heath reactor research center.

—, 539-42. The American HTGCR reactor.

Nucl. Engng. 5, No. 52 (1960)

J. Moore, 385-90. An analysis of shortcomings in research reactors using punch-card systems.

---, 393-94. Steam superheat in BWR-1 type reactors.

C. Braun, 395-396. Steam superheat in BWR-2 type reactors. Present state of the art and future outlook.

---, 400. Low-power and medium-power reactors.

U. Alfredsson, 405-408. Aluminum welding in reactor design.

D. Markham 413-14. Simulation of power reactors.

Nucl. Engng. 5, No. 54 (1960)

G. Emmerson, 493-500. Heat transfer during a boiling process.

---, 505-506. Choice of a reactor as a neutron source.

J. Griffin, 506-508. Design and building of the NESTOR reactor.

G. Ford, 513-516. Complex experiments in power reactor design.

Nucl. Power 5, No. 55 (1960)

J. Southwood et al., 74-76. The Berkeley nuclear electric power station. Construction and modifications of the original plan.

R. Vaughan et al., 77-79. The Bradwell nuclear electric power station. Construction and modifications of the original plan.

A. Bond, D. Angwin, 80-82. The Hunterston nuclear electric power station. Construction and modifications of the original plan.

W. Wadkin, D. Hutton, 83-85. The Hinkley Point nuclear electric power station. Construction and design.

J. Bishop, 86-88. The Trawsfynydd nuclear electric power station. Construction and design.

---, 89. The Soviet 50 Mw SM research reactor.

S. Hollands, 90-91. The opinion of British frims on reactor exports.

R. Guard, 92-94. Potential buyers of nuclear power stations.

---, 95. A storage pit for spent fuel elements at Harwell.

A. Powell, T. Leader, 97-100. The IAEA conference on low-power and medium-power reactors, September,1960.

C. Plumton et al., 101-103. Inner cathodic shielding of metals surfaces.

---, 109. A fuel element testing tower.

Nucl. Sci. and Engng. 8, No. 3 (1960)

H. Honeck, 193-202. Distribution of thermal neutrons in space and energy in reactor lattices. I. Theory.

H. Honeck, I. Kaplan, 203-209. Distribution of thermal neutrons in space and energy in reactor lattices. II. Comparison of theory and experiment.

R. Macklin et al., 210-220. Manganese bath measurements of neutron regeneration factor (eta) of U^{233} and U^{235}.

F. Kloverstrom et al., 221-225. Critical measurements of near-homogeneous BeO-moderated, enriched-uranium-fueled systems.

R. Lingenfelter, 225-32. Criticality calculations of BeO-moderated, enriched-uranium systems.

J. Chernik, 233-43. Dynamics of a xenon-controlled reactor.

E. Gyftopoulos, 244-50. Effect of delayed neutron precursors on nonlinear reactor stability.

R. Murray et al., 254-59. Control rod theory for asymmetrical arrays and reflected cores.

M. Wagner, 287-81. Spatial distribution of resonance absorption in fuel elements.

G. Rakavy, 281-82. Perturbation method applied to neutron transport theory.

Nukleonika V, No. 9 (1960)

P. Szulc, 503-12. Automation of power variation and of compensation of slow reactivity changes in the WWR-S reactor.

A. Selecki, 513-30. On the effect of some hydrodynamical factors on the catalytic exchange of deuterium between hydrogen and water vapor.

Z. Bieguszewski et al., 542-550. Analysis of primary coolant loop water in the WWR-S reactor.

Reactor Science 12, No. 4 (1960)

T. Högberg, 145-50. Monte Carlo computation of thermalization of neutrons in a heterogeneous system.
N. Sjöstrand, 151-54. Determination of the diffusion constant in one-group theory.
A. Kirchenmayer, 155-61. Kinetics of boiling-water reactors.
M. Cabell, 172-176. Thermal neutron cross section and resonance integral of Mo^{100}.
D. Ricabarra et al., 177. In-pile measurements of fast neutrons using threshold detectors.
B. Fastrup, 177-78. Cadmium cutoff measurements using thin and thick gold foils.

III. Nuclear Fuel and Materials

Nuclear geology and primary ore technology. Nuclear metallurgy and secondary ore technology. Chemistry of nuclear materials

Geokhimiya No. 6 (1960)

V. I. Baranov et al., 490-97. Neutron-borometric contouring.

Doklady akad. nauk SSSR 134, No. 1 (1960)

A. G. Zhabin, M. E. Kazakova, 164-67. On thorite from the alkali complex of the Vishnevy Mts. in the Urals.

Doklady akad. nauk SSSR 134, No. 4 (1960)

I. V. Batenin et al., 802-805. Effect of neutron irradiation on the fine crystal structure and properties of metals and alloys.

Zhur. neorgan. khim. 5, No. 9 (1960)

Vikt. I. Spitsyn et al., 1938-42. Some problems in the thermodynamics and kinetics of the dissolving of uranium oxides in an acid medium.
A. G. Kozlov, N. N. Krot, 1959-63. Spectrophotometric investigation of uranyl-EDTA complex formation.
A. S. Solovkin, 2119-31. Effect of salting-out agents on the distribution of uranyl nitrate between an aqueous solution and the di-isoamyl ether of methylphosphonic acid.

Zhur. prikladnoi khim. 33, No. 9 (1960)

P. P. Budnikov, R. A. Belyaev, 1921-40. Beryllium oxide and its properties.
I. F. Nichkov et al., 2136-39. Interaction between uranium-containing melts of halide salts and bismuth.

Izvestiya akad. nauk SSSR, Otdel. khim. nauk No. 8 (1960)

Vikt. I. Spitsyn, 1325-32. New data on the effect of radioactive radiation on solids and external radiation on some hetergeneous chemical processes. Report to the general session of the Division of Chemical Sciences of the USSR Academy of Sciences (April 20, 1960).

Kuznechno-shtampovochnoe proizvodstvo No. 9 (1960)

I. L. Perlin, V. A. Fedorchenko, 12-18. On the technology of extrusion of uranium and uranium alloys.

Prikladnaya geofizika No. 28 (1960)

E. M. Filippov, 201-11. Group-method study of the distribution of neutron densities in strongly absorbing rocks cored in drill-hole logging.

Trudy po khimii i khim. tekhnol. No. 2 (1960)

A. M. Petrov et al., 248-53. Chromatographic concentration of radioactive isotopes and various substances present in dilute solutions (report I).
M. N. Kulikova et al., 352-57. Regeneration of radiochlorine from discards of chlorine-36-tagged hexachlorane.

Uspekhi khimii XXIX, No. 9 (1960)

K. I. Sakodynskii, N. M. Zhavoronkov, 1112-37. Dual-temperature techniques of heavy water production.

Uspekhi khimii XXIX, No. 10 (1960)

D. I. Ryabchikov, E. A. Terent'eva, 1285-1300. New developments in techniques for rare-earth separation.

Uchenye zapisi Leningrad. univ., No. 297, seriya khim. nauk No. 19 (1960)

M. N. Gordeeva, M. N. Myazdrikova, 16-19. Separation of zirconium and uranium on EDE-OP anion exchange resin from sufate solutions.
I. A. Tserknovitskaya, N. S. Borovaya, 96-98. Behavior of zirconium in extraction of uranium and niobium diethyldithiocarbaminates.

Yu. V. Morachevskii, N. S. Borovaya, 99-101. Separation of traces of zirconium by extraction with tributylphosphate.

I. A. Tserknovitskaya, A. K. Charykov, 109-118. Development of a procedure for analyzing uraninite.

Yu. V. Morachevskii et al., 119-124. A new variant in the cupferron method of uranium separation.

Atomwirtschaft V, No. 9 (1960)

L. Bangert, 408-11. Zirconium and zirconium alloys as structural materials and cladding materials in maritime reactors.

Canad. J. Chem. 38, No. 10 (1960)

R. Bailey, L. Yaffe, 1871-80. Separation of some inorganic ions by high-voltage electromigration in paper (paper electrophoresis).

O. Sepall, S. Mason, 2024-25. Distribution of tritium between tritiated water and vapor.

Nucl. Energy No. 149 (1960)

F. Paulsen, 471-73. Heavy water. Research and production in France.

Nucl. Engng. 5, No. 52 (1960)

B. Eriksson, 409-12. Heavy water production in Sweden.

Nucl. Engng. 5, No. 54, (1960)

M. D'Amore, 501-504. Fuel element fabrication for a pressurized water reactor.

Nukleonika V, No. 9 (1960)

M. Taube, 531-39. Effect of concentration of nitric acid on the extraction of a plutonium (IV) complex using ammonium tetrabutylnitrate in mixed solvents.

M. Orman, A. Galanty, 551-58. Isolation of very pure potassium.

M. Perec et al., 559-68. Experimental work on production of uranium metal by reduction of uranium tetrafluoride with calcium metal.

J. Dobrowolski, 583-84. Study of uranium extraction from uranium ore solutions.

Reactor Science 12, No. 4 (1960)

W. Blackburn et al., 162-71. Effect of thermal cycling on creep in uranium.

IV. Nuclear Radiation Shielding

Radiobiology and radiation hygiene. Shielding theory and shielding techniques. Instrumentation

Biofizika 5, No. 5 (1960)

A. V. Bibergal', 628-30. Gamma facility for chronic exposures in a radiobiological experiment.

Med. radiologiya 5, No. 8 (1960)

M. N. Pobedinskii, 90-93. Conference of exports of the World Health Organization on radiogiology (Geneva, April, 1960).

Med. radiologiya 5, No. 9 (1960)

A. K. Arnautov, 93-95. The First Ukrainian republic-wide scientific conference on medicinal and diagnostic applications of radioactive isotopes, Kharkov, May, 1960.

Nauchnye trudy Severn.-Zapad. nauchno-issled. inst. sel'sko-khoz. No. 1 (1960)

V. M. Motkin, V. S. Rabinovich, 163-71. Radiophosphorus doses in vegetation experiments with spring wheat, and the effect of radioactive radiations on the productivity of spring wheat crops.

Priborostroenie No. 10 (1960)

A. V. Klimushev, V. S. Merkulov, 30-31. Criterion in the choice of protective membranes in measurements using the method of attenuation of beta radiation.

Trudy inst. biologii (Ural'sk. filial akad. nauk SSSR) No. 13 (1960)

N. V. Timofeev-Resovskii, 73-96. Development and present state of the art of radiation genetics.

Trudy Sverdlov. sel'sko-khoz. inst. vol. 7 (1960)

P. R. Borodin et al., 239-43. Some results of the effect on ionizing radiations on corn.

Atomkernenergie 5, No. 9 (1960)

W. Burkhardt, D. Herrmann, 324-32. Calibration of beta dosimeters.

R. May, H. Schneider, 333-35. Artificial radioactivity of spring water and river water.

W. Gerlach, K. Stierstadt, 335-40. Studies of radioactive fallout and radioactivity of air (VI).

Atomkernenergie 5, No. 10 (1960)

K. Lindackers, 379-83. Reactor radiation shielding design. II.

Atompraxis 6, No. 9 (1960)

R. Plesch, 348-52. Shielding design calculations observing existing radiation regulations.

Atompraxis 6, No. 10-11 (1960)

N. Hemmer, H. Wilimzig, 392-96. Scram monitoring system for nuclear reactors.

T. Musialowicz, F. Wachsmann, 404-407. Note on the problem of beta shielding.

H. Egelhaaft et al., 407-11. Use of the film blackening method for checking observation of radiation shielding measures in laboratories where radium and radioisotopes are handled.

F. Wachsmann, 411-413. Note on the preceding article.

F. Habashi, T. Shonfeld, 414-15. Gamma-ray spectrometry techniques for detecting settling of "fresh" fallout fission products into the biosphere.

Atomwirtschaft V, No. 9 (1960)

J. Pfaffelhuber, 384-90. A new law on radiation shielding in West Germany.

Atomwirtschaft V, No. 10 (1960)

L. Merz, 437-41. "Uncontrolled runaway" and "scramming" as shielding problems in nuclear electric power stations.

N. Hemmer, H. Wilimzig, 449-57. Scram monitoring system for nuclear reactors.

G. Boucke. 463-65. Counters in radiation measurements techniques.

P. Rinn, 465-72. Trends inscintillation counter development.

J. Schulz, 473-74. Use of transistors in dosimeters.

S. Müller, 475-78. Modular assembling of dosimeters.

Kerntechnik 2, No. 9 (1960)

M. Oberhofer, 276-81. Graduation and calibration of dosimetric instruments.

Kerntechnik 2, No. 10 (1960)

T. Friese, 322-23. Shielding devices in the power measurements hole of the Berlin reactor.

H. Fessler et al., 324-326. Simple anticoincidence circuits with two proportional flow counters.

E. Leiter, 327-29. A portable fast-neutron dosimeter.

Nucl. Energy No. 149 (1960)

A. Gould, 464-67. Radioactive contamination problems. Required safety measures.

Nucl. Energy No. 150 (1960)

J. Coltman, 530-532. Structural materials for thermionic generators.

Nucl. Engng. 5, No. 52 (1960)

K. Orton, 401-402. Review of papers read at the conference on radiation dosimetry, Vienna, June, 1960.

Nucl. Power 5, No. 55 (1960)

D. Taylor, 104-108. International conference and exhibit on instrumentation and measurements.

Nucl. Sci. and Engng. 8, No. 3 (1960)

D. Anderson, K. Shure, 260-69. Thermal neutron flux distribution in metal-hydrogenous shields.

S. Wexler, 270-73. Standard boron solutions for neutron absorption measurements.

J. Ayer et al., 274-76. Engineering aspects of the water vapor permeability of glove materials.

Nukleonika V, No. 9 (1960)

Z. Kachliki, 569-73. A linear pulse amplifier.

J. Andruszkiewicz et al., 576-82. Plastic scintillators.

V. Radioactive and Stable Isotopes

Labeled-atoms technique. Uses of radioactive radiations. Direct conversion of nuclear energy to electric energy

Avtomobil. prom. No. 9 (1960)

A. Kh. Éliava, 30-33. Procedure for utilizing tracers in studies on wear on carburetor engine parts.

Azerb. khim. zhur. No. 2 (1960)

M. M. Melik-Zade et al., 127-34. Evaluation of film formation of oil additives on rubbing surfaces, using tracer methods.

Vestnik akad. nauk SSSR XXX, No. 10 (1960)

V. D. Goroshko, 64-66. Radiometric dry method for coal dressing.

Vestnik vsesoyuz. nauchno-issled. inst. zhelez.-dorozhn. transporta No. 6 (1960)

V. S. Shadikyan, A. N. Toropchinov, 13-17. Procedure for estimating the wear-resistance properties of diesel oils, using tracer techniques.

Vestnik Mosk. univ., seriya 3. Fizika, astronomiya No. 4 (1960)

B. A. Nelepo, 64-70. Determination of the turbulent diffusion coefficient in sea water, using tracers.

Voprosy rats. vedeniya vinogradarstva No. 1 (1960)

P. I. Litvinov, 89-93. Radiophosphorus used in studying regeneration of grapevine roots and interrelations between separate parts of a grapevine.

Doklady akad. nauk SSSR 134, No. 2 (1960)

É. E. Vainshtein, Yu. I. Belyaev, 322-25. Tracer studies of spatial distribution of atoms in a constant-current arc plasma in different atmospheres.

I. I. Pokrovskii, M. M. Pavlyuchenko, 391-393. S^{35}-tracer investigation of the oxidation mechanism in oxidation of copper by molten sulfur.

Doklady akad. nauk SSSR 134, No. 3 (1960)

V. F. Oreshko et al., 636-38. Effect of ionizing gamma rays on the structural and mechanical properties of starch gels.

Doklady akad. nauk SSSR 134, No. 4 (1960)

V. E. Kazarinov, N. A. Balashova, 864-67. Tracer investigation of adsorption and desorption of iodine on smooth platinum.

Izvestiya akad. nauk Armyan. SSR. Biol. nauki 13, No. 5 (1960)

V. L. Ananyan, 87-90. On the radiometric method for determining total potassium content of a soil.

Izvestiya akad. nauk Latv. SSR No. 7 (1960)

G. Gaile, 162-71. On experience acquired in the assimilation of radioactive isotopes and nuclear radiations into the operations of enterprises in the national economy of the Latvian SSR.

Izvestiya vyssh. ucheb. zaved. Fizika No. 4 (1960)

———, 152-59. Effect of gamma radiation on the dielectric properties of some electrical insulator materials.

3. K. I. Vodop'yanov et al. Lacquers and varnishes. 4. K. I. Vodop'yanov et al. Polyethylene.

Izvestiya vyssh. ucheb. zaved. Chernaya metallurgiya No. 8 (1960)

N. A. Chelyshev et al., 48-58. Tracer studies of metal flow during rolling on a 750 rolling mill.

Liteinoe proizvodstvo No. 10 (1960)

V. I. Dobatkin, B. I. Simakovskii, 34-36. Tracer investigation of aluminum crystallization in continuous casting.

Mineral'noe syr'e (Vsesoyuz. nauchno-issled. inst. mineral'nogo syr'ya) No. 1 (1960)

E. I. Zheleznova, D. V. Tokareva, 277-82. Use of a scintillation beta counter in determining zircon content.

Prom. énergetika No. 9 (1960)

A. D. Grober, 33-34. Applications for radioactive level gage annunciators in the cotton processing industry.

Trudy vsesoyuz. nauchno-issled. kinofotoinst. No. 37 (1960)

A. V. Borin et al., 78-94. Tracer studies of adsorption of thiosulfate by microcrystals of silver bromide in photographic emulsions, using radiosulfur tracer atoms.

Trudy Mosk. inst. neftekhim. i. gaz. prom. No. 31 (1960)

K. I. Yakubson, Sh. A. Guberman, 81-99. Experimental investigation of the space and energy distribution of neutrons, using a plastic model.

Trudy. Kharkov. avtomobil.-dorozhn. inst. No. 23, (1960)

A. I. Danilenko, 125-28. On the use of radiometric techniques in highway construction.

Uspekhi fiz. nauk LXXII, No. 2 (1960)

N. S. Gorbunov, V. I. Izvekov, 273-306. Tracer study of diffusion in metal oxides.

Khim. i tekhnol. topliv i masel No. 9 (1960)

A. A. Kuznetsov, V. S. Luneva, 61-64. Quantitative tracer determination of anticorrosion properties of high-consistency lubricants.

Atomkernenergie 5, No. 10 (1960)

——, 384, Possibilities of utilizing underground explosions for scientific and industrial purposes.

Atompraxis 6, No. 10-11 (1960)

H. Langel, 337-379. A summing instrument for comparing values obtained in tracer measurements of the thickness of materials.

P. Gerke, 380-85. Applications for radiation-measuring instruments in the petroleum and petrochemical industry.

K. Waechter, 385-91. Choice of a proper detector for gaging the thickness of relative thick specimens.

Atomwirtschaft V, No. 9 (1960)

H. Krauch, 411-13. Radiochemistry in engineering and industry. II.

Kerntechnik 2, No. 9 (1960)

W. Kühn, F. Herrmann, 268-70. Possibilities of utilizing tritium bremsstrahlung in industrial applications.

———, 285-86. A new cobalt facility for weighing commercial freight cars.

Kerntechnik 2, No. 10 (1960)

———, 331. Use of radioactive tracers in West Germany.

Nucl. Energy No. 149 (1960)

———, 490, ff. Copenhagen international conference on the uses of radioactive isotopes in science and industry. Review of papers on industrial applications.*

W. Arnold, V. Stonehocker, 492-93. Tracer applications for determining wear on reciprocating piston engines.

Nucl. Engng. 5, No. 52 (1960)

———, 517-22. Radiography applications for accelerators.

* See article, this issue JAE, page 182.

3 titles of immediate interest!

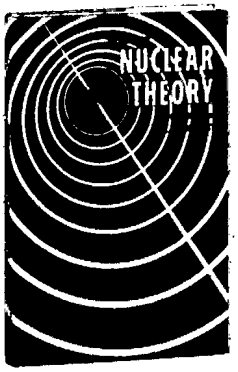

LECTURES ON NUCLEAR THEORY

by L. Landau and Ya. Smorodinsky

Translated from Russian

A concise presentation by these world-famous Soviet physicists of some of the basic concepts of nuclear theory. Originally published at $15.00 per copy.

". . . a real jewel of an elementary introduction into the main concepts of nuclear theory . . ."—NUCLEAR PHYSICS

". . . a decidedly worth-while addition to any experimental nuclear physicist's library."—E. M. Henley, PHYSICS TODAY

cloth 108 pages $5.25

Order from: **PLENUM PRESS 227 W. 17th Street, New York 11, N.Y.**

— of major interest to all researchers in low-temperature physics.

A SUPPLEMENT TO "HELIUM"

By E. M. Lifshits and E. L. Andronikashvili

Translated from Russian

This notable volume consists of two supplementary chapters, by these outstanding Soviet physicists, which were added to the Russian translation of W. H. Keesom's classic book "Helium."

The first chapter, by Lifshits, presents a concise resume of the Landau theory of superfluidity. The second chapter reports in considerable detail the experimental work conducted by Peter Kapitza and E. L. Andronikashvili.

cloth 167 pages illustrated $7.50

Order from: **CONSULTANTS BUREAU 227 W. 17th St. • New York 11, N. Y.**

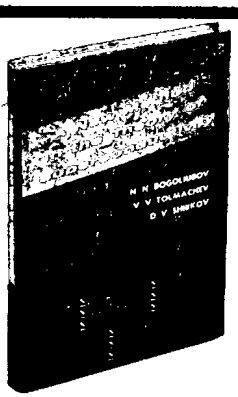

A NEW METHOD IN THE THEORY OF SUPERCONDUCTIVITY

By N. N. Bogoliubov, V. V. Tolmachev and D. V. Shirkov

Translated from Russian

The Soviet authors put forth a systematic presentation of a new method in the theory of superconductivity, developed as a result of the research of N. N. Bogoliubov and V. V. Tolmachev—based on a physical and mathematical analogy with superfluidity. This new method is an immediate generalization of the method developed by Bogoliubov in formulating a microscopic theory of superfluidity.

The authors give calculations for the energy of the superconducting ground state using Frohlich's Hamiltonian, as well as of the one-fermion and collective elementary excited states. A detailed analysis of the role of the Coulomb interaction between the electrons in the theory of superconductivity is included. The authors also demonstrate how a system of fermions is treated with a fourth-order interaction Hamiltonian and establish the criterion for its superconductivity.

cloth 121 pages illustrated $5.75

Order from: **CONSULTANTS BUREAU 227 W. 17th St. • New York 11, N. Y.**

Descriptive folders upon request.

Research by Soviet Experts
Translated by Western Scientists

Soviet Research on the LANTHANIDE AND ACTINIDE ELEMENTS, 1949-1957

An important contribution to the literature of nuclear chemistry, this collection of papers is a comprehensive presentation of Soviet research on the chemistry of lanthanides and actinides. The 106 reports included in this collection appeared in the major Soviet chemical journals translated by Consultants Bureau, as well as in the Soviet Journal of Atomic Energy, 1949-1957.

The five sections, totalling 657 pages, provide broad representation of contemporary Soviet research in this important aspect of nuclear science. This collection should be accessible to all nuclear researchers, whether theoretical or applied.

Each part may be purchased as follows:

Basic Chemistry (25 papers) **$15.00**
Analytical and Separation Chemistry (30 papers) **$20.00**
Nuclear Chemistry (and Nuclear Properties) (32 papers) ... **$22.50**
Geology (10 papers) **$7.50**
Nuclear Fuel Technology (9 papers) **$7.50**
Complete collection **$65.00**

RADIATION CHEMISTRY, PROCEEDINGS OF THE FIRST ALL-UNION CONFERENCE MOSCOW, 1957

More than 700 of the Soviet Union's outstanding research scientists participated in this conference sponsored by the Academy of Sciences and the Ministry of the Chemical Industry. Each of the 56 reports read in the various sessions covers either the theoretical or practical aspects of radiation chemistry, and special attention is given to radiation sources used in radiation-chemical investigations. The general discussions which followed each report and reflected various points of view on the problem under analysis are also included.

Primary Acts in Radiation Chemical Processes
heavy paper covers 5 reports, plus discussion ..... illustrated **$25.00**

Radiation Chemistry of Aqueous Solutions (Inorganic and Organic Systems)
heavy paper covers 15 reports, plus discussion ..... illustrated **$50.00**

Radiation Electrochemical Processes
heavy paper covers 9 reports, plus discussion ..... illustrated **$15.00**

The Effect of Radiation on Materials Involved in Biochemical Processes
heavy paper covers 6 reports, plus discussion ..... illustrated **$12.00**

Radiation Chemistry of Simple Organic Systems
heavy paper covers 9 reports, plus discussion ..... illustrated **$30.00**

The Effect of Radiation on Polymers
heavy paper covers 9 reports, plus discussion ..... illustrated **$25.00**

Radiation Sources
heavy paper covers 3 reports ..... illustrated **$10.00**

Individual volumes may be purchased separately.

NOTE: Individual reports from each volume are available at $12.50 each. Tables of contents sent upon request.

special price for the 7-volume set **$125.00**

Payment in sterling may be made to Barclay's Bank in London, England.

CONSULTANTS BUREAU
227 West 17th Street · New York, N.Y., U.S.A.